

In-Vitro Studies on the Intestinal Absorption Mechanisms of
Quercetin and Related Glycosides

Ying Zheng

A Thesis Submitted in Partial Fulfillment
of the Requirements for the Degree of
Master of Philosophy
in
Pharmacy

The Chinese University of Hong Kong
October 2001

©The Chinese University of Hong Kong holds the copyright of this thesis. Any person(s) intending to use a part of the materials in the thesis in a proposed publication must seek copyright release from the Graduate School.

UL



ABSTRACT

In-Vitro Studies on the Intestinal Absorption Mechanisms of Quercetin and Related Glycosides

YING Zheng

Keywords:- Flavonoids, Quercetin and related glycosides, Absorption, Caco-2 Cell Monolayers, Brush Border Membrane Vesicles, SGLT1, P-glycoprotein.

Purpose. Quercetin is one of the most abundant flavonoids present in human diet. *In vitro* and *in vivo* studies have demonstrated the beneficial effects of quercetin and related glycosides. Bioavailability studies conducted thus far have shown different absorption characteristics for quercetin and its various glycosides. It has been suggested that quercetin glucosides may be actively absorbed by specific glucose transporters. The aims of the present study are to characterize the physicochemical properties of quercetin and four of its glycosides, and to investigate the intestinal transport mechanisms of quercetin, and in particular, the impact of the sugar moiety on its absorption.

Methods. Quercetin and four of its glycosides were characterized by thermal analysis, partition coefficient and solubility measurements, and stability assessment in water at various pHs. Permeability coefficients of quercetin and its glycosides across Caco-2 cell monolayers were measured as a function of direction of transport, concentration of the flavonoid, existence of sodium ions, and in the presence or absence of verapamil, an inhibitor of the efflux pump P-gp. Rabbit's brush border membrane vesicles (BBMVs) were employed to study the competition of quercetin-3-glucoside and quercetin-3-galactoside with D-glucose for the glucose transporters.

Results. Quercetin (aglycone) has been shown to be poorly soluble in water and prone to hydrolytic degradation under intestinal pH condition. Incubation of quercetin in water at intestinal pH 6.8 resulted in the formation of three degradation products. Substitution of quercetin at position 3 with sugar led to lower lipophilicity (lower partition coefficient) and higher stability and higher aqueous solubility.

Apparent permeability coefficient (P_{app}) of quercetin, quercetin-3-rhamnoside,

quercetin-3-galactoside, quercetin-3-glucoside, and quercetin-3-rutinoside, at 50 μM in the donor compartment were, respectively, $15.50 \pm 1.64 \times 10^{-6}$, $2.71 \pm 0.61 \times 10^{-6}$, $2.46 \pm 0.36 \times 10^{-6}$, $1.50 \pm 0.22 \times 10^{-6}$ and $2.73 \pm 0.32 \times 10^{-6}$ cm/s from apical to basolateral side (AP to BL), and $16.93 \pm 0.61 \times 10^{-6}$, $2.67 \pm 0.37 \times 10^{-6}$, $2.42 \pm 0.13 \times 10^{-6}$, $2.43 \pm 0.19 \times 10^{-6}$ and $2.15 \pm 0.58 \times 10^{-6}$ cm/s from basolateral to apical side (BL to AP). Except for quercetin-3-glucoside, there was no significant bi-directional difference in P_{app} at 5% significance level among the glycosides. P_{app} of quercetin-3-glucoside was 12.6-, 3.4-, 1.6- and 1.3- fold higher in the BL to AP direction at 25, 30, 50 and 100 μM , respectively. The efflux of quercetin-3-glucoside was reduced in the presence of verapamil, a P-glycoprotein (P-gp) substrate. At 50 μM , the transport of quercetin-3-glucoside from AP to BL side was independent of the presence of sodium ions, while the presence of sodium/D-glucose co-transporter (SGLT1) inhibitor phloridzin at 100 μM in Caco-2 cells monolayers had no inhibitory effect on the transport of quercetin-3-glucoside. Quercetin-3-glucoside and quercetin-3-galactoside at 0.05, 0.1 and 0.2 mM had no significant inhibitory effects on the uptake of 0.1 mM D-glucose on BBMVs.

Conclusions. The above results are indicative of transcellular transport predominantly by passive diffusion for quercetin and its glycosides except for quercetin-3-glucoside, whose transport also involves interaction with the P-gp efflux system. Being more lipophilic, the aglycone quercetin is expected to be better absorbed than its glycosides. However, metabolism by Phase II enzymes in the intestine cells and reduced chemical stability at intestinal pH may limit the amount of the free form of quercetin *in vivo*. In contrast, the various glycosides exhibit low lipophilicity (partition coefficient) and poor permeabilities which may be a limiting factor for their absorption. The absence of inhibitory effect of quercetin-3-glucoside and quercetin-3-galactoside on the uptake of D-glucose by BBMVs suggests that they may not compete with D-glucose for the same binding sites on the glucose transporter SGLT1.

摘 要

黄酮肠道吸收机理的体外研究

郑 颖

关键词：黄酮，斛皮素及其糖甙，吸收，Caco-2 单层细胞，微囊(上皮细胞膜刷状缘侧)，依赖钠离子的葡萄糖转运载体，P-糖蛋白

目的： 斛皮素是一种在人们的饮食中大量存在的黄酮。体内及体外研究证明斛皮素及其糖甙有益健康。迄今为止，对其的生物利用度研究显示，斛皮素及其各种糖甙的吸收过程很不相同。有假设认为，斛皮素的葡萄糖甙可被特异性的葡萄糖载体转运而被吸收。本研究的目的在于考察斛皮素及其四个糖甙的理化性质，吸收机理，特别是不同糖基对斛皮素吸收的影响。

方法： 首先研究了斛皮素及其糖甙的理化性质，包括热力学分析,分配系数及溶解度测定和在不同 pH 值水溶液中的稳定性考察。斛皮素及其糖甙通过 Caco-2 单层细胞的渗透系数在下列不同条件下进行考察： 不同的转运方向；不同的初始浓度；是否存在钠离子及是否存在 P-蛋白反转运系统的抑制剂。利用兔子的上皮细胞膜(刷状缘侧)制成的微囊来研究斛皮素-3-葡萄糖甙和斛皮素-3-半乳糖甙是否可与 D-葡萄糖竞争葡萄糖转运载体。

结果： 斛皮素(甙元)水溶性较差，在肠液 pH(6.8)条件下分解并形成三个分解产物。斛皮素的 3 位被糖基取代后使脂溶性降低(分配系数)，同时稳定性及水溶性得以提高。

在 50 微摩尔/升的浓度下，斛皮素， 斛皮素-3-鼠李糖甙，斛皮素-3-半乳糖甙，斛皮素-3-葡萄糖甙和芦丁在从 Caco-2 单层细胞粘膜侧到浆膜侧的表观渗透系数分别为(厘米/秒)： $15.50 \pm 1.64 \times 10^{-6}$ ， $2.71 \pm 0.61 \times 10^{-6}$ ， $2.46 \pm 0.36 \times 10^{-6}$ ， $1.50 \pm 0.22 \times 10^{-6}$ 及 $2.73 \pm 0.32 \times 10^{-6}$ ；从浆膜侧到粘膜侧分别为(厘米/秒)： $16.93 \pm 0.61 \times 10^{-6}$ ， $2.67 \pm 0.37 \times 10^{-6}$ ， $2.42 \pm 0.13 \times 10^{-6}$ ， 2.43 ± 0.19

$\times 10^{-6}$ 和 $2.15 \pm 0.58 \times 10^{-6}$ 。除了斛皮素-3-葡萄糖甙，其余糖甙的表观渗透系数在两个方向上没有显著性差异 ($P > 0.05$)。斛皮素-3-葡萄糖甙在 25, 30, 50 和 100 微摩尔/升浓度下的表观渗透系数从浆膜侧到粘膜侧分别为从粘膜侧到浆膜侧的 12.6, 3.4, 1.6 和 1.3 倍。加入 P-蛋白的抑制剂惟拉帕米减少斛皮素-3-葡萄糖甙的反向转运(浆膜侧到粘膜侧)。在 50 微摩尔/升浓度下，斛皮素-3-葡萄糖甙从粘膜侧到浆膜侧的表观渗透系数与钠离子的存在无关。根皮甙(钠离子依赖的葡萄糖转运载体抑制剂)，在 100 微摩尔/升浓度下，在单层细胞模型中，对斛皮素-3-葡萄糖甙从粘膜侧到浆膜侧的转运无抑制作用。在 0.05, 0.1 和 0.2 毫摩尔/升条件下，斛皮素-3-葡萄糖甙和斛皮素-3-半乳糖甙对微囊(上皮细胞膜刷状缘侧)摄入 D-葡萄糖(0.1 毫摩尔/升)无显著性的抑制作用。

结论：上述结果提示在选定的黄酮中，除去斛皮素-3-葡萄糖甙，斛皮素及其它糖甙主要通过被动扩散机理被吸收，而斛皮素-3-葡萄糖甙的转运还与 P-蛋白反转运系统关联。由于甙元斛皮素相对较高的脂溶性，预计斛皮素的转运比其糖甙好。但是，斛皮素在肠细胞中被二相酶代谢和其在肠液 pH 条件下较差的稳定性会影响体内斛皮素(原形)的量。与其相反，斛皮素糖甙的脂溶性(分配系数)较低，而且渗透性差，这些可能成为影响其口服吸收的限速步骤。斛皮素-3-葡萄糖甙和斛皮素-3-半乳糖甙对微囊摄入 D-葡萄糖无显著性的抑制作用，提示它们可能不能与 D-葡萄糖竞争葡萄糖转运载体上相同的结合位点。

ACKNOWLEDGEMENTS

I would like to thank my supervisor, Prof. Albert H.L. Chow for his guidance and kind assistance. I also want to thank Prof. Joan Z. Zuo for her helpful comments and suggestions on the experimental work and preparation of thesis, and Prof. Clara B.S. Lau for her helpful guidance in the studies with brush border membrane vesicles. Special thanks are due to Prof. W.H. Ko and his technician in the Department of Physiology for assistance with the cell culture work and to the staff in the multidisciplinary laboratory for providing the space and equipment for some of the studies.

My heartiest thanks also go to the professors and technicians in our School for their helpful advice and technical support, especially to Ms. Cindy M.Y. Lo and Ms. Sherry S.L. Lam who performed the HPLC/MS analysis. Living and studying with other postgraduate students in our School enables me to learn a lot from their rich experience and perseverance.

Last but not the least, I would like to thank my parents and my friends for their continual encouragement and support.

TABLE OF CONTENTS

TITLE PAGE	
ABSTRACT	ii
中文摘要	iv
ACKNOWLEDGEMENTS	vi
TABLE OF CONTENTS	vii
LIST OF FIGURES	x
LIST OF TABLES	xii
ABBREVIATIONS	xiii
CHAPTER 1. Introduction	1
1.1. Rationale of the Study	2
1.2. Flavonoids	3
1.2.1. Introduction	3
1.2.2. Potential Health Effects	5
1.2.3. Absorption Studies	6
1.3. Drug Absorption	9
1.3.1. Pathways and Mechanisms of Intestinal Absorption	9
1.3.2. Transporters Potentially Involved in the Absorption of Flavonoids	11
1.3.2.1. Glucose Transporters	11
1.3.2.2. Multidrug Resistance Systems	13
1.3.2.2.1. P-glycoprotein	13
1.3.2.2.2. Non-P-glycoprotein Efflux Mechanisms	15
1.4. <i>In vitro</i> Models to Study Absorption	15
1.4.1. Ussing Chamber	16
1.4.2. Cultured Cells	17
1.4.2.1. Choice of Cells	17
1.4.2.2. Caco-2 Cell Monolayers as <i>in vitro</i> Model	18
1.4.2.3. Correlation Between <i>in vivo</i> Absorption and <i>in vitro</i> Permeability Coefficients	19
1.4.3. Everted Gut Sacs	20
1.4.4. Brush Border Membrane Vesicles (BBMVs)	20
1.4.5. <i>In situ</i> Experiments	21
1.5. Aims and Scope of the Present Study	23
CHAPTER 2. Materials & Methods	25
2.1. Materials	26
2.1.1. Chemicals	26
2.1.2. Materials for Cell Culture	27
2.1.3. Instruments	28
2.1.4. Animals	28
2.2. Methods	29
2.2.1. Preformulation Studies on Selected Flavonoids	29
2.2.1.1. Determination of Stability	29
2.2.1.2. Thermal Analysis	29
2.2.1.3. Determination of Solubility	29
2.2.1.4. Determination of Partition Coefficient	30

2.2.2. Validation of <i>in vitro</i> Models	30
2.2.2.1. Ussing Chamber	30
2.2.2.1.1. Tissue Preparation	30
2.2.2.1.2. Electrical Measurements	31
2.2.2.1.3. Experimental Protocols	31
2.2.2.1.4. Calculations of Permeability	32
2.2.2.2. Caco-2 Cell Monolayers	32
2.2.2.2.1. Preparation of Caco-2 Cell Monolayers	32
2.2.2.2.2. Validation of Caco-2 Cell Monolayers	32
2.2.2.2.3. Calculation of Permeability	34
2.2.3. Transport Studies of Selected Flavonoids	34
2.2.4. Brush Border Membrane Vesicles (BBMVs)	35
2.2.4.1. Preparation of BBMVs	35
2.2.4.2. Uptake of D-glucose by BBMVs	38
2.2.4.3. Counting of ³ H-D-glucose in BBMVs	39
2.2.4.4. Calculation of Glucose Uptake	39
2.2.4.5. Total Protein Assay	40
2.2.5. Analytical Methods	41
2.2.5.1. HPLC Analysis	41
2.2.5.1.1. HPLC Analysis of Quercetin and Related Glycosides	41
2.2.5.1.2. HPLC-MS Analysis of Degradation Products	41
2.2.5.1.3. HPLC Analysis of Propranolol	42
2.2.5.2. UV Analysis	42
2.2.5.3. Fluorescence Analysis	42
2.2.5.4. Analysis of Radiolabeled Markers	42
2.2.6. Statistical Analysis	42
CHAPTER 3. Results & Discussions	44
3.1. Preformulation Studies on Selected Flavonoids	45
3.1.1. Stability	45
3.1.2. Thermal Analysis	52
3.1.3. Aqueous Solubility	58
3.1.4. Partition Coefficient	61
3.2. Validation of <i>in vitro</i> Models	62
3.2.1. Selection of Marker Compounds	62
3.2.2. Validation of Ussing Chamber	63
3.2.3. Validation of Caco-2 Cell Monolayers	64
3.2.3.1. Integrity of Caco-2 Cell Monolayers	64
3.2.3.2. Permeabilities of Marker Compounds	65
3.2.3.3. Selection of <i>in vitro</i> Models	66
3.2.3.3. Validation of Sodium/Glucose Cotransporter (SGLT1)	66
3.3. Transport Studies of Quercetin and Related Flavonoids	67
3.3.1. Direction of Transport	67
3.3.2. Concentration Dependence	69
3.3.3. Inhibition of P-gp by Verapamil	71
3.3.4. Metabolism of Quercetin in Caco-2 Cells	72
3.3.5. Studies of Quercetin-3-glucoside with Sugar Transporters	73
3.4. Uptake of D-glucose by Brush Border Membrane Vesicles (BBMVs)	75
CHAPTER 4. Conclusions	80

LIST OF FIGURES

Chapter 1. Introduction	1
Figure 1.1. Structures of flavonoids.	4
Figure 1.2. Potential model of transport of molecules across the intestinal epithelium	11
Figure 1.3. Glucose transport systems in the small intestine	12
Figure 1.4. Ussing Chamber	22
Figure 1.5. Caco-2 cell monolayers	22
Figure 1.6. Structures of quercetin and related glycosides.	24
Chapter 2. Materials and Methods	25
Figure 2.1. Preparation of frozen rabbit's small intestine.	36
Figure 2.2. Preparation of BBMVs from frozen small intestine.	37
Figure 2.3. Procedure of uptake of D-glucose into BBMVs.	38
Chapter 3. Results & Discussions	44
Figure 3.1a. Stability of quercetin-3-galactoside at pH 7.4, 6.8 and 1.2 in aqueous solutions at 37 °C .	45
Figure 3.1b. Stability of quercetin-3-glucoside at pH 7.4, 6.8 and 1.2 in aqueous solutions at 37 °C .	46
Figure 3.1c. Stability of quercetin-3-rutinoside at pH 7.4, 6.8 in aqueous solutions at 37 °C.	46
Figure 3.1d. Stability of quercetin-3-rhamnoside at pH 7.4, 6.8 in aqueous solutions at 37 °C .	46
Figure 3.1e. Stability of quercetin at pH 7.4, 6.8 and 1.2 in aqueous solutions at 37 °C.	48
Figure 3.2a. HPLC chromatograms of quercetin.	49
Figure 3.2b. HPLC chromatogram of quercetin and its degradation products.	49
Figure 3.3a. UV scan of degradation product 1.	50
Figure 3.3b. UV scan of degradation product 2.	50
Figure 3.3c. UV scan of degradation product 3.	51
Figure 3.3d. UV scan of quercetin	51
Figure 3.4a. TGA of quercetin.	53

Figure 3.4b.	DSC thermogram of quercetin.	53
Figure 3.5a.	TGA of quercetin-3-glucoside.	54
Figure 3.5b.	DSC thermogram of quercetin-3-glucoside.	54
Figure 3.6a.	TGA of quercetin-3-rhamnoside.	55
Figure 3.6b.	DSC thermogram of quercetin-3-rhamnoside.	55
Figure 3.7a.	TGA of quercetin-3-rutinoside.	56
Figure 3.7b.	DSC thermogram of quercetin-3-rutinoside.	56
Figure 3.8a.	TGA of quercetin-3-galactoside.	57
Figure 3.8b.	DSC thermogram of quercetin-3-galactoside.	57
Figure 3.9.	Van't Hoff plots on the saturated aqueous concentration of glycoside.	59
Figure 3.10a.	Transepithelial flux of quercetin-3-glucoside across the Caco-2 cell monolayers from apical to basolateral side.	69
Figure 3.10b.	Transepithelial flux of quercetin-3-glucoside across the Caco-2 cell monolayers from basolateral to apical side.	70
Figure 3.10c.	P_{app} vs. TEER of Caco-2 cell monolayers	70
Figure 3.11.	Time course of 30 μ M quercetin-3-glucoside transport across the Caco-2 cell monolayers in the absence or presence of 100 μ M verapamil.	71
Figure 3.12.	Concentration of quercetin aglycone on basolateral side before and after hydrolysis.	72
Figure 3.13.	Effect of SGLT1 inhibitor phloridzin (100 μ M) on the transport of quercetin-3-glucoside (100 μ M) from apical to basolateral in Caco-2 cell monolayers.	74
Figure 3.14.	Time course plot of D-glucose uptake by rabbit intestinal BBMV's.	76
Figure 3.15a.	Uptake of D-glucose with quercetin-3-glucoside by rabbit intestinal BBMV's.	77
Figure 3.15b.	Uptake of D-glucose with quercetin-3-galactoside by rabbit intestinal BBMV's.	77

LIST OF TABLES

Chapter 3.	Results & Discussions	44
Table 3.1.	Bound water of flavonoids.	58
Table 3.2a.	Solubility of quercetin glycosides in aqueous solution (pH 7.4).	58
Table 3.2b.	Van't Hoff equation and calculated ΔH^S .	59
Table 3.3.	Partition coefficient of quercetin and its glycosides.	62
Table 3.4.	Physicochemical data, MW, pKa values, Log P (Octanol/Water, pH 7.4) and absorption in human of 6 markers studied in the Ussing Chamber and Caco-2 cell monolayers.	62
Table 3.5.	Apparent permeability coefficients of 6 marker compounds obtained in rat ileum using the Ussing Chamber.	64
Table 3.6.	Apparent permeability coefficients of 5 marker compounds obtained in Caco-2 cell monolayers.	65
Table 3.7.	The effect of SGLT1 inhibitor phloridzin (100 μ M) on P_{app} and uptake of D-glucose (100 μ M) from apical to basolateral in the Caco-2 cell monolayers.	67
Table 3.8.	Bi-directional permeability of quercetin (12.5 μ M) and its glycosides (50 μ M) in the Caco-2 cell monolayers.	69
Table 3.9.	The effect of sodium ions on P_{app} of quercetin-3-glucoside (50 μ M) from apical to basolateral in Caco-2 cell monolayers.	74

ABBREVIATIONS

AP	Apical
BBMVs	Brush Border Membrane Vesicles
BL	Basolateral
HEPES	N-2-Hydroxyethylpiperazine-N'-2-ethanesulphonic acid
MRP	Multidrug Resistance Protein
P_{app}	Apparent Permeability Coefficient
P-gp	P-glycoprotein
PD	Potential Difference
R	Resistance
SCC	Short Circuit Current
SGLT1	Na ⁺ /Glucose Co-transporter
TEER	Transepithelial Electrical Resistance
Tris	2-amino-(hydroxymethyl) propane-1,3-diol

CHAPTER 1.
INTRODUCTION

1. Introduction

1.1. Rationale of the Study

Quercetin belongs to the group of flavonoids, a major group of secondary plant metabolites occurring widely in plant. Flavonoids are polyphenolic compounds present in daily diet. They also occur in foods, usually as O- β -glycosides with various sugar residues (Kühnau, 1976). Due to their potential anticancer activities and protective effects in cardiovascular diseases (Hollman *et al*, 1996), there has been an increasing commercial interest in developing some of these biologically active flavonoids into drug candidates.

Despite the well-established biological effects of quercetin, the absorption mechanisms of quercetin and related glycosides (which represent the major form of quercetin in foods consumed) are not well understood. It is generally believed that the glycosides need to be hydrolyzed first in the gastrointestinal tract before being absorbed into the blood (Kühnau, 1976; Erlund *et al*, 2000). However, Hollman *et al* (1995, 1997) reported that quercetin conjugated with glucose could be readily absorbed in humans without undergoing prior hydrolysis, and the absorption was even significantly better than that of the quercetin aglycone. Thus they inferred that sodium/glucose co-transporter (SGLT1) may be actively involved in transporting quercetin glucoside across the intestinal cells, and this glucose transporter may provide an effective way for enhancing the oral absorption of glucoside. Olthof *et al* (2000) also observed that quercetin-3-glucoside and quercetin-4'-glucoside displayed rapid and comparable absorption in humans, and proposed that it is the chemical nature rather than the position of the attached sugars that determines the absorption of flavonoids.

The present project was aimed at providing a better understanding of the

mechanisms of absorption of quercetin across the intestinal epithelial cells and the influence of sugar moiety on the absorption process. For this purpose, quercetin and four related glycosides, namely, quercetin-3-glucoside, quercetin-3-galactose, quercetin-3-rutinoside and quercetin-3-rhamnoside, have been investigated for their intestinal transport characteristics using well-established *in vitro* models. In addition, potential absorption-limiting factors such as chemical instability, efflux and metabolism have also been studied.

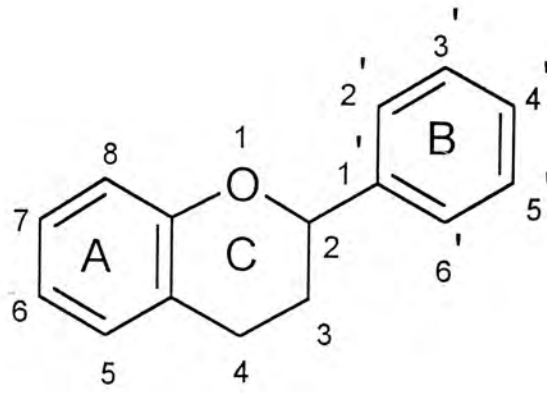
Presented below is a concise account of the background of the present research.

1.2. Flavonoids

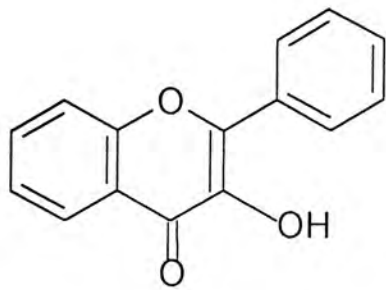
1.2.1. Introduction

Flavonoids are secondary plant metabolites occurring widely in plant. More than 4000 flavonoid glycosides have been described to date, which are based on a small number of flavonoid aglycones and a large variety of combinations with different sugar substituents (Cook and Samman, 1996).

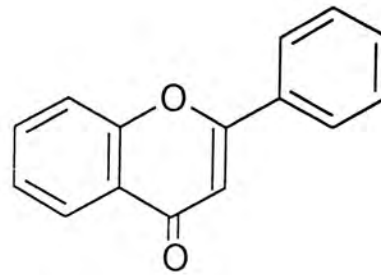
Flavonoids are a group of polyphenolic compounds based on the flavan nucleus. They can be divided into several classes according to the degree of oxidation of the oxygen heterocycle, namely, flavonols, flavones, isoflavones, flavanones, dihydroflavonols, and chalcones as shown in Figure 1.1 (Cook and Samman, 1996). They have antioxidant activities that are related to their chemical structures. Comparison of the aglycones with their respective glycosides showed that glycosylation at 7-OH and 3-OH on the B ring reduced their antioxidant activity (Rice-Evans *et al*, 1996).



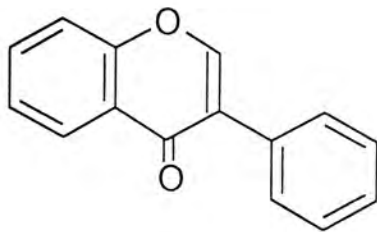
Basic structure of flavonoids



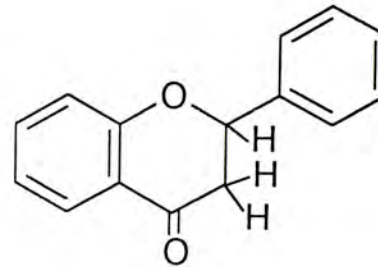
Flavonols



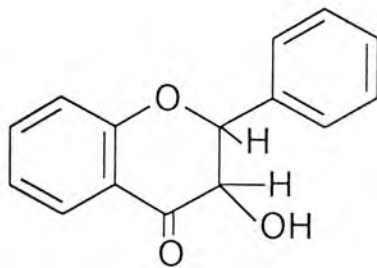
Flavones



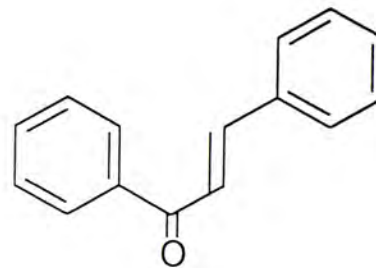
Isoflavones



Flavanones



Dihydroflavonols



Chalcones

Fig. 1.1 Structures of Flavonoids

In USA, the daily intake of flavonoids per person was estimated to be 1 g expressed as glycosides, equivalent to about 115 mg flavonol and flavone aglycones (Kühnau, 1976). However, this estimate was most likely too high as it was based on incomplete food composition data. In the Netherlands, the estimated average daily intake of flavonols and flavones was 23 mg, out of which 16 mg was quercetin (5,7,3',4'-hydroxyflavonol) (Hollman *et al*, 1999). Quercetin is commonly present in foods with relatively high concentration found in tea, onions and apples.

1.2.2. Potential Health Effects

In recent years, there has been a growing commercial interest in flavonoids, particularly in quercetin due to their potential beneficial effects on human health. Quercetin and other flavonoids have been shown to modify eicosanoid biosynthesis, protect low-density lipoprotein from oxidation, prevent platelet aggregation and promote relaxation of cardiovascular smooth muscle. In addition, they possess antiviral and carcinostatic properties (Formica *et al*, 1995).

The potential health benefits of quercetin and other flavonols and flavones in humans have been reviewed by Hollman *et al* (1996, 1999). Epidemiological studies on these flavonoids conducted to date at several sites have not revealed any strong association between cancer risk and intake of flavonol and flavone except for one study involving about 10,000 men and women aged 15-99, which demonstrated a reduction of lung cancer risk by about 50% (Knekt *et al*, 1997; Hertog *et al*, 1995; Goldbohm *et al*, 1995). Epidemiological findings from other studies also point to a protective effect of antioxidant flavonols in cardiovascular diseases but it is inconclusive (Keli *et al*, 1996; Hertog *et al*, 1997; Rimm *et al*, 1996).

1.2.3. Absorption Studies

Due to the high oral consumption of flavonoids in our daily diet and their potential benefits to human health, the absorption of flavonoids has attracted considerable attention in recent years. It is generally assumed that flavonoids in the form of glycosides cannot be absorbed from the small intestine, and the absorption of such glycosides will not occur until they reach the large intestine where they are hydrolyzed by the enzymatic activities of microflora to the respective aglycones (Kühnau, 1976). However, it has been found recently that the cytosolic β -glucosidase and a membrane-bound β -glucosidase (lactase phlorizin hydrolase) in the small intestine were capable of hydrolyzing some of these flavonoid glycosides to their aglycones, suggesting that the small intestine may also be a significant absorption site for the hydrolyzed products (Day *et al*, 1998, 2000a). Hollman *et al* (1997) observed widely different absorption characteristics for several quercetin glycosides when nine subjects were fed with a large single quantity of onions (containing glucose conjugates of quercetin), apples (containing both glucose and non-glucose quercetin glycosides), or pure quercetin-3-rutinoside. Absorption of quercetin glycosides from the apples or of pure quercetin-3-rutinoside was 30% of that for onions. Peak levels for these three groups of flavonoids were reached in about 0.7, 2.5 and 9 h respectively. In order to avoid the possible hydrolysis of the glycosides caused by the colonic bacteria, healthy ileostomy volunteers were recruited for the study. The extent of absorption was 52% for quercetin glucoside from onions, 17% for quercetin-3-rutinoside and 24% for quercetin aglycone (Hollman *et al*, 1995). The significantly higher absorption of the quercetin glucoside relative to the quercetin suggested that intestinal sugar transport carriers may be implicated in the absorption of the glucoside. It must be pointed out, however, that the chemical analysis of quercetin glycosides in

this reported study involved acid hydrolysis of the glycosides to the quercetin (aglycone), and it was not known if the absorbed flavonoids might also have included some aglycone resulting from hydrolysis in the gastrointestinal tract. Such a possibility has indeed been demonstrated by Walle *et al* (2000) who conducted similar studies on the onion glycosides. These authors found that only quercetin could be detected in the plasma of ileostomy subjects after being given an onion meal. Thus they concluded that quercetin-4'-glucoside and quercetin-3,4'-glucoside were efficiently hydrolyzed to the quercetin in the small intestine before being absorbed into the blood (Walle *et al*, 2000). Similarly, oral intake of quercetin-4'-glucoside and quercetin-3-rutinoside in pure form or in food did not afford any free form of the glycosides in human plasma and urine (Graefe *et al*, 2001). However, Aziz *et al* (1998) reported the detection of small amounts of unchanged quercetin-4'-glucoside in the plasma and urine of human subjects following the consumption of onions. Maximum accumulation in plasma and excretion in urine of this glycoside were 0.13% and 0.2% respectively of the amount of intake. These results further support the view that the absorption of quercetin in the form of glycosides is very limited, and hydrolysis may be required prior to absorption.

In addition to the aforementioned *in vivo* studies, several *in vitro* transport models have also been employed to elucidate the absorption process of flavonoids. *In vitro* perfusion of the isolated rat jejunum with quercetin-3-rutinoside demonstrated that neither the quercetin aglycone nor its potential glucuronide metabolites but only the original glycoside could be detected after passage of the flavonoid through the intestinal cells. However, for perfusion with quercetin-3-glucoside, small amounts of unchanged glucoside together with quercetin and quercetin glucuronides were found (Spencer *et al*, 1999). *In vitro* studies involving Caco-2 cell monolayers showed that

the carrier, sodium/glucose cotransporter SGLT1, was likely involved in transporting quercetin 4'- β -glucoside across the apical membrane of the monolayer (Walgren *et al*, 2000b), but such involvement could not be readily demonstrated owing to the counteracting effect of the apical multidrug resistance-associated protein 2 (Walgren *et al*, 1998, 2000a). [The multidrug resistant system is as an energy-dependent efflux pump that exports drug substrates out of the cells and thereby decreases their absorption (see later discussion)]. The efflux mechanism was also found to reduce the transport of genistein-7-glucoside, an isoflavone (Walle *et al*, 1999).

The significant role of metabolising enzymes present in the gut in the absorption process of quercetin (aglycone) has been demonstrated both *in vivo* and *in vitro*. Pharmacokinetic studies on quercetin showed that extensive glucuronidation occurred following oral administration of 50 mg of the pure compound to human volunteers, the amount of unconjugated quercetin observed at 12 h was 10.7% of the total quercetin (Erlund *et al*, 2000). *In vitro* studies have shown that both quercetin and chrysin could induce UDP-glucuronosyltransferase (UGT) in Caco-2 cells (Galijatovic *et al*, 2000). It has also been found that the ease of glucuronidation at different positions of the quercetin (see Figs. 1.1 and 1.2) by UGT followed the order: 4'- >3'- >7- >3-, and the resulting glucuronides except for quercetin-3-glucuronide retained part of the biological activities of the native quercetin (Day *et al*, 2000b). The latter was further substantiated by the observation that the conjugation derivatives of quercetin recovered from human plasma still possessed half of the antioxidant properties of quercetin (Manach *et al*, 1998).

All of the above observations indicate that the absorption process of quercetin glycosides possibly involves a complex interplay of a number of transport carriers/proteins and metabolising enzymes. The findings emphasize that not only the

native forms of quercetin and its glycosides, but also their potential metabolites in the body need be considered when assessing the beneficial effects of these flavonoids on human health.

1.3. Drug Absorption

1.3.1 Pathways and Mechanisms of Intestinal Absorption

A compound may transport across the intestinal epithelial barriers by two routes, namely, transcellular and paracellular routes as shown in Figure 1.2. The transcellular transport pathway is the most significant pathway since the cell membrane surface constitutes more than 99% of the total surface area of the intestine (Artursson, 1991). The paracellular pathway is characterized by the presence of tight junction on the apical side of the epithelial cells. This pathway accounts for less than 1% of the surface area of the intestinal epithelium, and transepithelial transport through this pathway is restricted by the size of transported species. Hydrophilic compounds with a molecular weight over 200 are only absorbed in small amounts by the paracellular route in humans (Lennernäs, 1995).

Broadly, there are four mechanisms of absorption, *viz* passive diffusion, active transport, facilitated transport and endocytosis, which are described below and shown in Figure 1.2.

(1) Passive Diffusion

It is the predominantly utilized mechanisms for drug transport. The driving force for diffusion across the membrane is the concentration gradient of the compound across that membrane. The process of membrane penetration is described by Fick's first law.

(2) Active transport

Active transport is mediated by means of carriers under the expenditure of energy (i.e. utilization of ATP). Each drug or group of drugs needs a specific carrier. Absorption proceeds against a concentration gradient and in the case of ions, against an electrochemical potential. The active transport becomes saturated if there are more drug molecules present than carriers available. The carriers are located on the external surface of the membrane. They form a complex with the drug molecule, which moves across the membrane by utilizing the energy provided by ATP. Many essential nutrients (e.g. monosaccharides, amino acid and vitamins) are transported by this mechanism.

(3) Facilitated transport

The facilitated transport is the same as active transport, the only difference is that the process does not operate against a concentration gradient.

(4) Endocytosis

Endocytosis is the uptake of extracellular material, exogenous molecules, or macromolecules into a cell by invagination of the plasmalemma and vesicle formation. It is the only transport process in which a drug or compound does not have to be in aqueous solution in order to be absorbed. Large peptides and other macromolecules may be absorbed by this route (Ritschel *et al*, 1999).

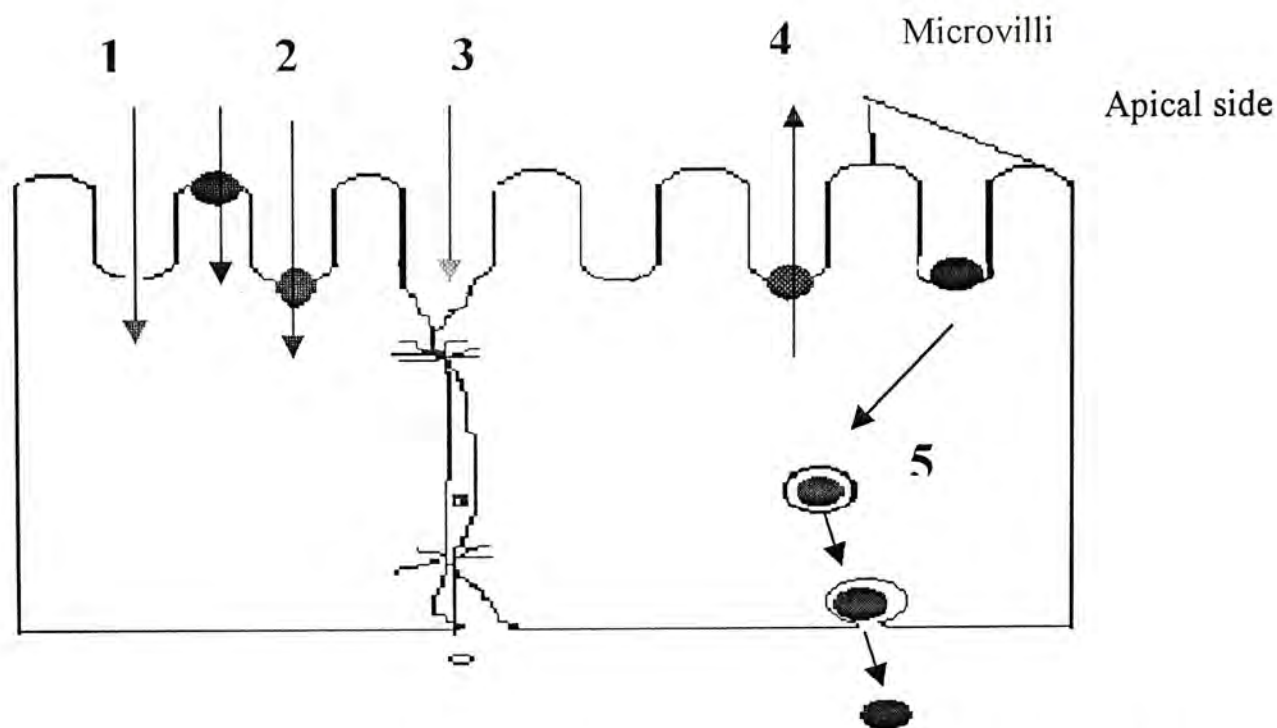


Fig. 1.2. Potential model of transport of molecules across the intestinal epithelium

1. Passive diffusion
2. Carrier-mediated transport (active or facilitated transport)
3. Paracellular transport
4. P-glycoprotein efflux system
5. Endocytosis

1.3.2. Transporters Potentially Involved in the Absorption of Flavonoids

1.3.2.1. Glucose Transporter

Shoji *et al* (1992) investigated whether the conjugation of a glucose or galactose moiety to a model compound (i.e. *p*-nitrophenol or β -naphthol) could result in active transport of that compound by the glucose transport system from the mucosal side to the serosal side. Their findings supported the feasibility of exploiting the glucose transport carrier as an alternative and possibly more efficient route in the intestinal absorption of non-glucose flavonoids through substitution with a glucose or galactose group.

It is well established that glucose absorption is specific, saturable, and energy-dependent. D-glucose can be absorbed from the gut against its concentration gradient. The conceptual breakthrough for glucose transport originated from the Na^+ /glucose

co-transport hypothesis presented by Crane and his colleagues. It was proposed that sugar transport was coupled to the Na^+ gradient across the brush border membrane and that the Na^+ gradient was maintained by the Na^+/K^+ pump. This hypothesis was tested, verified, refined, and extended to include the active transport of sugars, amino acids, and ions into cells. D-glucose uptake from gut lumen into enterocytes is driven by the Na^+ electrochemical potential gradient across the brush border. The intracellular Na^+ activity is low compared with the gut fluid, and a membrane potential of -40 to -60 mV exists across the brush border membrane (Wright *et al*, 1994).

Two distinctly different glucose transport systems have been shown to be present in the epithelial membranes isolated from the small intestine as shown in Figure 1.3. The major transport mechanism in the brush border membrane is the Na^+ /glucose co-transport system, SGLT1, where glucose is transported across the membrane into the cells against its concentration gradient through a coupling to the sodium ions across the membrane. A low intracellular concentration of Na^+ is maintained by the Na^+/K^+ -ATPase localized in the basolateral membrane. The glucose accumulated into the intestinal epithelial cells is then transported across the basolateral membrane by a Na^+ -independent facilitated diffusion system located on the basolateral membrane.

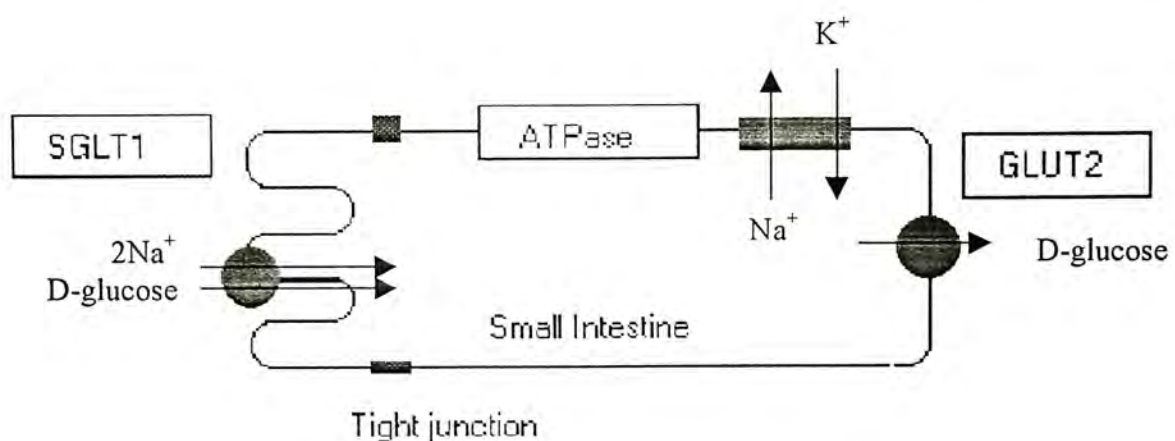


Fig. 1.3. Glucose transport systems in the small intestine

1.3.2.2. Multi-drug Resistance Systems

As alluded to earlier, the transports of quercetin-4'-glucoside and genistein-7-glucoside are associated with the multidrug resistant systems (Walle *et al*, 1999; Walgren *et al*, 2000a).

Multi-drug resistance (MDR) is defined as the ability of cells exposed to a single drug to develop resistance to a broad range of structurally and functionally unrelated drugs, due to enhanced outward transport (efflux) of drugs, which is mediated by a membrane glycoprotein 'drug transport pump'. The most consistent alteration found in MDR cell lines is an increased expression of a surface glycoprotein (i.e. P-glycoprotein), which will be elaborated in the following section (Hunter, 1997).

1.3.2.2.1. P-glycoprotein

(1) Distribution in normal tissues of human

Thiebaut (1987) employed an immunohistochemical technique using the anti-P-glycoprotein monoclonal antibody, MRK16 to examine frozen normal tissues. P-glycoprotein (P-gp) expression was found on the biliary canalicular surface of hepatocytes and the apical surface of small biliary ductules of the liver, the apical surface of proximal tubular epithelial cells of the kidney, the epithelial cells of small pancreatic ductules and the luminal surface of columnar epithelial cells of the jejunum and colon. The adrenal gland expressed P-gp in both the cortex and medulla, while no expression was identified in stomach, lung, ovary, uterus, spleen, skin or central nervous system tissues. P-gp was expressed at the apical brush border in confluent epithelial layers of human Caco-2 cells (Hosoya *et al*, 1996; Hunter *et al*, 1993a).

The specific location of P-gp expression indicates that it could be a factor that

limits intestinal absorption and diffusion of xenobiotics, as well as a feature that participates in the biliary, renal and intestinal clearance of drugs.

(2) Structure and function of P-glycoprotein

P-gp is an ATP-dependent glycoprotein located at the apical side of the membrane and has a molecular weight of 170 KDa. It is encoded by MDR1 gene in humans and *mdr1a* and *mdr1b* in mouse. It was shown to encode a protein of 1280 amino acids, the polypeptide chain consisting of two similar regions each containing six putative transmembrane segments and an intracellular adenosine triphosphate (ATP) binding site. It is recognized as a member of the ATP-binding cassette (ABC) super-family of membrane transport protein. The P-gp acts as an energy-dependent efflux pump that exports its drug substrates out of the cells, thus making the cell resistant to multiple cytotoxic compounds (Tanigawara, 2000).

The multidrug resistant systems play an important role in the pharmacokinetic behaviours of those drugs that are P-gp substrates/inhibitors. A well-known example is the cardiac glycoside, digoxin, which showed significant interactions with verapamil, nifedipine and quinidine, which are P-gp inhibitors. The plasma levels and half-life of the digoxin were observed to increase in the presence of these drugs (Hunter *et al*, 1997). *In vitro* transport studies using Caco-2 cell monolayers confirmed the involvement of P-gp in the absorption of digoxin (Cavet *et al*, 1996). Another example is celiprolol, a β -adrenoceptor blocking agent that exhibits dose-dependent bioavailability in rat (Kuo *et al*, 1994). It is a substrate of P-gp, as evidenced by the *in vitro* observation that the basal-to-apical transport of celiprolol through Caco-2 cell monolayers was 5 times higher than that determined in the reverse direction. Net celiprolol secretion (efflux) obtained in the concentration range

of 0.01 to 5 mM displayed saturable kinetics and the secretion was inhibited by several substrates of P-gp, i.e. vinblastine, verapamil and nifedipine (Karlsson *et al*, 1993). A more recent study also showed that the component, bergamottin, in grapefruit juice is a P-gp inhibitor and potentially can increase the absorption of those drugs that are P-gp substrates (Wang *et al*, 2001). It has been suggested that inhibition of P-gp by constituents of grapefruit juice could present ways both to enhance bioavailability of therapies without increasing the dose and to reduce drug resistance in refractory cells.

P-gp possesses the ability to recognize and transport a chemically and pharmacologically diverse range of compounds. Its substrates include calcium channel blockers, antibiotics, cyclosporines, peptides etc (Hunter *et al*, 1997). The mechanisms by which P-gp recognizes a wide range of substrates are not clear at present, but all P-gp substrates are at least somewhat hydrophobic (Tanigawara, 2000).

1.3.2.2.2. Non-P-glycoprotein Efflux Mechanisms

In addition to P-gp, other non-P-gp efflux mechanisms also exist, including the multi-drug resistance-associated protein (MRP). MRP is a 190 kDa protein distributed broadly similar to that described for P-gp (Hunter *et al*, 1997), and is also functionally expressed in Caco-2 cells (Gutmann *et al*, 1999).

1.4. *In vitro* Models to Study Absorption

To screen new drug candidates for intestinal absorption at an early stage of the drug development process, scientists in the pharmaceutical industry have often resorted to new efficient techniques that are amenable to high throughput screening

and require only minimal quantity of drug material. These techniques are based on defined *in vitro* and *in situ* models, which can be readily applied to estimate the permeability of drug candidates through a defined biological barrier, elucidate the transport pathways of drugs, determine the structure-transport relationship, and to determine the most optimal physicochemical characteristics for drug transport. Presented below are some of the models commonly employed in drug absorption screening.

1.4.1. Ussing Chamber

This model was first proposed by Ussing *et al* (1951) as shown in Figure 1.4. Small sections of a tissue are clamped between two compartments. The compound under test is added to one of the compartments called 'donor' chamber. The accumulation of the compound at the other side of the membrane is called 'receiver' chamber. The flux of compound across the tissue is defined as the rate of accumulation normalized for tissue surface area. In most studies, the intestinal tissue is prepared before mounting by stripping off the serosa and the outer musculature. Such stripped tissue is considered desirable for studies designed to determine the mechanism and rate of transport since permeation through the serosa and musculature does not contribute in any significant way to the overall drug bioavailability (Smith *et al*, 1996).

The unique feature of Ussing Chamber is that it allows measurement of the electrical parameters of the tissue throughout the course of the experiment. It is equipped with electrodes and a voltage clamp for monitoring epithelial potential difference (PD), short-circuit current (SCC) and tissue resistance (R). These electrical parameters can be used to verify the viability and integrity of the tissue during the

experiment. To minimize viability problems, experiments should be limited in time. The major drawback of the technique is that the viability of the tissue may be changed during the incubation, as has been observed in some studies (Polentarutti *et al*, 1999). Nevertheless, the technique has proved useful for studying the regional difference in absorption along the gastrointestinal tract (Ungell *et al*, 1998). In terms of utility and functional expression of carrier-mediated transport, the Ussing Chamber was ranked between the Caco-2 model and the single-pass perfusion model (Lennernäs *et al*, 1997).

1.4.2. Cultured Cells

1.4.2.1. Choice of Cells

In vitro intestinal absorption models are polarized systems mimicking the small intestine. Primary cultures of enterocytes have very poor viability and do not form an organized monolayer that will differentiate. The most commonly used cell culture models are derived from immortalized cell lines.

Twenty intestinal adenocarcinoma cell lines have been classified into four types according to their degree of differentiation. **Type 1** cells undergo spontaneous differentiation under normal cell culture conditions, i.e. polarization of the cells with formation of domes and well-developed apical brush borders with several hydrolases. Only one cell line, Caco-2, belongs to this group. **Type 2** cells do not differentiate spontaneously. However, they can be induced to differentiate when the cell culture conditions are altered by replacement of glucose by galactose. The well-characterized cell line HT29 is an example of a type2 cell line. **Type 3** cells are organized into polarized monolayers with formation of domes without differentiation. **Type 4** cells grow in multilayers without any signs of differentiation. Only the cell lines that form polarized monolayers with well-developed barrier properties can be considered in

drug absorption studies. The type 1 cell line Caco-2 is preferred in most cases (Artursson, 1991).

1.4.2.2. Caco-2 Cell Monolayers as *In Vitro* Model

Caco-2 cell line is an immortal cell line derived from a human colon carcinoma and can be grown as a single layer on porous support. Normal intestinal epithelial cells are attached to a basement membrane. Usually, some type of collagen is used to support the attachment. The use of permeable substrata may also be important for the differentiation process. The cells obtain access to nutrients not only from the apical but also from the basolateral side. Caco-2 cells grown on plastic has poorly developed microvilli compared to those grown on filters (Artursson, 1991).

Caco-2 cell lines exhibit structural/morphological as well as biochemical/functional similarities to the small intestinal epithelium (Pinto *et al*, 1983; Hidalgo *et al*, 1989). Morphologically, they resemble small intestine with a well-defined brush border on the apical side, and well-formed tight junctions between the cells. Brush border membrane-associated enzymes such as aminopeptidase, alkaline phosphatase, sucrase and dipeptidyl aminopeptidase are present in the Caco-2 cell monolayers (Pinto *et al*, 1983). The existence of phases I and II metabolizing enzymes, glutathione S-transferase, glucuronidase, and sulfotransferase, in this cell system has been reported (Rosenberg and Leff, 1993; Peters *et al*, 1989; Bjorge *et al*, 1991; Abid *et al*, 1995). Several active transport systems that are located in the intestinal epithelium (e.g. sugars, amino acids, dipeptides, bile acids) are also expressed in Caco-2 cell monolayers (Blais *et al*, 1987; Smith *et al*, 1991; Yoshioka *et al*, 1991; Hu *et al*, 1990; Dantzig *et al*, 1990). Several drug efflux systems are also found in Caco-2 cells, such as P-gp and multi-drug resistant systems (Hosoya *et al*,

1996; Hunter *et al*, 1993).

The Caco-2 cell monolayers model has several advantages. Firstly, it can be used to determine both cellular uptake and transepithelial transport. Secondly, it expresses cell polarity, which makes it possible to determine the directionality of uptake/transport and to elucidate transport mechanisms. Thirdly, the cells are isolated from humans and species-related differences are therefore not a concern. However, the Caco-2 cell model does have certain limitations. The model is devoid of mucin-producing goblet cells, and thus the impact of the mucus layer normally present on the intestinal epithelium cannot be evaluated. The tight junctions in the differentiated Caco-2 cell monolayers are more reflective of those in the colon than in the small intestine, thus affording higher transepithelial resistance than normally found across the small intestinal epithelium (Artursson, 1990).

1.4.2.3. Correlation Between *In Vivo* Absorption and *In Vitro* Permeability Coefficients

The permeability coefficients of drugs measured using the Caco-2 cell monolayer model has been found to correlate well with their absorption in humans (0-100%). The relationship between oral absorption and permeability coefficients is generally sigmoidal in trend. The good correlation and the sigmoidal relationship between *in vitro* permeability coefficients and *in vivo* absorption have been observed for most drugs, irrespective of their modes of transport (i.e. transcellular, paracellular, or carrier-mediated pathway). However, the best correlation was demonstrated for the passively transported drugs (Artursson *et al*, 1996). In addition, while such permeability-absorption correlation has been widely verified in different laboratories, significant variations in the measured permeability coefficients have been found

among the laboratories (Bailey *et al*, 1996). In view of such interlaboratory variations, it is important to validate the *in vitro* Caco-2 cell model by determining the permeability coefficients of a set of known markers for comparison against literature values before applying the model to absorption prediction of the unknown test compounds.

1.4.3. Everted Gut Sacs

The everted gut was first described by Wilson and Wiseman in 1954 (Wilson and Wiseman, 1954). In the everted gut sac method, the mucosa becomes the outer side of the sac and is in contact with the incubation medium. The sac is filled with buffer and immersed in a flask filled with oxygenated (95:5 CO₂:O₂) buffer containing the compound under investigation. At the end of the experiment, the sac is cut opened at one end, and the serosal fluid is collected. Viability of the sac can be monitored during the experiment by measuring the transport of a marker. This method is an inexpensive and relatively simple technique. By preparing the segment from different parts of the intestine, the absorption from different sites can be compared. However, the serosal compartment is a closed compartment, which may distort the transport kinetics of the drug upon prolonged incubation or if the drug is very rapidly absorbed (Barthe *et al*, 1999).

1.4.4. Brush Border Membrane Vesicles (BBMVs)

This model has been well validated and widely used to study glucose transport for several years (Hopfer *et al*, 1973; Kessler *et al*, 1978). In this approach, frozen small intestine of rabbit was treated by CaCl₂ precipitation followed by centrifugation. The final pellet contains the luminal wall-bound proteins and phospholipids, which

contain most of the enzymatic and carrier activities of the brush border, such as Na⁺-glucose cotransporter SGLT1 (Hopfer *et al*, 1973).

In order to investigate the possible interaction of selected quercetin glycosides with sugar transporter SGLT1, BBMVs were employed in the present study. Uptake of D-glucose into BBMVs was used as control and compared with uptake of D-glucose in the presence of selected glycosides.

Compared with other *in vitro* models, BBMVs mainly contain the brush border components, typically only the apical transcellular transporters and enzymes. Therefore, BBMVs are more suitable for studying glucose transport. The major drawbacks with this approach are that radio-labeled compound need be used for improving the sensitivity of analysis and the technique is subject to day-to-day variation in BBMVs preparation (Tukker, 2000).

1.4.5. *In situ* Experiments

In situ experiments for studying intestinal drug uptake was first introduced in the late 1960s. Segments of the intestine of anesthetized animals are cannulated and perfused by a solution of the drug. Input of the drug compound can be closely controlled in terms of concentration, pH, osmolality, intestinal region, and flow rate. The technique is the nearest to the *in vivo* system and is good for generating kinetic data. However, being a perfusion system, it affords no information on the events at the cellular membrane level. Another disadvantage of this model is that it consumes more animals than the other *in vitro* models. Moreover, surgical manipulation and anesthesia decrease the intestinal blood flow and may affect the intestinal absorption (Barthe *et al*, 1999).

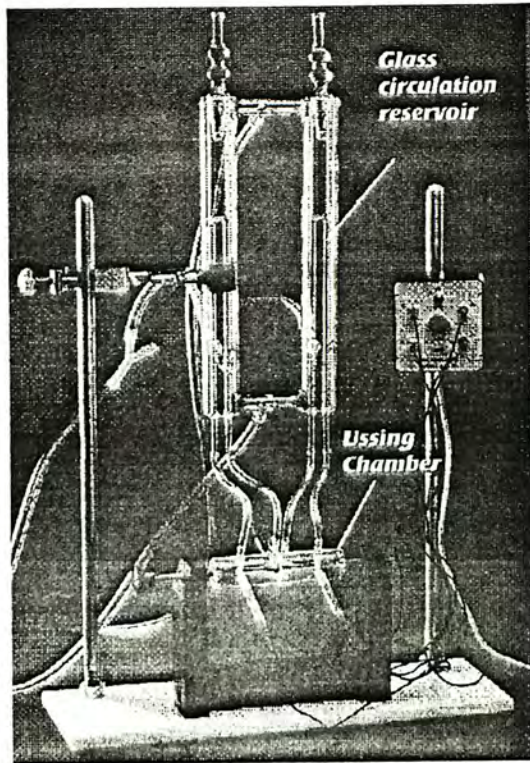


Fig. 1.4 Ussing Chamber

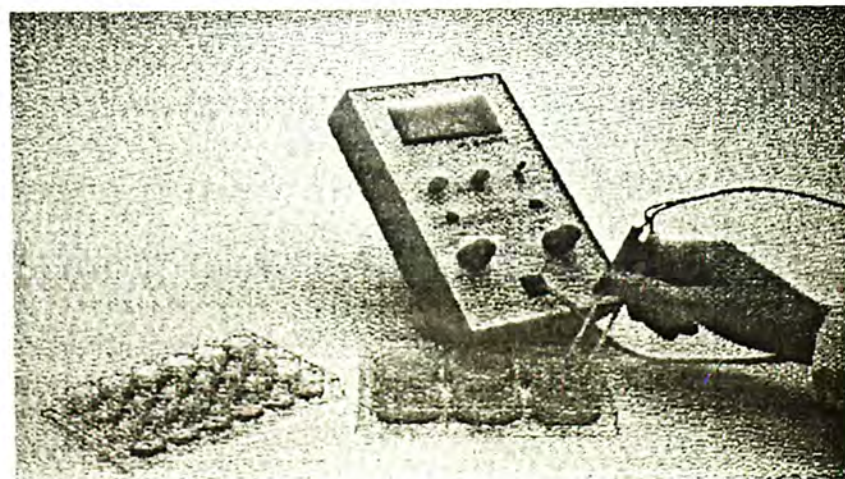
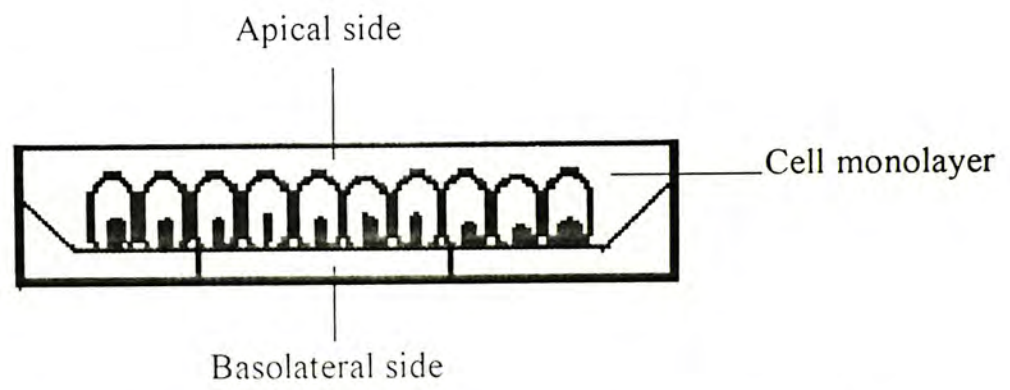
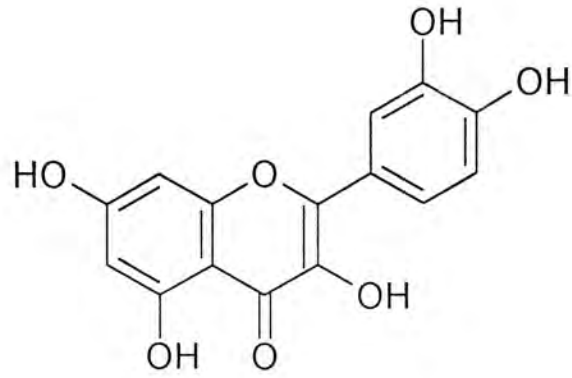


Fig. 1.5. Caco-2 cell monolayers

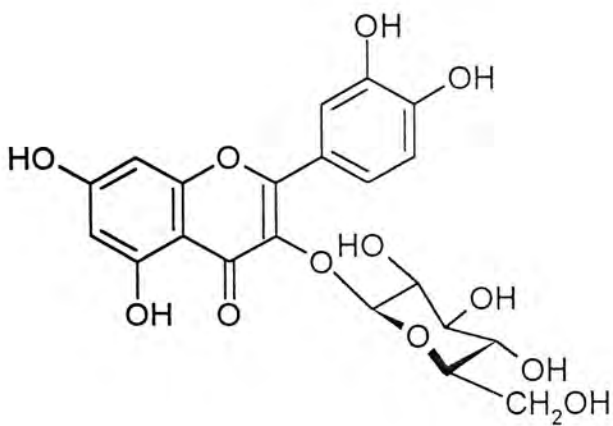
1.5. Aims and Scope of Study

In view of the potential beneficial effects of quercetin flavonoids for certain diseases (e.g. cancer, cardiovascular diseases) and the relative dearth of information on the oral absorption of these compounds, the present project aimed to elucidate the absorption mechanism(s) of quercetin, and in particular, the impact of the sugar substituents on the absorption of quercetin with a view to developing formulation strategies to improve its oral absorption. To this end, quercetin and four related glycosides, *viz* quercetin-3-glucoside, quercetin-3-galactose, quercetin-3-rutinoside and quercetin-3-rhamnoside (Fig. 1.2), were investigated for their intestinal transport characteristics using well-established *in vitro* models. Additionally, potential absorption-limiting factors including chemical instability, efflux effect and gut metabolism have also been examined. The specific objectives of the present thesis were as follows:

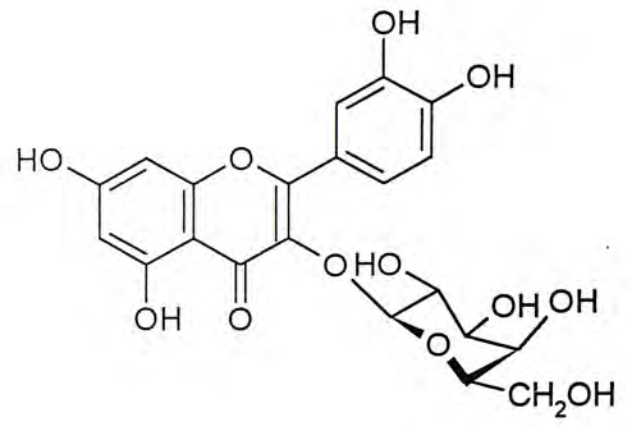
- 1) to conduct (preformulation) characterization studies on quercetin and four related glycosides, including thermal analysis, partition coefficient and aqueous solubility measurements, and stability assessment in water at different pHs;
- 2) to investigate the transport mechanisms of quercetin and its glycosides using validated *in vitro* Caco-2 cell monolayer model;
- 3) to examine the possible involvement of glucose transporters in the intestinal transport of quercetin glucoside using isolated brush border membrane vesicles from the small intestine of rabbit.



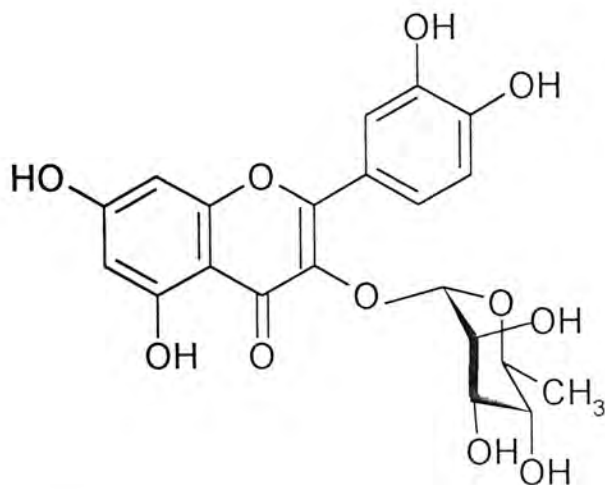
Quercetin



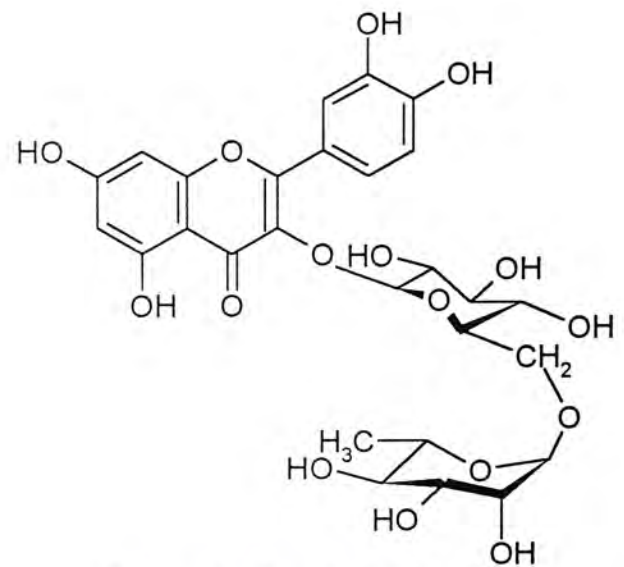
Quercetin-3-glucoside



Quercetin-3-galactoside



Quercetin-3-rhamnoside



Quercetin-3-rutinoside

Fig. 1.4. Structures of quercetin and related glycosides

CHAPTER 2.
MATERIALS & METHODS

2.1. Materials

2.1.1. Chemicals

All solvents and chemicals used were of HPLC and analytical grade respectively unless otherwise specified.

Studied compounds:

Quercetin (purity > 98%), quercetin-3-rutinoside (purity > 95%), quercetin-3-rhamnoside (purity > 89%) and fisetin (purity > 99%) were purchased from Sigma (USA). Quercetin-3-glucoside and quercetin-3-galatoside were supplied by Carl Roth (Germany).

Marker compounds:

Lucifer yellow, atenolol, phloridzin, verapamil hydrochloride were obtained from Sigma. [³H]-D-glucose (1mCi/ml) was purchased from Amersham Life Science (UK). [³H]-polyethylene glycol-4000 (250 μCi), [³H]-mannitol (250 μCi) were purchased from NEN Life Science Product, Inc. (USA).

Media for cell culture:

DMEM (Gibco12430-054), FBS (Qualified), trypsin-EDTA (0.05% in 0.53mM EDTA), Penicillin-Streptomycin, L-glutamine and non-essential amino acids were obtained from GibcoBRL, Life & Technologies (USA).

Collagen type I (from rat tail), sterile DMSO and sodium pyruvate was supplied by Sigma.

Buffers for *in vitro* studies:

KH buffer (pH 7.4) was prepared by mixing 100 ml 1.17 M sodium chloride (B.P. grade), 100 ml 0.248 M sodium bicarbonate (B.P. grade), 10 ml 0.47 M potassium chloride, 12 ml 100 mM magnesium chloride hexahydrate, 10 ml 120 mM potassium dihydrogen phosphate, 10 ml 0.256 M calcium chloride dihydrate and 2 g D-glucose (B.P. grade) with water to the final volume of 1 L. All water used was freshly distilled, de-ionized and filtered.

PBS⁺ buffer was prepared by dissolving 1 tablet of phosphate buffered saline tablets (Sigma) containing 0.01 M phosphate buffer, 0.0027 M potassium chloride and 0.137 M sodium chloride, pH 7.4 in 200 ml water. Then calcium chloride and magnesium chloride were added to a final concentration of 0.9 mM and 0.4 mM respectively.

Other chemicals:

β -Glucuronidase was purchased from Sigma. It was diluted with 1 M sodium acetate (pH 5.0) to 5×10^6 U/l.

Dimethyl sulfoxide, bovine serum albumin and folin-cicalteu's reagent were obtained from Sigma. Octan-1-ol was obtained from BDH (England).

2.1.2. Materials for Cell Culture

Caco-2 cells were obtained from the American Type Culture Collection (USA) Centrifuge tube, tissue culture flask, filters (0.22 μ m) were purchased from Iwaki (Japan). Six-well transwell[®] plate (0.4 μ m pore size, 4.71 cm², polycarbonate filter, Costar 3410), six-well transwell[®] plate (0.4 μ m pore size, 4.71 cm² collagen coated PTFE filter, Costar 3491) and pipette (5 ml) were purchased from Corning Costar

Corp. (USA).

MF-Millipore membrane filters (mixed cellulose acetate and cellulose nitrate, 0.45 μm pore size) used in BBMV studies were purchased from Millipore, Inc. (USA).

2.1.3. Instruments

The HPLC column employed was a reversed phase C_{18} column (4.6 \times 250mm, particle size 5 μm) connected with an ODS guard column (Alltech Associates, Inc., USA). The HPLC system consisted of Waters 2690 separations module, Waters 996 photodiode array detector and Waters 464 pulsed electrochemical detector.

Mass spectrometry was performed on API 2000 Triple Quadrupole LC/MS/MS spectrometer (USA).

UV absorption was measured by Spectronic[®] Genesys[™] 5 spectrophotometer. Fluorescence was measured by fluorescence spectrophotometer (Model F2000, Hitachi, Japan).

The radioactive samples were counted in low activity liquid scintillation counter (LS2900TR and LS6000).

All electrical measurements on the tissues were taken using multi-channel voltage/current clamp, voltage/current electrode and epithelial voltohmmeter supplied by World Precision Instruments, Inc. (USA).

2.1.4. Animals

Male Sprague-Dawley rat (220-250 g) and white New Zealand rabbit were bred at and supplied by the laboratory Animal Service Center at the Chinese University of Hong Kong. Animals were allowed free access to food and water before sacrifice.

2.2. Methods

2.2.1. Preformulation Characterization of Selected Flavonoids

2.2.1.1. Determination of Stability

100 μM quercetin glycosides and 15 μM quercetin were prepared in PBS buffer (pH 7.4 or 6.8, DMSO < 0.5%) or simulated gastric fluid, TS (pH 1.2, USP24). They were incubated at 37 °C with agitation and collected at different time points for 4 hours. Collected samples were analyzed by HPLC.

10 $\mu\text{g/ml}$ quercetin (in 10% methanol) dissolved in PBS buffer (pH 6.8) was incubated at 37 °C with shaking. Sample collected at 2, 5, 20, 25, 80 hours were analyzed by HPLC-MS for the degradation products of quercetin.

2.2.1.2. Thermal Analysis

Thermogravimetric analysis (TGA) was performed in an open pan using a Perkin Elmer Thermogravimetric Analyzer TGA 7 with Thermal Analysis Controller TAC 7/DX (Perkin Elmer, CT, USA).

Differential Scanning Calorimetry (DSC) profiles were generated using a Perkin Elmer Pyris 1 differential scanning calorimeter (with Pyris Manager software) (Perkin Elmer, CT, USA). Indium ($T_m = 156.6$ °C; $\Delta H_f = 28.45$ J g⁻¹) was used for routine calibration. Samples were placed in pin-hole pans. Scanning speed at 20 °C min⁻¹ was employed.

2.2.1.3. Determination of Solubility

Excess amounts of quercetin glycosides were placed in PBS buffer (pH 7.4). The suspensions were equilibrated at different temperatures over night. The equilibrated sample was centrifuged at 13000 rpm for 5 minutes and the supernatant was assayed by

UV spectrophotometry at 360 nm.

2.2.1.4. Determination of Partition Coefficient

Small amounts of quercetin-3-rutinoside, quercetin-3-glucoside, quercetin-3-rhamnoside and quercetin-3-galactoside were added in PBS buffer (pH 7.4, pre-saturated with n-octanol) as stock solution. The stock solution was centrifuged at 4000 rpm for 5 minutes. Concentration of the supernatant (C_1) was measured by UV at 360 nm. The supernatant (V_1) was mixed with n-octanol (V_2) pre-saturated with PBS and shaken up and down at room temperature. After equilibration for 20 minutes, the aqueous phase sample was collected and centrifuged at 2500 rpm for 3 minutes. The concentration of the aqueous phase (C_2) was measured by UV at 360 nm except for quercetin-3-rhamnoside, whose concentration of the aqueous phase was measured by HPLC at λ_{\max} 360 nm.

Partition coefficient was calculated by the following equation (Martin *et al*, 1983).

$$\text{Log } P = \log [(V_1/V_2) \times (C_1 - C_2)/C_2].$$

2.2.2. Validation of *in vitro* models

2.2.2.1. Ussing Chamber

2.2.2.1.1. Tissue Preparation

For preparation of the tissue segment, ileum from the anesthetized rat was rapidly removed, washed with cold KH solution and put into beakers with KH solution on ice. The ileum was allowed to rest for approximately 30 minutes for lowering the tissue temperature before further treatment to minimize tissue damage during preparation. Ileum was cut into 2 cm pieces along their mesenteric border and the serosa were removed using blunt dissection under microscope. Care was taken to avoid taking segment of the Peyers patches (Polentarutti *et al*, 1999). During preparation, the tissue was submerged in

ice-cold KH solution bubbled with gas mixture O₂/CO₂ (95:5).

The stripped tissues were mounted in Ussing Chamber over a surface area of 0.636 cm². 10 ml of KH solution was added to each compartment of the Ussing Chamber and the solutions were bubbled as before. The chambers were kept at 37 °C by means of a thermostatic water circulator. Prior to each experiment, the electrical parameters of the tissue were allowed to stabilize for 30-40 minutes to permit recovery of the tissue from the preparation and to attain equilibrium at 37 °C.

2.2.2.1.2. Electrical Measurements

The following electrical parameters were recorded during the experiment using four channels Voltage Clamp (WPI): potential difference (PD) which reflects the voltage gradient generated by the tissue; resistance (R) which reflects the tissue integrity, and short-circuit current (SCC) which indicates the ionic fluxes across the epithelium. Electrical parameters are widely accepted for monitoring the viability and integrity of the tissue for the Ussing Chamber technique.

Potential difference of ileum prepared above was measured before each experiment, any ileum with PD < 4mV was omitted (Polentarutti *et al*, 1999).

2.2.2.1.3. Experimental Protocols

After the equilibration period, the compound to be studied was added to the apical or basolateral side called donor chamber; the other side is the receiver chamber. At 0, 15, 30, 60, 90, 120 minutes, the samples (1 ml) were removed from the receiver chamber. Following removal of each sample, the same volume of a blank buffer was added back to the same chamber to maintain the volume constant. Concentrations of the markers were measured by fluorescence spectrophotometry, HPLC or scintillation counting, depending

on the markers.

2.2.2.1.4. Calculation of Permeability

The apparent permeability coefficient was calculated from the following equation.

$P_{app} = [dC/dt \times V] / (A \times C)$, where dC/dt is the change in concentration in the receiver chamber per unit time, V is the receiver volume and A is the area available for diffusion or transport, C is the initial concentration of the donor chamber (Smith *et al*, 1996)

2.2.2.2. Caco-2 Cell Monolayers

2.2.2.2.1. Preparation of Caco-2 Cell Monolayers

Caco-2 cells were maintained at 37 °C in Dulbecco's modified Eagle's medium, containing 10% fetal bovine serum, 1 % nonessential amino acids, 1 % L-glutamine in an atmosphere of 5 % CO₂ and 95 % relative humidity. Cells grown in 75 cm² flasks were passaged every 4 days at 80 %-90 % confluence and the cells detached by using 0.05 % trypsin-0.53 mM EDTA. Cells were seeded at a density of 3×10^5 cells/well in Transwell[®] inserts previously coated with a thin collagen layer and dried for at least 5 hours (Hidalgo *et al*, 1989). The medium (1.5 ml in the apical side and 2.6ml in the basolateral side) was changed every other day.

2.2.2.2.2. Validation of Caco-2 Cell Monolayers

Integrity of the Monolayers:

In the validation experiments, monolayers' integrity was determined by measuring the transepithelial electrical resistance (TEER) using an epithelial voltohmmeter, and by following the transepithelial transport of poorly absorbed markers, mannitol and lucifer yellow. The potential difference was expressed as TEER (ohms.cm²), after subtraction of

the intrinsic resistance of the cell-free inserts. A monolayer with a low TEER, or with a high transport rate with mannitol or lucifer yellow, was assumed to exhibit extensive leakage in the monolayer and was discarded (Grès *et al*, 1998). Transport studies on the selected flavonoids used TEER to monitor the integrity of the monolayers.

PBS⁺ was used as transport buffer involved calcium ions to maintain the integrity of the tight junction between the cells.

Permeabilities of marker compounds:

Caco-2 cells grown in Transwell[®] insert for 3 weeks were used for all transport studies. Complete culture medium was removed from both the apical and basolateral sides and the monolayers were washed twice with transport buffer. Marker compounds dissolved in PBS⁺ were added on apical or basolateral side called the donor side, then the samples (1ml) at the other side, i.e. the receiver side, was collected at regular time intervals for 2 hours. The same volume of the blank PBS⁺ was added back to the same compartment to maintain the volume constant.

Marker compounds were analyzed by fluorescence spectrophotometry, HPLC or scintillation counting as before.

Validation of sodium/glucose co-transporter (SGLT1):

1.5 ml 100 μ M D-glucose containing 0.5 μ Ci [³H]-D-glucose was added on apical side of the Caco-2 cell monolayers. Transport studies were performed as above. The Caco-2 cell monolayers were rinsed with PBS⁺ and residual buffer removed by turning the Transwell insert over. The whole filter was cut from the insert and put into a mini-vial for scintillation counting.

For inhibition of SGLT1, 100 μ M phloridzin was preloaded on both sides of

Caco-2 cell monolayers for 20 minutes, then removed from apical side. 100 μM phloridzin with 1.5 ml 100 μM D-glucose were added together to the apical side. Transport studies were carried out as mentioned above.

2.2.2.2.3. Calculation of Permeability

The apparent permeability coefficient (P_{app}) was calculated from the following equation: $P_{\text{app}} = [(dC/dt) \times V] / (A \times C)$, where dC/dt is the change in concentration in the receiver side per unit time, V is the receiver volume and A is the area available for diffusion or transport. C is the initial concentration of the compound on the donor side.

2.2.3. Transport Studies of Selected Flavonoids

Direction of Transport:

20 mM quercetin glycosides (or 5 mM quercetin) were dissolved in DMSO as stock solution and diluted with PBS⁺ to 50 μM (or 12.5 μM). Flavonoid in the transport buffer was applied to either the apical or the basolateral side of Caco-2 cell monolayers. Samples were collected as described previously in 2 hours and analyzed by HPLC. At the end of the experiments, 100 μl sample was removed from the donor side.

Recovery was defined as the percentage of total amount of the flavonoids found on donor and receiver side at the end of the experiments.

Concentration dependence:

Transport experiments were performed from apical to basolateral side and from basolateral to apical side for quercetin-3-glucoside at 25, 30, 50 and 100 μM .

Inhibition of P-gp with verapamil:

100 μM verapamil was added to both sides and preloaded for 20 minutes, followed by the addition of 30 μM quercetin-3-glucoside to the donor side. Then transport experiments were conducted as mentioned above.

Enzymatic hydrolysis:

12.5 μM quercetin was added on apical side, and transport experiments were conducted as mentioned above. Samples containing glucuronides collected from basolateral side of Caco-2 cell monolayers was hydrolyzed by β -Glucuronidase.

Studies of quercetin-3-glucoside with sugar transporters:

100 μM phloridzin was added to both sides and preloaded for 20 minutes. Then it was added with 100 μM quercetin-3-glucoside to the apical side. Then transport experiments were conducted as mentioned above.

2.2.4 Brush Border Membrane Vesicles (BBMVs)

2.2.4.1 Preparation of BBMVs

Brush border membrane vesicles were prepared from the tips of the microvilli of the frozen rabbit small intestine. Frozen rabbit intestine were prepared as in Fig. 2.1. BBMVs were prepared using the Mg^{2+} precipitation method (Hopfer *et al*, 1973) as outlined in Fig. 2.2.

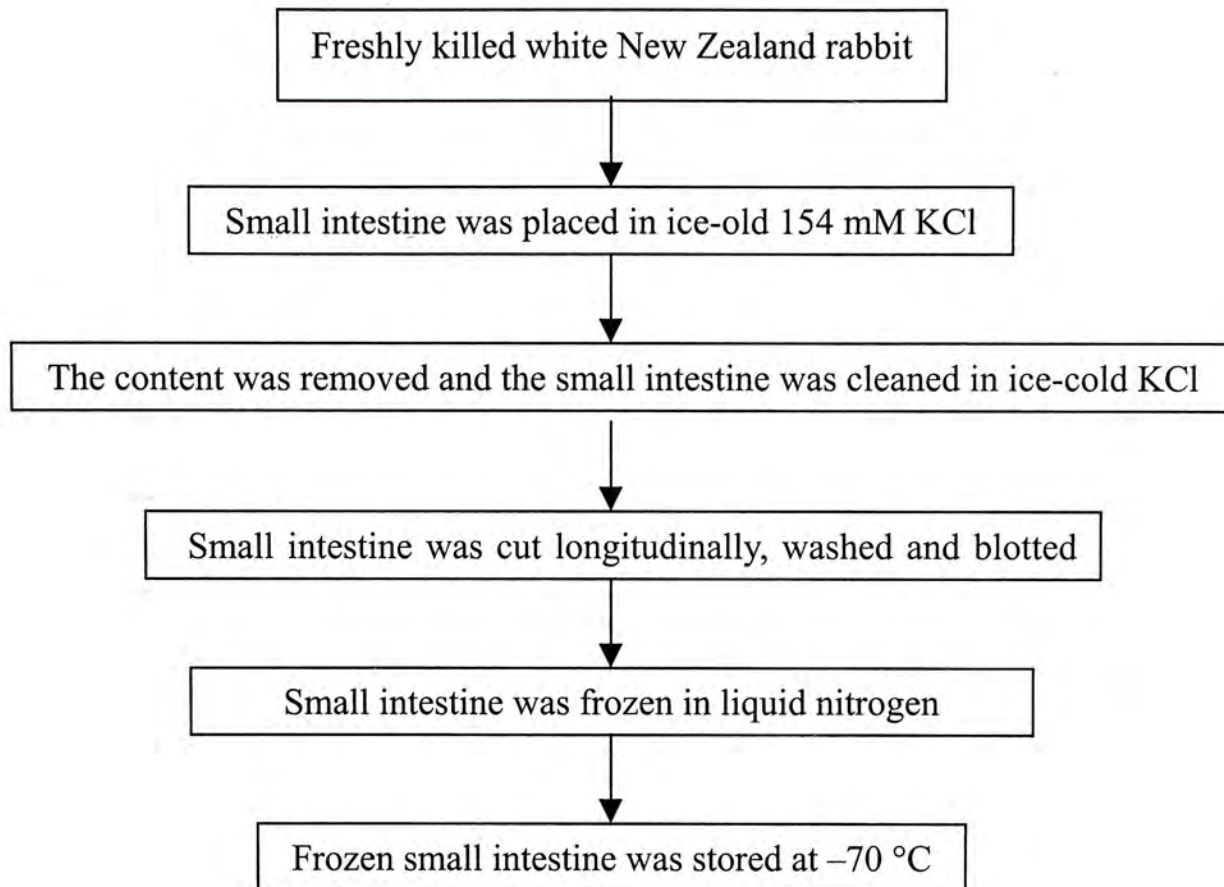


Fig. 2.1. Preparation of frozen rabbit small intestine

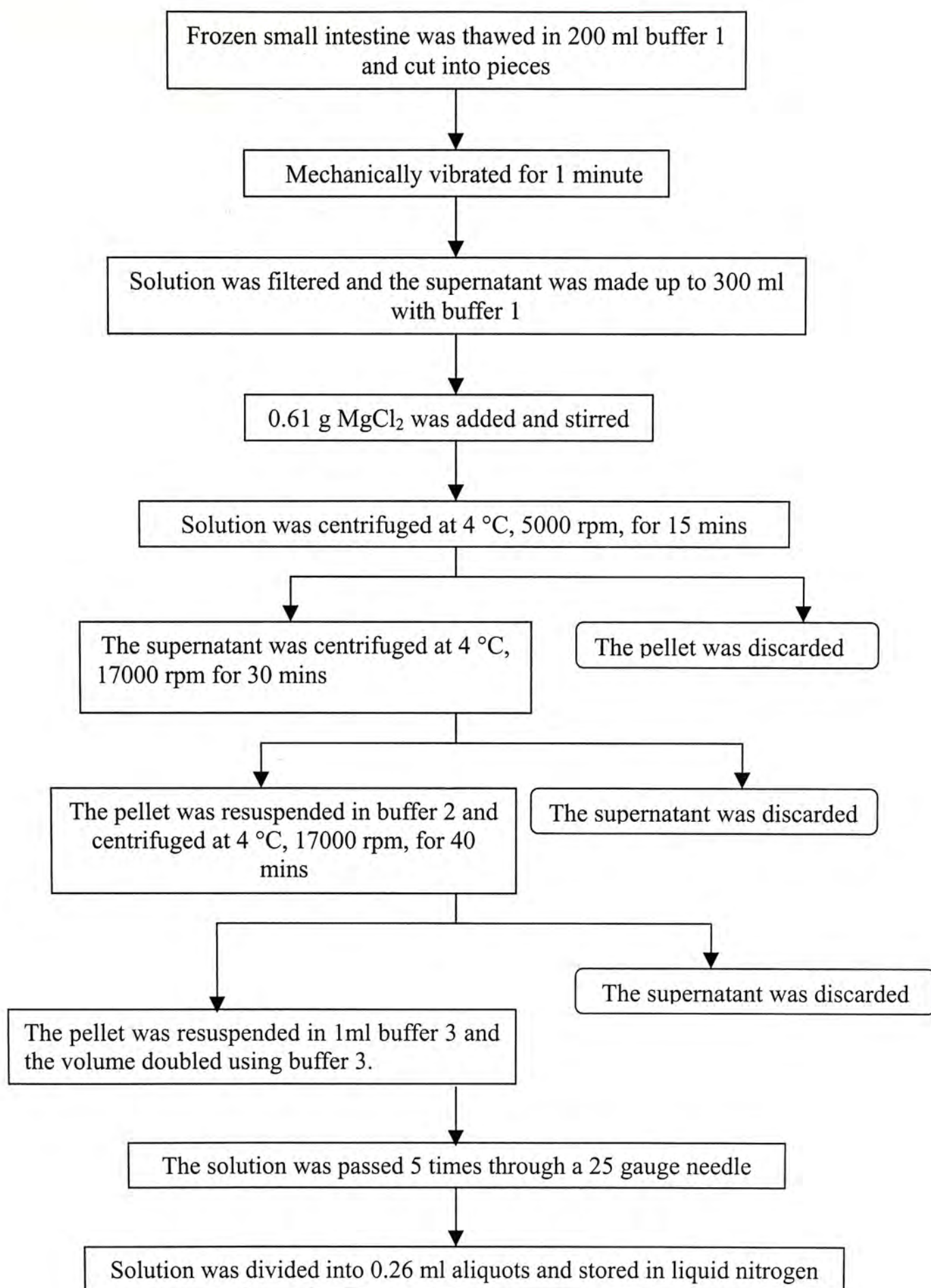


Fig. 2.2. Preparation of BBMVs from frozen small intestine

2.2.4.2. Uptake of D-glucose by BBMVs

The uptake of D-glucose into BBMVs was performed according to the rapid filtration technique of Hopfer *et al* (1973) as shown in Figure 2.3.

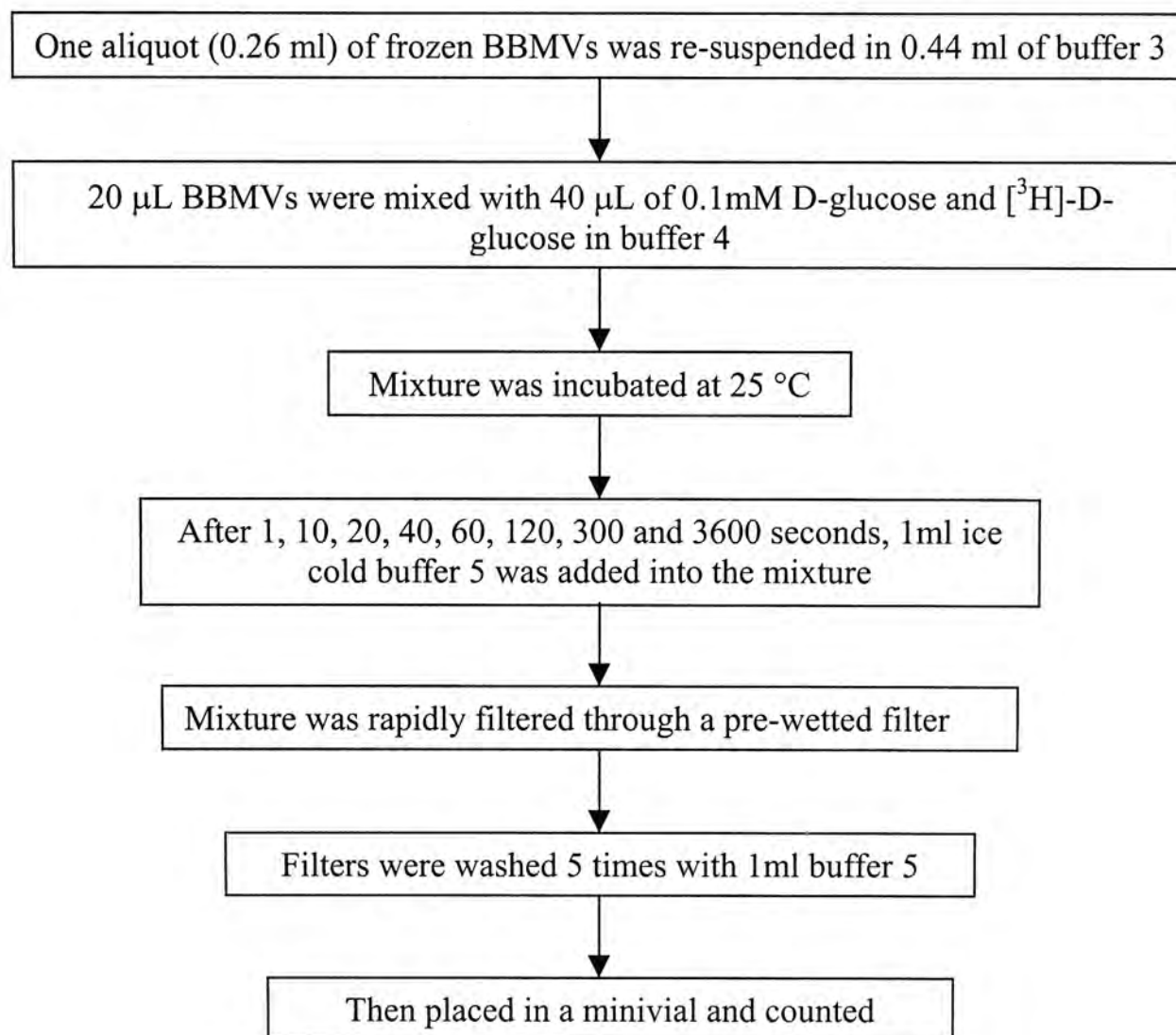


Fig. 2.3. Procedure of uptake of D-glucose into BBMVs

Buffer 1: 10mM mannitol, 2mM HEPES adjust with Tris to pH 7.1

Buffer 2: 100mM mannitol, 0.1mM MgSO₄, 2mM HEPES adjust with Tris to pH 7.4

Buffer 3: 300mM mannitol, 0.1mM MgSO₄, 10mM HEPES adjust with Tris to pH 7.4

Buffer 4: 100 mM NaCl, 100 mM mannitol, 10 mM HEPES-Tris, pH 7.4

Buffer 5: 200 mM NaCl, 10 mM HEPES-Tris, 250 µM phlorizin, pH 7.4

HEPES = N-2-Hydroxyethylpiperazine-N'-2-ethanesulphonic acid

Tris = 2-amino-(hydroxymethyl)propane-1,3-diol

The procedure for measuring the uptake of D-glucose by BBMV's in the presence of quercetin-3-glucoside/quercetin-3-galactoside was the same as above except for incubation of the added flavonoid glycoside (0.05 mM, 0.1 mM or 0.02 mM) together with 0.1 mM D-glucose with BBMV's. The uptake of D-glucose by BBMV's was calculated as before. The control incubation was performed without the quercetin glycosides.

2.2.4.3. Counting on ³H-D-glucose in BBMV's

The filters with the BBMV's were each placed in a minivial containing 3 ml scintillation fluid and were counted for 3 minutes.

2.2.4.4. Calculation of Glucose Uptake

Glucose uptake was expressed as picomoles (pmoles, 10⁻¹²) of glucose/mg protein using the following equation:

Glucose uptake =

$$\frac{\text{corrected cpm} \times \text{amount of glucose added (pmoles)}}{\text{mean cpm for control samples} \times \text{protein concentration of BBMV} \times \text{volume of BBMV(ml)}}$$

Note:

Corrected cpm (counts per minute) = actual measured value – value for non-specific binding to filter.

(Non-specific binding to the filter was measured by control incubation containing 40 µl of 0.1 mM D-glucose without BBMV).

Mean control cpm = total activity (the activity of 40 µl 0.1mM radiolabelled D-glucose)

2.2.4.5. Total Protein Assay

Preparation of BBMV test samples:

One aliquot (0.26 ml) of frozen BBMVs was re-suspended in 0.44 ml of water. Three dilutions (using water) were made for the assay: 1 in 10; 1 in 20 and 1 in 50 dilutions

Preparation of protein assay agent

Buffer1 was prepared by mixing 4 % sodium carbonate (Na_2CO_3) with 0.2 M sodium hydroxide (NaOH), (1:1 v/v).

Buffer2 was prepared by mixing 1 % copper sulphate pentahydrate ($\text{CuSO}_4 \cdot 5\text{H}_2\text{O}$) with 1 % sodium tartrate ($\text{Na}_2\text{C}_4\text{H}_4\text{O}_6$), (1:1 v/v).

Bovine serum albumin (BSA) was prepared to 1mg/ml.

Protein assay

Lowry method was used for total protein determination (Lowry *et al*, 1951). BSA was used as standard protein solution. For the calibration curve, 0 - 500 μl BSA (1mg/ml), were made up to the final volume of 500 μl with water. 2.5 ml mixture (buffer 1: buffer 2 = 50:1) was then added into to the above BSA solution and shaken for 10 minutes. Then 0.25 ml Folin-ciocalteu's phenol reagent was added and agitated for 30 minutes. All samples were measured at 750 nm by visible spectrometry. The same assay procedure was used for the BBMV test samples. The protein concentration of BBMV was calculated by taking the mean of the three results obtained from the 3 dilutions. The protein assay was carried out for each batch of BBMVs.

2.2.5. Analytical Methods

2.2.5.1. HPLC Analysis

2.2.5.1.1. HPLC Analysis of Quercetin and Related Glycosides

The mobile phase for HPLC analysis consisted of two solvent compositions: acetonitrile (solvent A) and 25 mM phosphate buffer (solvent B) adjusted to pH 2.4 by concentrated phosphate acid (Hertog *et al*, 1992). The mobile phase at a flow rate of 1.0 ml/min was composed of 30 % A and 70 % B for quercetin and 25 % A and 75 % B for quercetin glycoside with UV detection at 360 nm or electrochemical detection at 800 mV.

At the end of the transport experiments with quercetin, 100 µl sample was mixed with 25 µl 1 M sodium acetate (pH 5.0), 25 µl β-glucuronidase (5×10^6 U/l, pH 5.0) and incubated in a mini-vial for 30 minutes at 37 °C. Then 50 µl 400 ng/ml fistin (dissolved in methanol) as internal stand and 25 µl (20%, pH 2.15) ascorbic acid were added to the sample (Nielsen *et al*, 1998). The sample was centrifuged at 13000 rpm for 10 minutes and analyzed by HPLC.

2.2.5.1.2. HPLC-MS Analysis of Quercetin Degradation Products

Degraded samples were injected into RP C₁₈ column with a mobile phase composed of acetonitrile (solvent A) and 2 mM ammonium formate adjusted to pH 3.0 with formic acid (solvent B). Gradient elution was carried out according to the following program: solvent A was kept at 10% in the first 5 minutes, then increased from 10 to 40% from 5 to 20 minutes, and then decreased back to 10% in 10 minutes. The flow rate was 1 ml/min. The eluent was monitored by UV detection (220-400 nm) to obtain the UV scan of each degradation products and by electrochemical detection at 800 mV.

Mass Spectrum (MS) was carried out in the negative (degradation product 1 and 2) and positive (degradation product 3) mode with electrospray ionization, by scanning from 80-305 amu to obtain molecular weight information.

2.2.5.1.3. HPLC Analysis of Propranolol

The mobile phase for HPLC analysis consisted of two solvent compositions: acetonitrile (solvent A) and 50 mM phosphate buffer adjusted to pH 3.0 by concentrated phosphoric acid (solvent B). The mobile phase at a flow rate of 1.0 ml/min consisted of 30 % A and 70 % B with UV detection set at 230 nm.

2.2.5.2. UV Analysis

The concentration of quercetin glycoside for the solubility studies was measured by UV spectrophotometry at 360 nm.

2.2.5.3. Fluorescence Analysis

Samples of atenolol was measured by fluorescence spectrometry at excitation (E_x) 259 nm and emission (E_m) 600 nm. Lucifer yellow was measured at 424 nm (E_x) and 525 nm (E_m) (Reardon *et al*, 1993).

2.2.5.4. Analysis of Radio-labeled Markers

^3H -labeled D-glucose, PEG-4000, L-leucine and mannitol were counted by scintillation counter.

2.2.6. Statistical Analysis

All experiments were done in at least triplicate and data were expressed as mean

\pm standard deviation. The difference between mean values were analyzed using the Student t-test. A minimum p value of 0.05 was used as significance level for t-tests.

CHAPTER 3.
RESULTS & DISCUSSIONS

3.1. Preformulation Studies on Selected Flavonoids

3.1.1. Stability

The chemical degradation of flavonoids was studied at 37 °C in PBS buffer with pH adjusted to 7.4 and 6.8, and in simulated gastric fluid (pH 1.2), which mimic the pH condition of the plasma, intestine and stomach respectively, (Fig.3.1a-e.). All the flavonoids except for the aglycone quercetin, were relatively stable under the above conditions. The percentages of flavonoids remaining after incubation were above 90%.

These results suggest that substitution of the OH group at position 3 of quercetin by a sugar moiety enhances the chemical stability of quercetin.

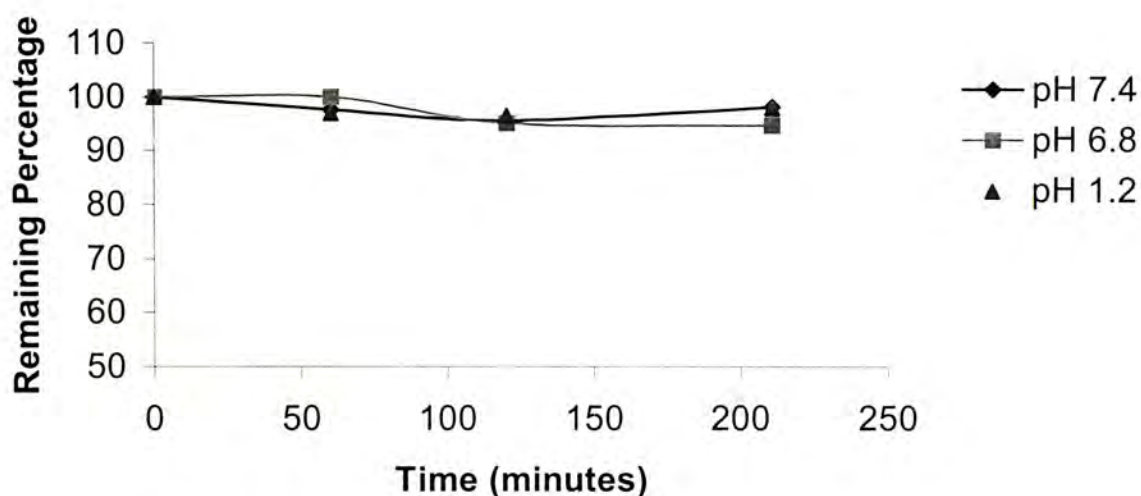


Fig. 3.1a. Stability of quercetin-3-galactoside at pH 7.4, 6.8 and 1.2 in aqueous solutions at 37 °C.

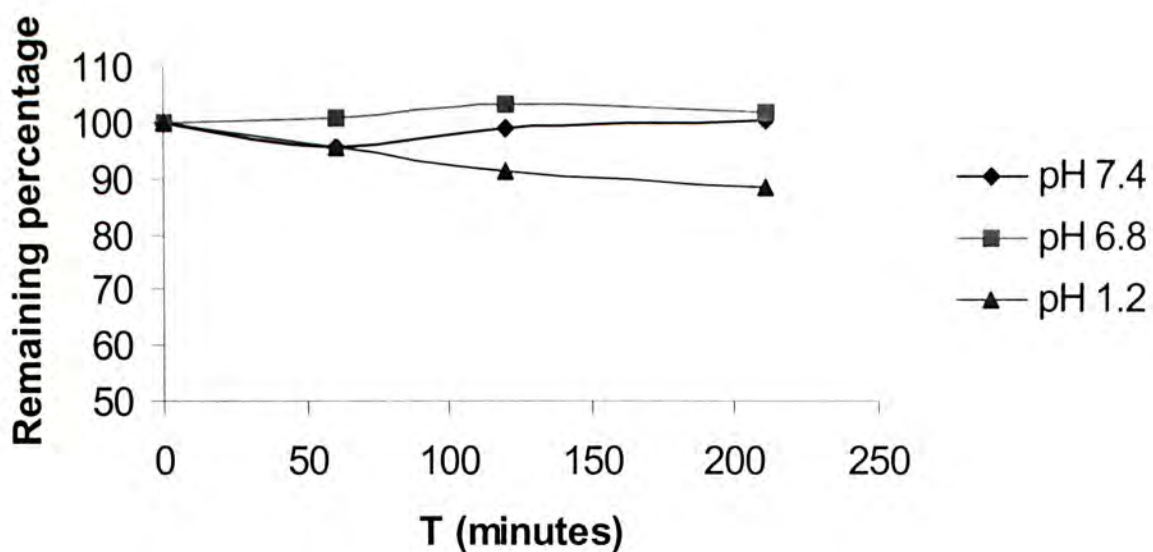


Fig. 3.1b. Stability of quercetin-3-glucoside at pH 7.4, 6.8 and 1.2 in aqueous solution at 37 °C.

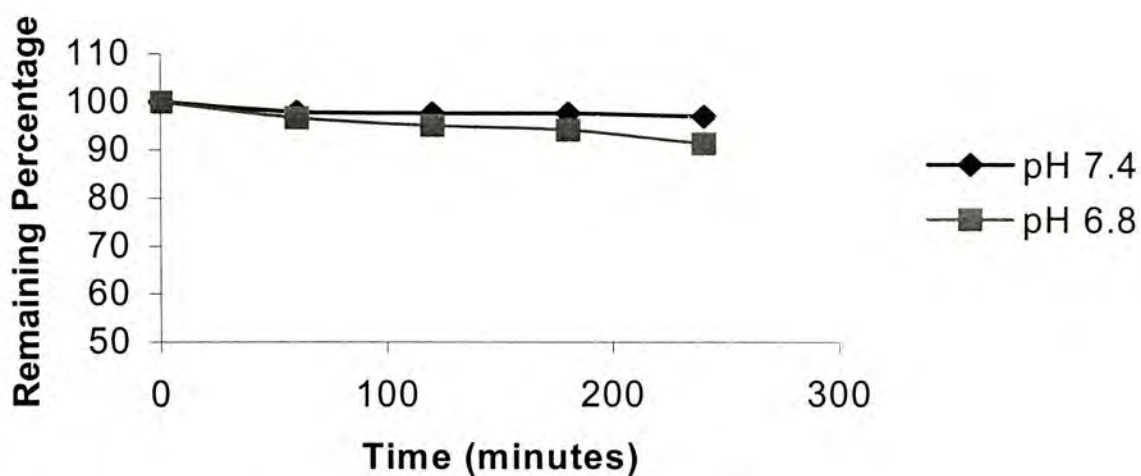


Fig. 3.1c. Stability of quercetin-3-rutinoside at pH 7.4, 6.8 in aqueous solutions at 37 °C.

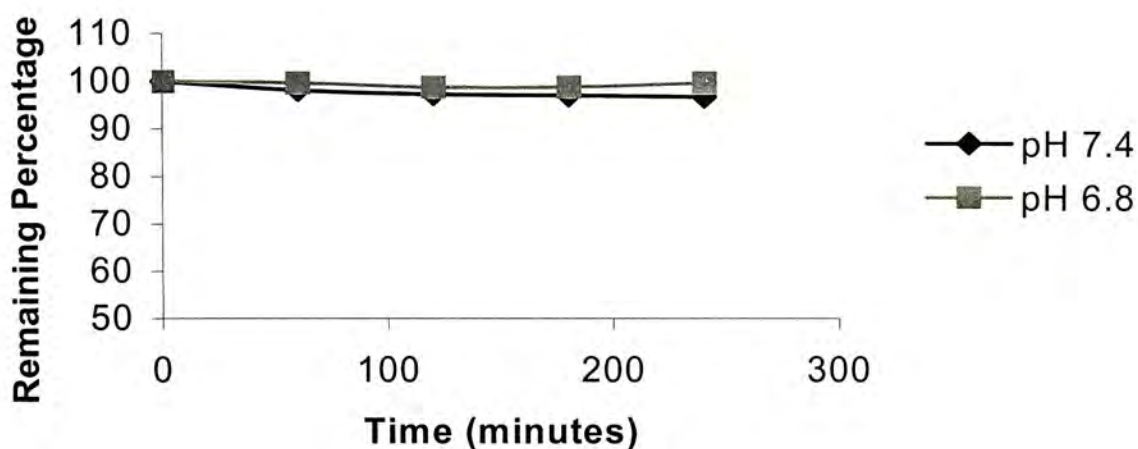
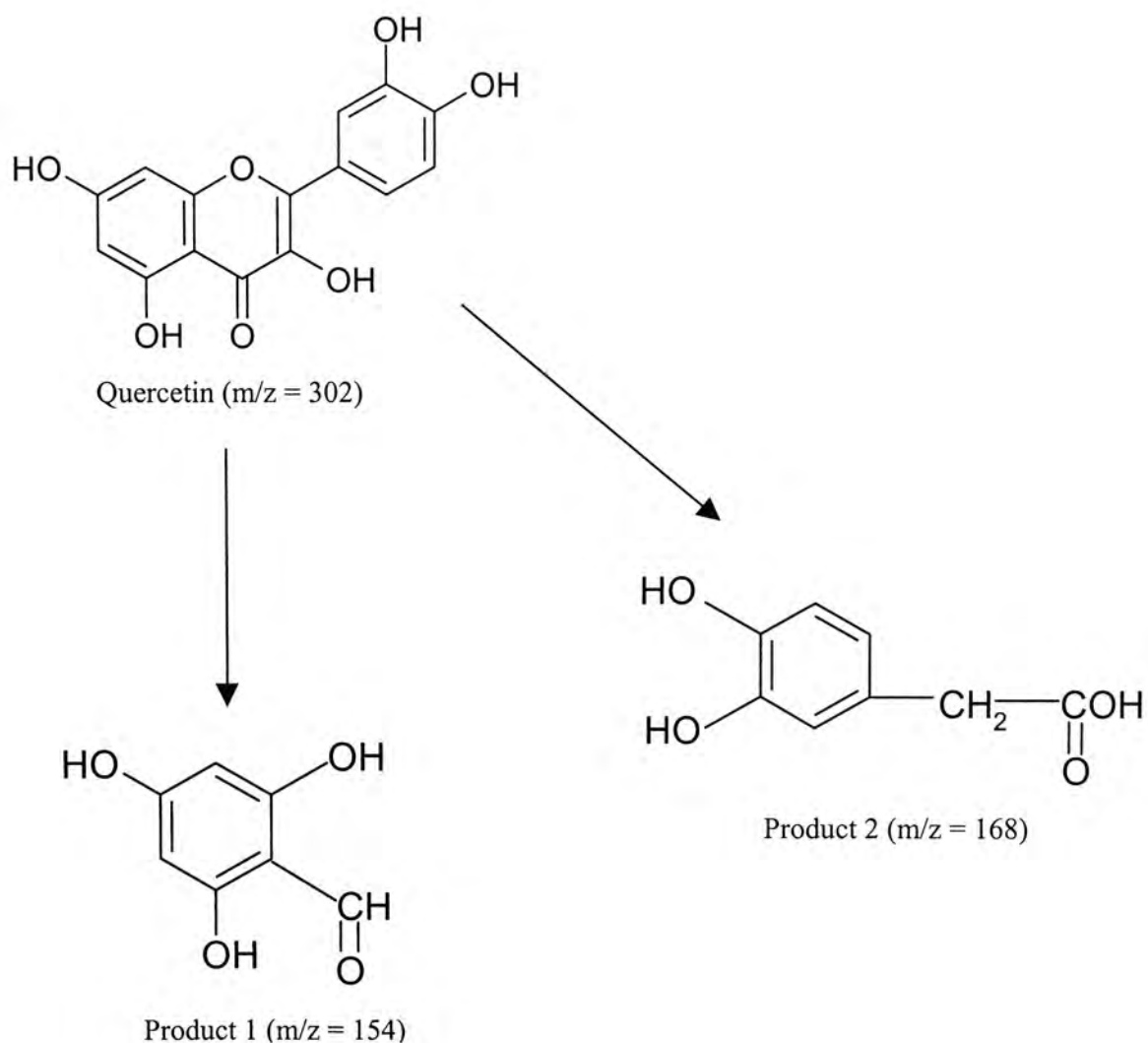


Fig. 3.1d. Stability of Quercetin-3-rhamnoside at pH 7.4, 6.8 in aqueous solutions at 37 °C.

Quercetin became more unstable at higher pH condition. Only 30% of the compound left after three hours of incubation at pH 7.4 (Fig. 3.1e.). Incubation of quercetin at pH 6.8 in PBS aqueous buffer resulted in the formation of three degradation products, as evidenced by HPLC (Figs. 3.2a,b.). The polarity based on retention time decreased in the order: product1 > product 2 > product 3 > quercetin. Their UV scans are shown in Figs.3.3a-d. UV scan was useful for selecting the λ_{max} of degradation products for further assay. LC/MS analysis of the degradation products showed that product 2 has an m/z of 168, product 3 has m/z of 272 and 300 and product 1 has m/z of 110 and 154. The possible degradation pathways of quercetin in aqueous solution at pH 6.8 are shown below.



Justesen *et al* (2001) reported the mass spectra of the degradation products of quercetin obtained by *in vitro* fermentation with faecal material from humans. However, further investigation employing preparative HPLC (to collect the degradation products) and solution NMR will be necessary to identify/confirm their chemical structures.

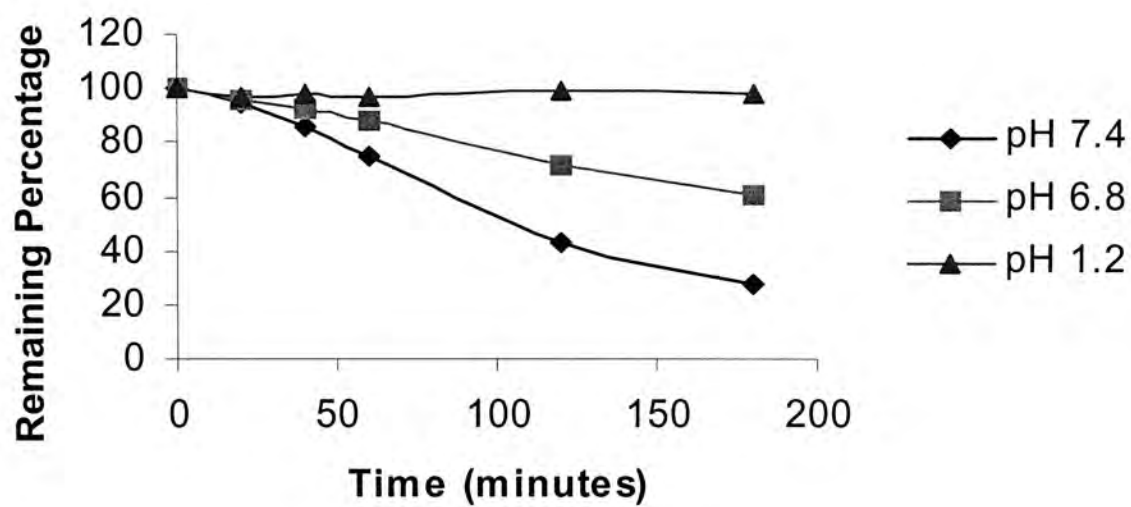


Fig. 3.1e. Stability of Quercetin at pH 7.4, 6.8 and 1.2 in aqueous solutions at 37 °C.

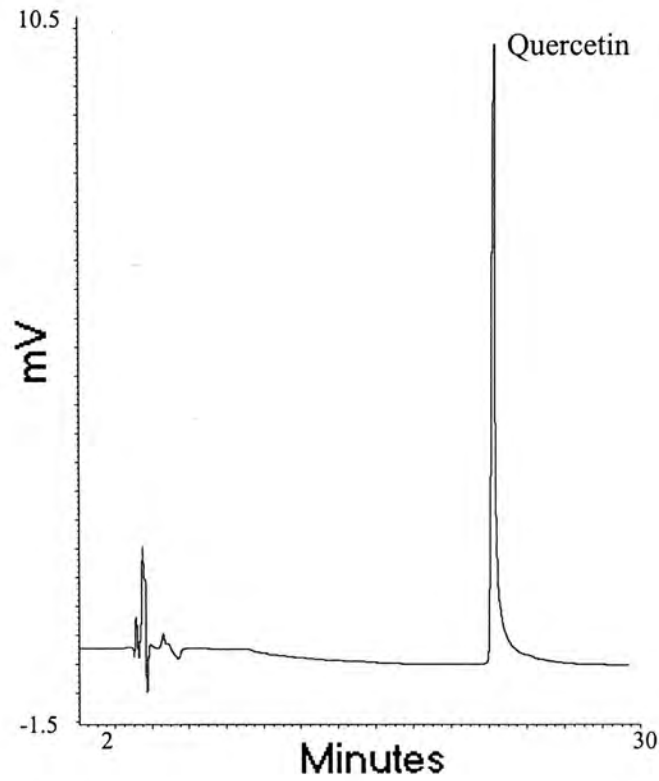


Fig. 3.2a. HPLC Chromatogram of quercetin.
The retention time (R_t) of quercetin is 22.3 minutes.

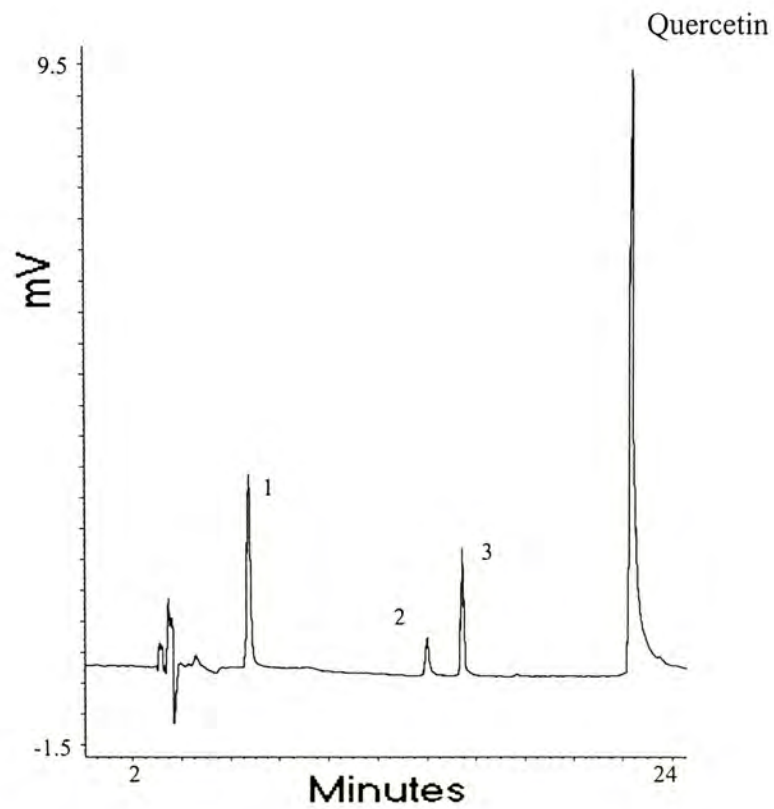


Fig. 3.2b. HPLC chromatogram of quercetin and its degradation products.
Quercetin was incubated in PBS buffer (pH 6.8) at 37 °C for 20h.
The Retention time of degradation products 1, 2, 3 is 6.7, 13.8 and 15.3 minutes.

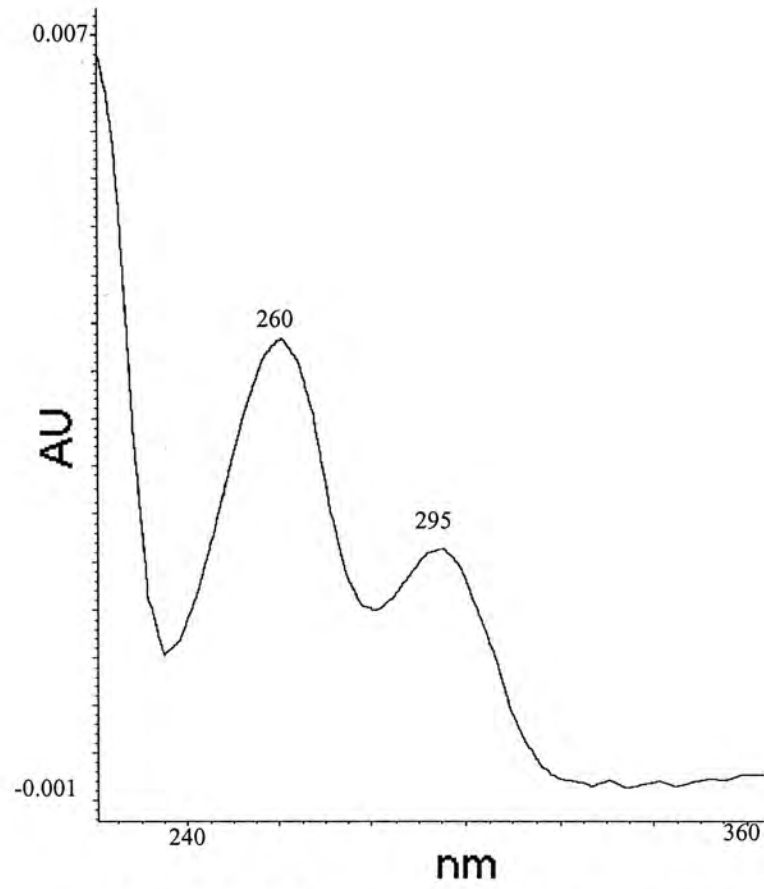


Fig. 3.3a. UV scan of degradation product 1.

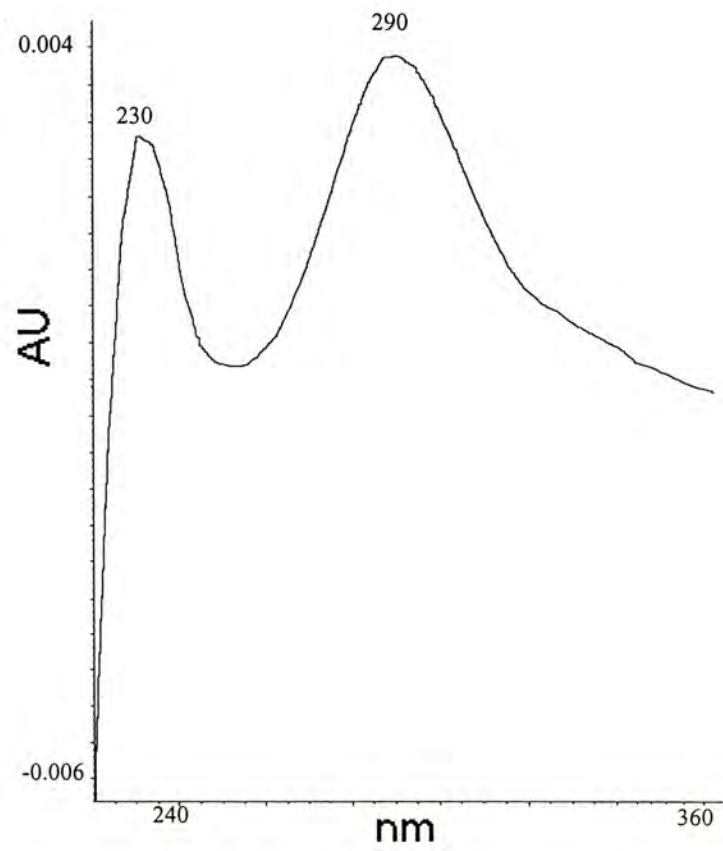


Fig. 3.3b. UV scan of degradation product 2

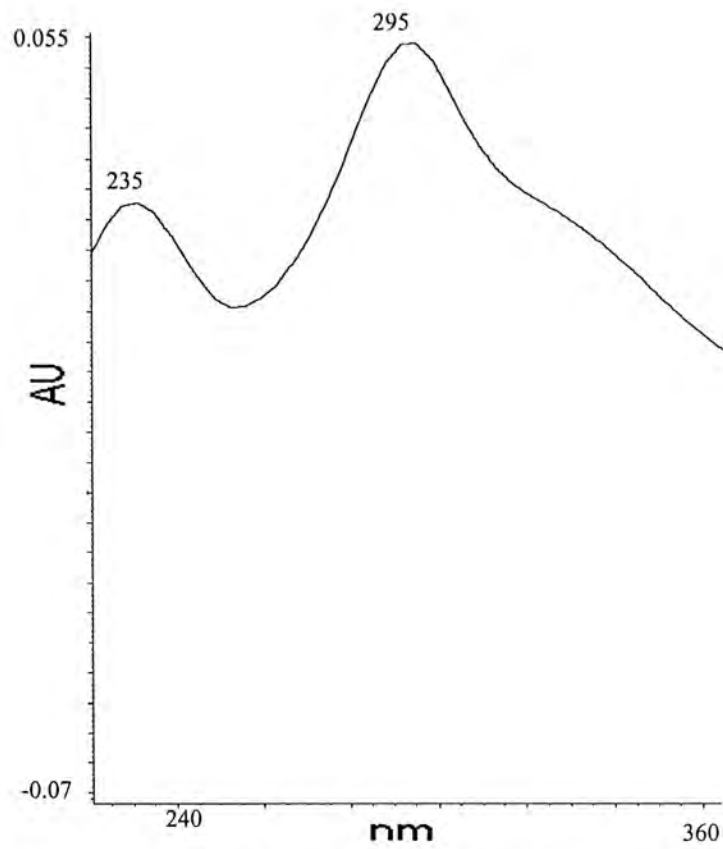


Fig. 3.3c. UV scan of degradation product 3

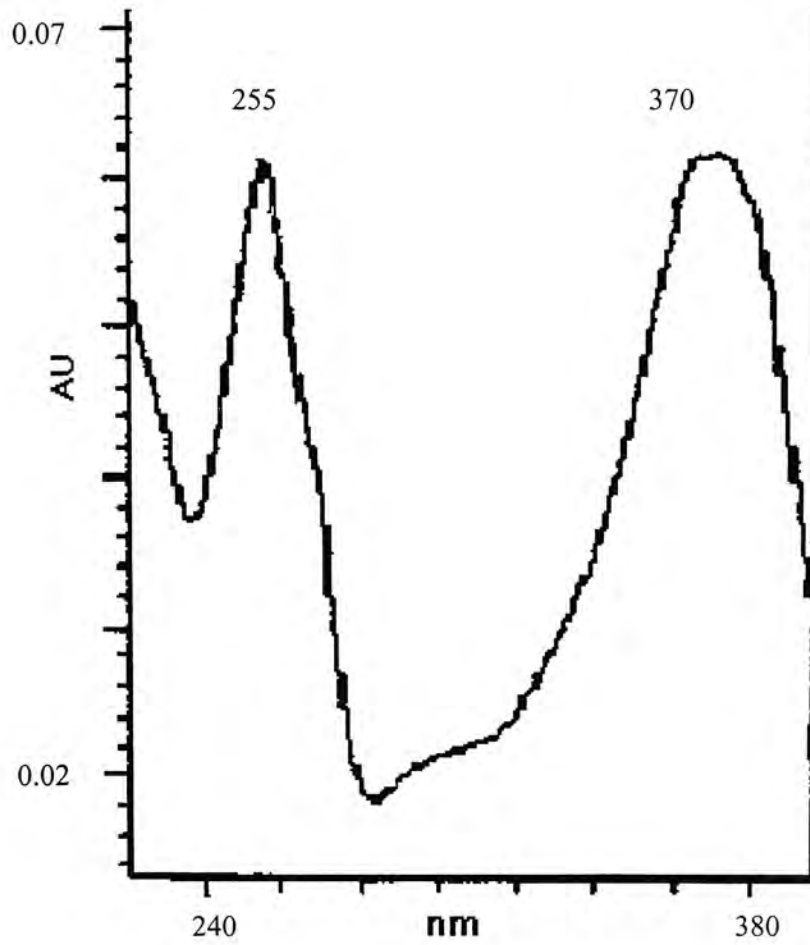


Fig. 3.3d. UV scan of quercetin

3.1.2. Thermal Analysis

Thermal analysis generally refers to any method involving heating the sample and measuring the change in some physical property. The most important thermal methods for the study of solid-state behavior are thermogravimetry (TG), differential scanning calorimetry (DSC) and thermal microscopy. TG measures the change in mass of the sample as the temperature is varied. DSC measures the difference in temperature or energy between the sample and a reference material as the temperature of the system is changed. The technique is most frequently employed for studying solid phase transitions such as polymorphism and desolvation. Thermal methods of analysis are important analytical tools for characterizing crystal forms, an important parameter governing the solubility and possibly the oral absorption of drugs.

Quercetin and the four related glycosides were all found to be stoichiometric hydrates as confirmed by DSC and TGA (Figs. 3.4-3.8, Table 3.1). A sharp endothermic peak (corresponding to dehydration) at ~ 100-120 °C was evident for quercetin-3-galactoside and quercetin (Figs. 3.4b, 3.8b), suggesting the dehydration process was complete within a narrow temperature range. For the other 3 flavonoids, the dehydration endotherm was not clearly discernable, indicating that the dehydration occurred over a much wider temperature range. Based on TGA data (Table 3.1), it can be deduced that quercetin and quercetin-3-rutinoside are dihydrates whereas quercetin-3-glucoside, quercetin-3-rhamnoside and quercetin-3-galactoside are monohydrates.

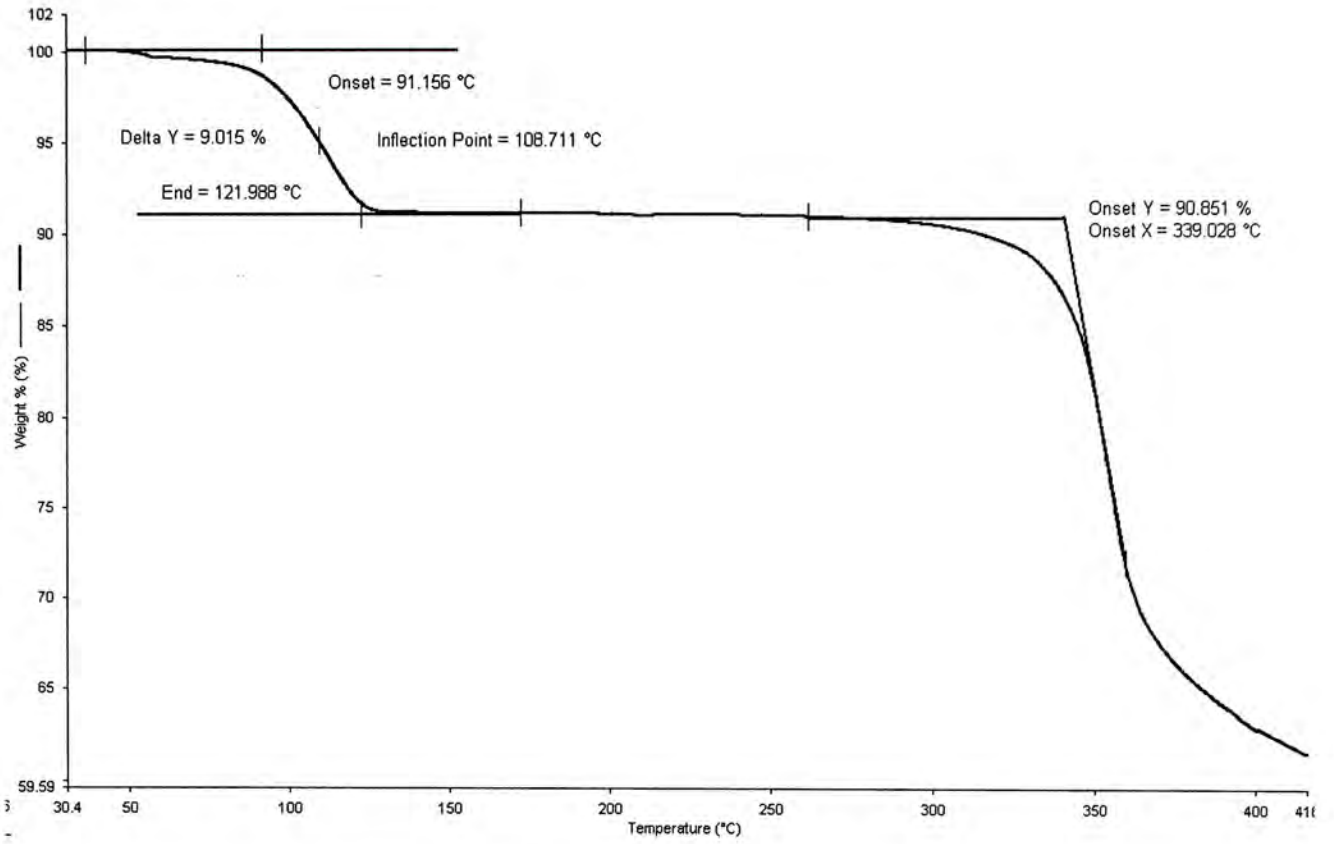


Figure 3.4a. TGA of Quercetin

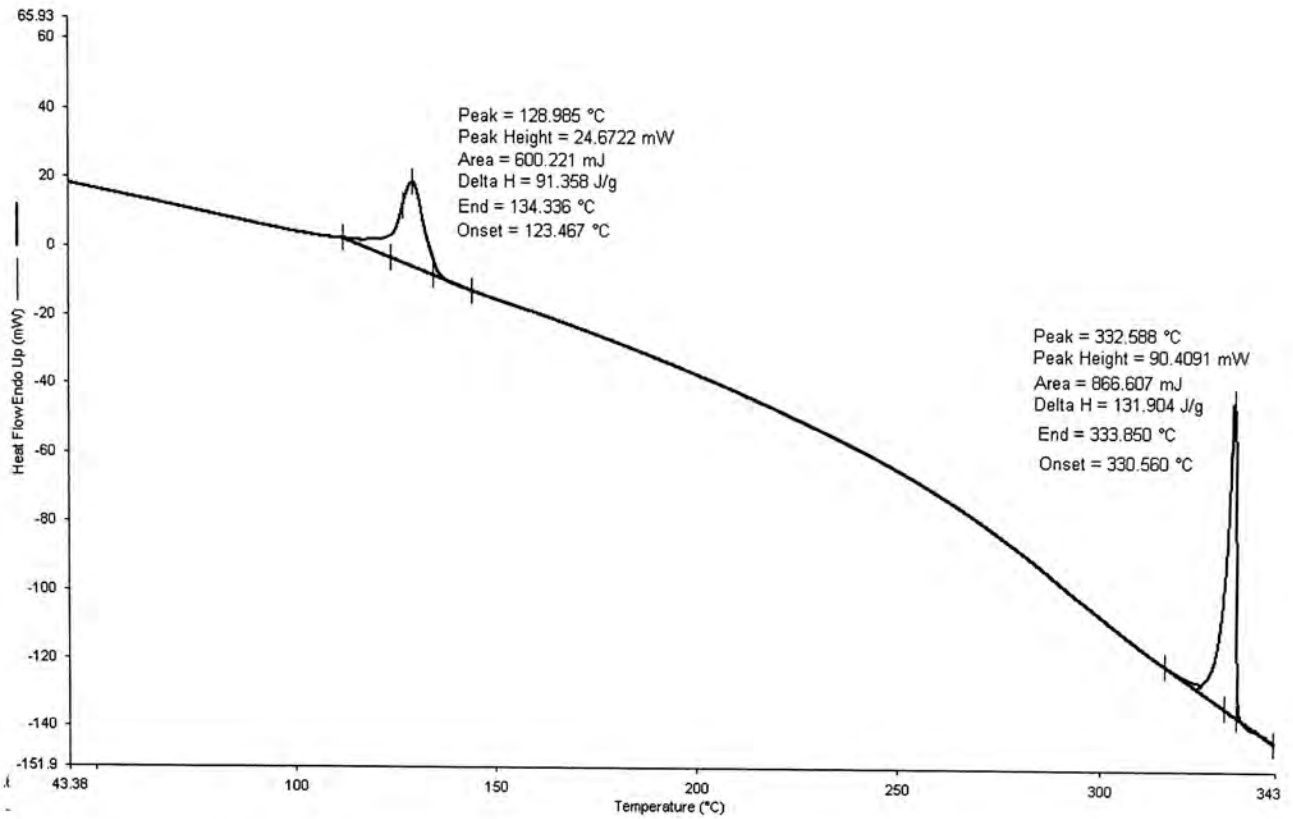


Figure 3.4b. DSC thermogram of Quercetin

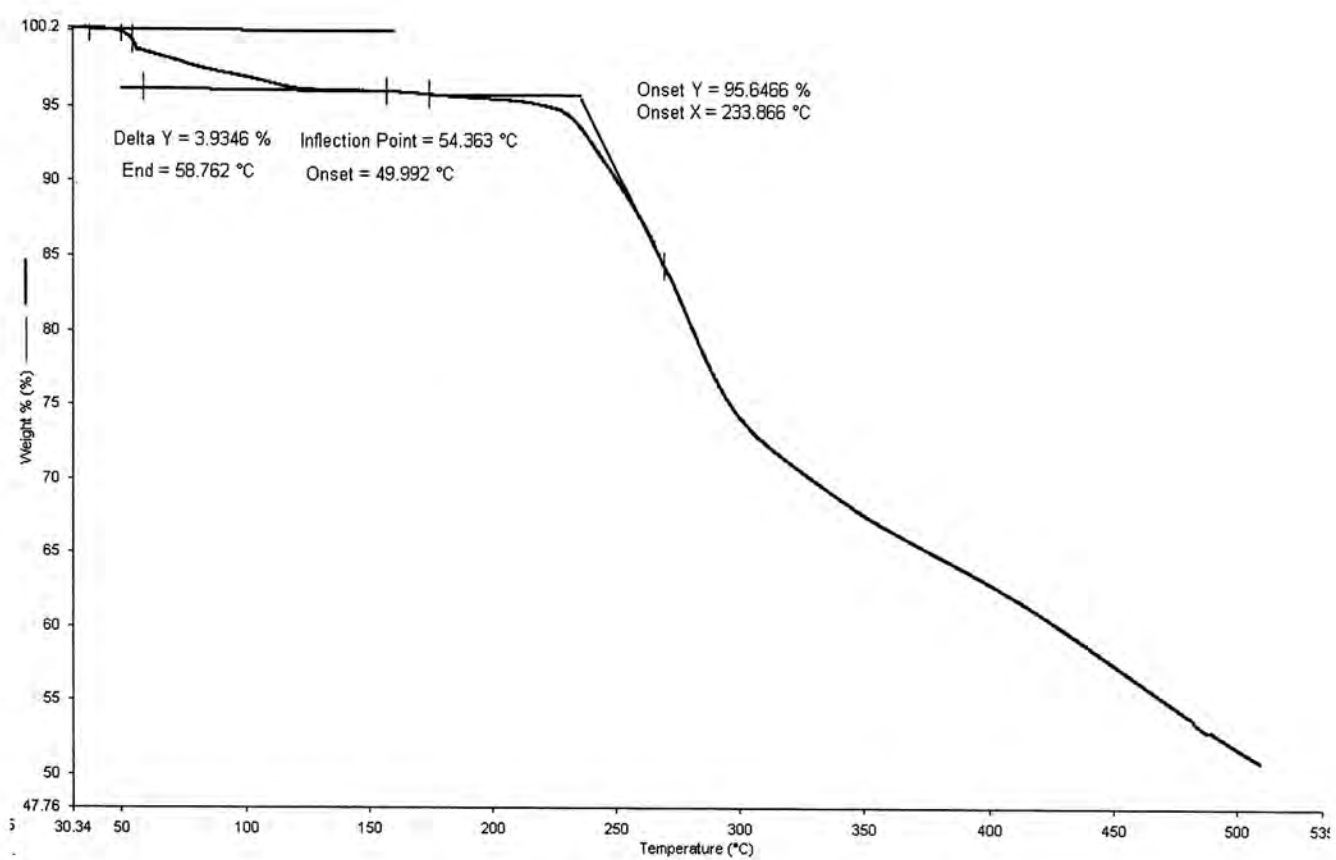


Figure 3.5a. TGA of Q-3-glucoside

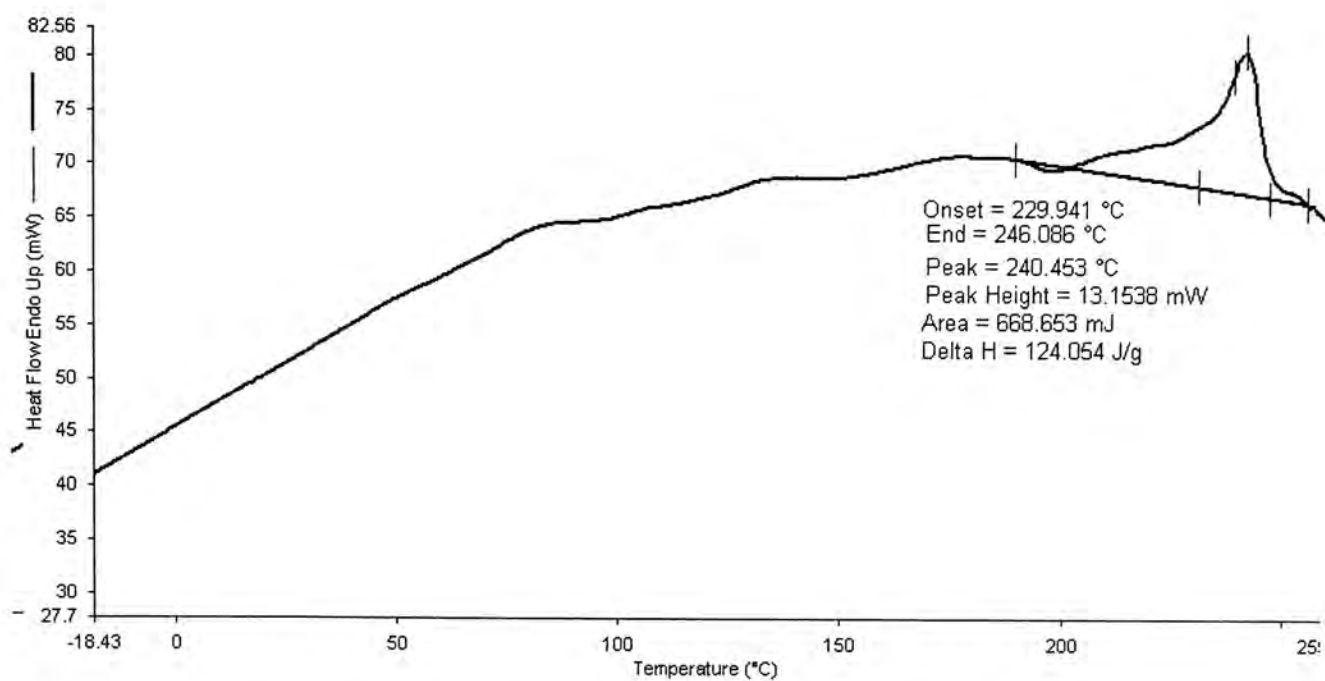


Figure 3.5b. DSC thermogram of Q-3-glucoside

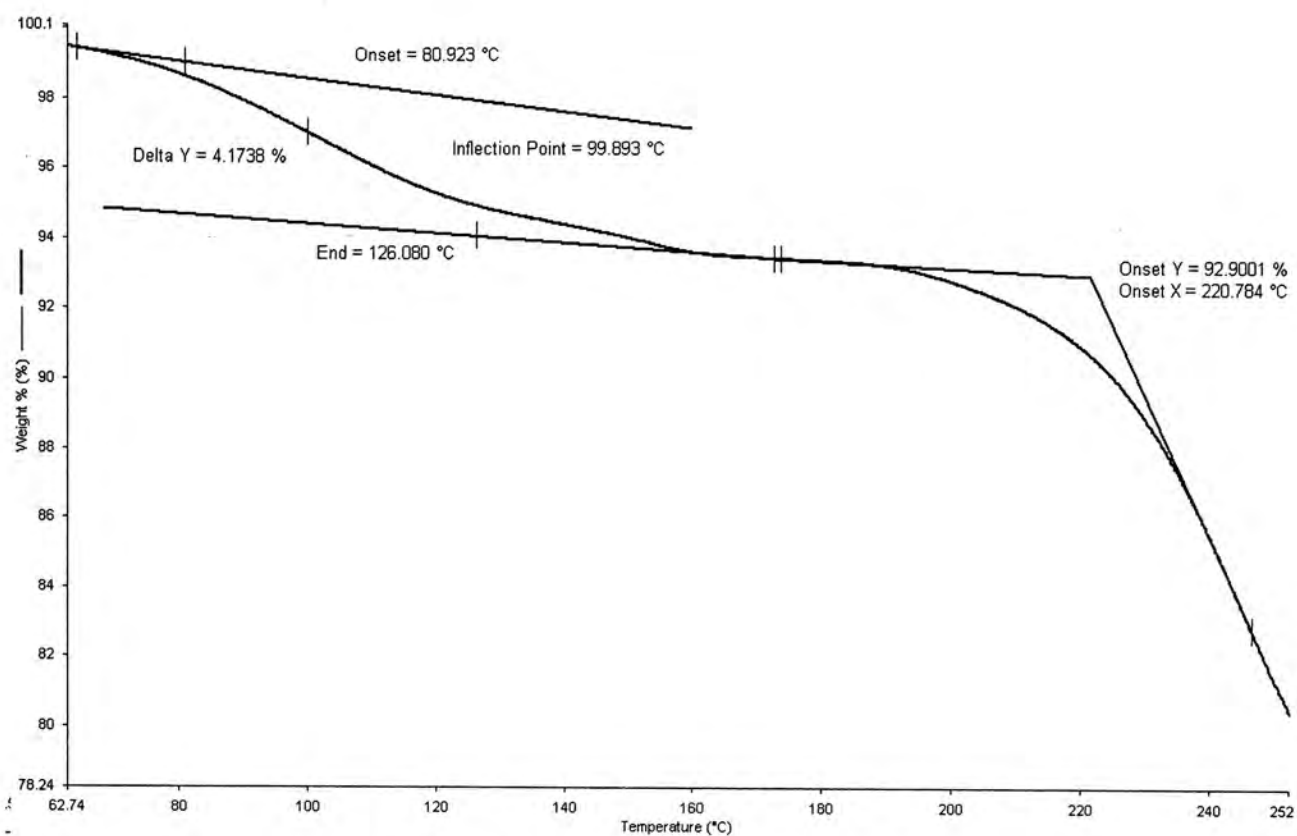


Figure 3.6a. TGA of Q-3-rhamnoside

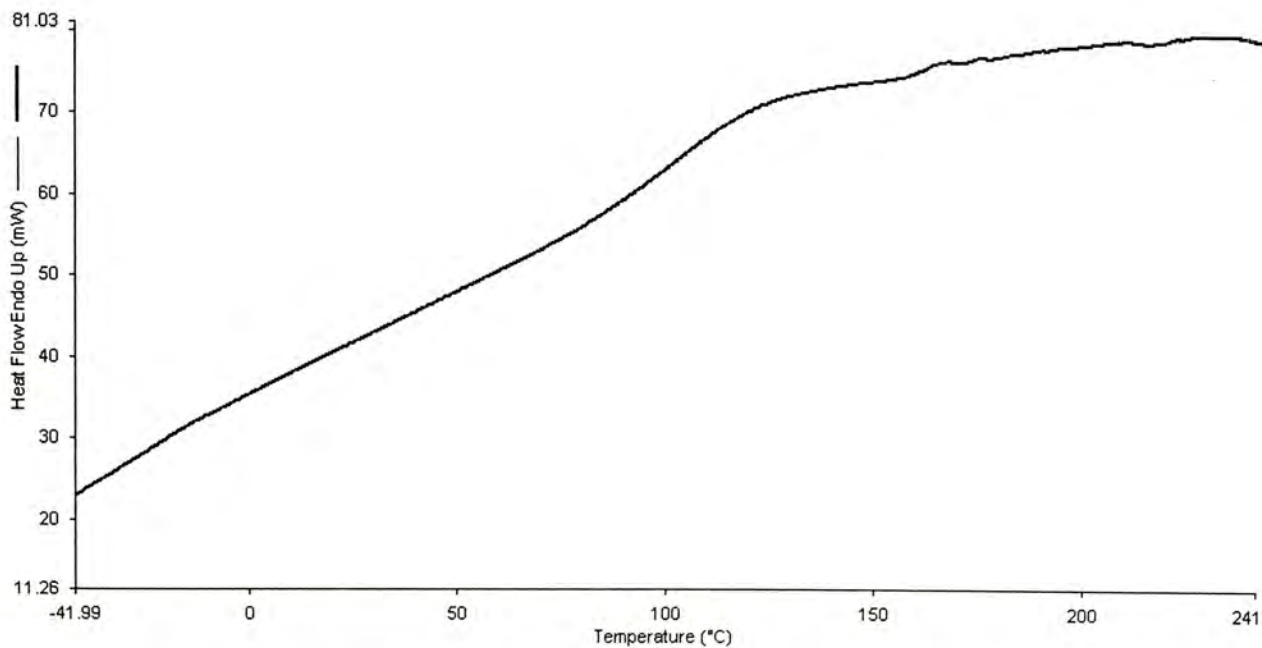


Figure 3.6b. DSC thermogram of Q-3-rhamnoside

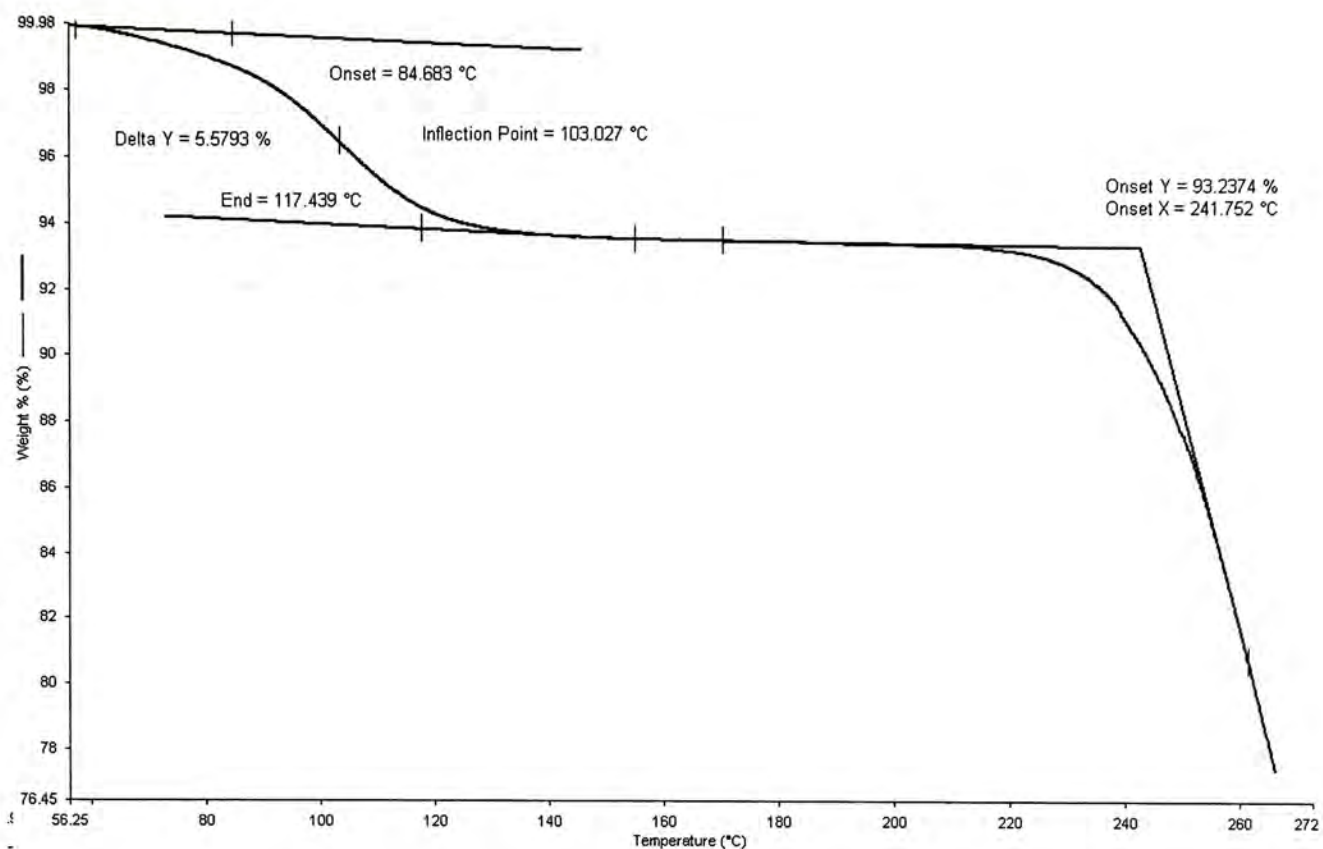


Figure 3.7a. TGA of Q-3-rutinoside

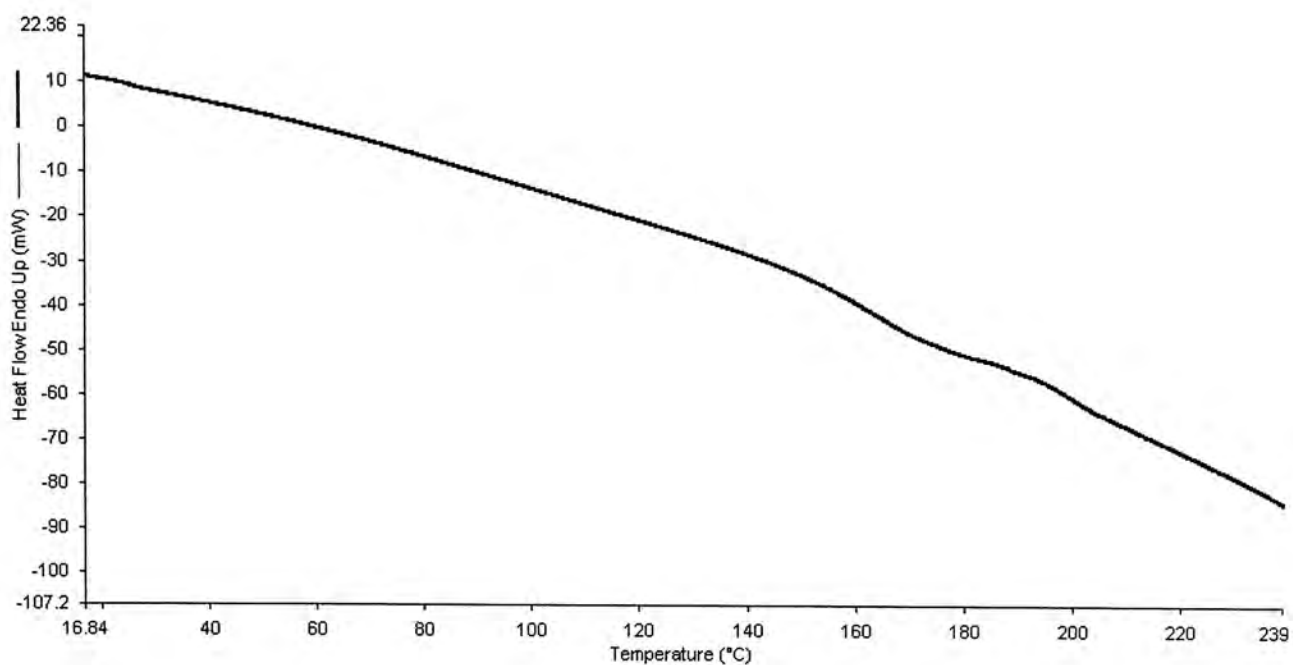


Figure 3.7b DSC thermogram of Q-3-rutinoside

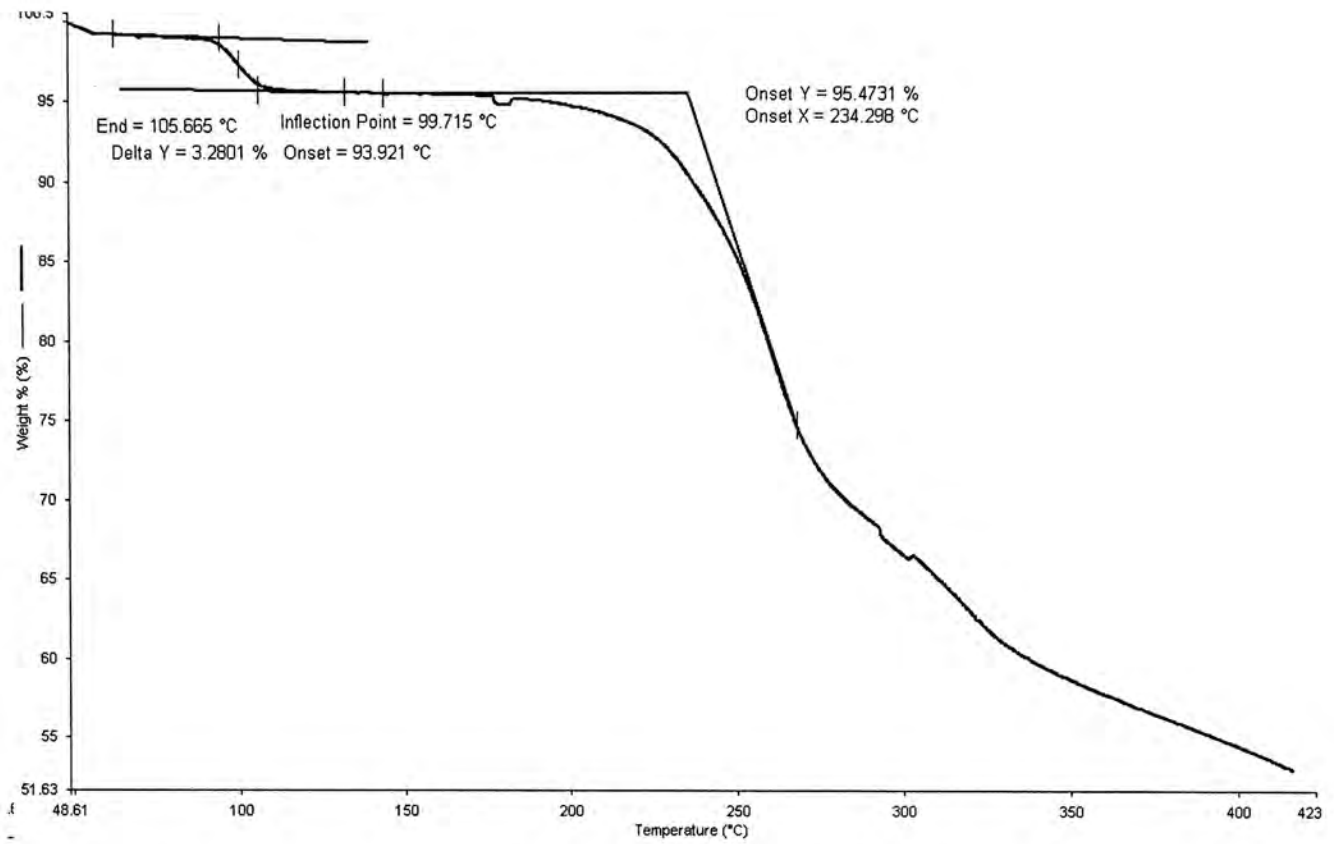


Figure 3.8a. TGA of Q-3-galactoside

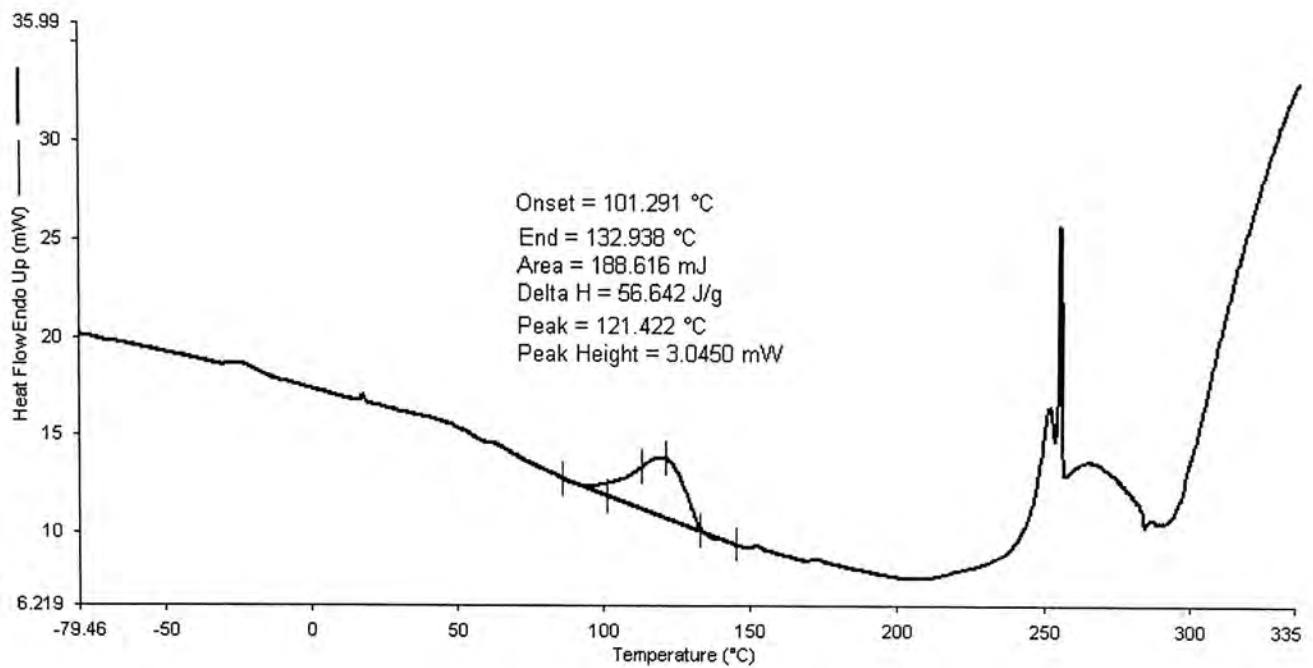


Figure 3.8b. DSC thermogram of Q-3-galactoside

Table 3.1. Bound water of flavonoids.

Flavonoids	Percentage of bound water		Number of bound water
	Mean value	Theoretical value	
Quercetin	9.02	10.6	2
Q-3-glucoside	3.93	3.73	1
Q-3-rhamnoside	4.17	3.86	1
Q-3-rutinoside	5.58	5.57	2
Q-3-galactoside	3.28	3.73	1

3.1.3. Aqueous Solubility

Dissolution is an important factor affecting the absorption of the poorly soluble drugs. The aqueous solubilities of the four quercetin glycosides determined at different temperatures are presented in Table 3.2a. The solubility of quercetin was not measured since it is relatively unstable in water (see Fig.3.1e).

The solubility of various glycosides in water increased with an increase in temperature. In addition, the solubilities depended on the sugar substituent at position 3 of the quercetin structure, and followed the order: quercetin-3-glucosides \approx quercetin-3-galactoside > quercetin-3-rhamnoside > quercetin-3-rutinoside.

Table 3.2a. Solubility of quercetin glycosides in aqueous solution (pH 7.4, n = 3).

T (C)	Fraction $\times 10^6$ [(mole of glycosides)/(mole of solvent)]			
	Quercetin-3-rutinoside	Quercetin-3-glucoside	Quercetin-3-galactoside	Quercetin-3-rhamnoside
4	1.218 \pm 0.0186	1.609 \pm 0.0390	1.687 \pm 0.0558	1.678 \pm 0.0193
15	1.681 \pm 0.0449	2.302 \pm 0.0395	3.036 \pm 0.0745	2.820 \pm 0.0146
25	2.465 \pm 0.0782	5.377 \pm 0.0908	3.916 \pm 0.0517	4.380 \pm 0.0577
30	3.731 \pm 0.0431	11.39 \pm 0.209	7.120 \pm 0.0577	5.579 \pm 0.145
37	5.222 \pm 0.184	12.33 \pm 0.252	15.25 \pm 0.152	9.628 \pm 0.138
50	10.62 \pm 0.0839	17.20 \pm 0.0300	34.69 \pm 0.314	14.12 \pm 0.0999

The solubility data were analyzed using the Van't Hoff equation, and the associated plots are shown in Fig. 3.9. The regression equation and apparent molar enthalpy of solution, ΔH^S (calculated from the slope of the plot) of each glycoside are shown in Table 3.2b. The van's Hoff plots for the various glycosides displayed good linearity ($R^2 = 0.93-0.99$; $n = 6$), showing that the van's Hoff equation was obeyed by all the glycosides.

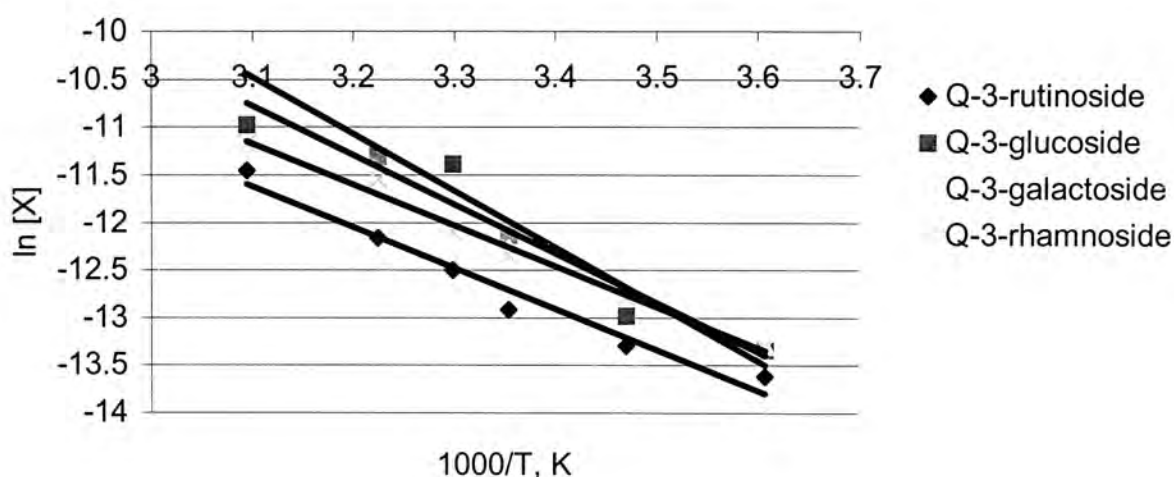


Fig. 3.9. Van't Hoff plots on the saturated aqueous concentration of glycosides

Table 3.2b. Van't Hoff equation and calculated ΔH^S

Compound	Equation	R^2	ΔH^S (kJ/mol)
Q-3-glucoside	$Y = -5.154 x + 5.20$	0.93	42.85 ± 5.89
Q-3-galactoside	$Y = -5.955 x + 7.98$	0.97	49.51 ± 4.24
Q-3-rhamnoside	$Y = -4.283 x + 2.02$	0.99	35.61 ± 2.01
Q-3-rutinoside	$Y = -4.281 x + 1.65$	0.97	35.59 ± 3.30

All the quercetin glycosides displayed positive ΔH^S values, suggesting that the dissolution process is endothermic.

As shown in Table 3.1, the ΔH^S values are statistically indistinguishable for quercetin-3-glucosides and quercetin-3-galactoside and for quercetin-3-rhamnoside and quercetin-3-rutinoside. Quercetin-3-glucoside and quercetin-3-galacoside had higher ΔH^S than quercetin-3-rhamnoside and quercetin-3-rutinoside. The differences

or similarities in the observed ΔH^S among the various samples are closely related to the lattice energy, as can be deduced from the following thermodynamic reasoning.

The dissolution of a solid in a solvent (e.g. water) can be viewed as being equivalent to the breaking of the crystal lattice of the sample (solute-solute interaction) followed by solvation of the separate solute molecules (solute-solvent interaction). The enthalpy of solution, ΔH^S of the solid is therefore given by

$$\Delta H^S = \Delta H_{cl} + \Delta H_{solv}$$

where ΔH_{cl} is the change in crystal lattice enthalpy (i.e. heat absorbed when the solute molecules of the crystal are separated by an infinite distance against their intermolecular forces) and ΔH_{solv} is the change in solvent enthalpy (i.e. heat evolved when the solute interacts with the solvent). ΔH_{cl} is positive, (i.e. endothermic transition) since energy is required to break the solute-solute interactions while ΔH_{solv} is generally negative (i.e. exothermic transition) if there exists an affinity between the solute and the solvent.

For the quercetin-3-glucoside monohydrate and the quercetin-3-galactoside monohydrate, the 2 sugar moieties, glucose and galactose, are closely similar in terms of chemical structure and the numbers of hydrophilic groups present. Thus the interaction of these two glycosides with water should be comparable (i.e. similar $-\Delta H_{solv}$). Since the measured ΔH^S are statistically equivalent, the lattice energy of both monohydrates, as reflected by ΔH_{cl} , should also be comparable. However, for the quercetin-3-rhamnoside monohydrate, the rhamnose moiety has one OH group less compared with glucose or galactose. Thus its interaction with water should be weaker both in solution (i.e. less negative ΔH_{solv}) and in the crystal lattice (i.e. lower ΔH_{cl}), as evidenced by a lower ΔH^S . On the other hand, the rutinose dihydrate has a glucose and rhamnose linked together. The additional glucose in the rutinose provides

additional hydrophilic sites (OH groups) for interaction with water both in solution and in the crystal lattice, and will yield a more negative ΔH_{solv} and a higher ΔH_{cl} . It is interesting to note that the rhamnoside monohydrate and the rutinoside dihydrate have virtually identical ΔH^{S} , suggesting that the difference between solvation (hydration) enthalpy (ΔH_{solv}) and lattice enthalpy (ΔH_{cl}) governing the dissolution process is the same for the two samples.

The higher ΔH_{cl} estimate deduced from thermodynamic reasoning for the rutinoside dihydrate is consistent with the generally accepted principle that the dihydrate is always more stable and stronger in intermolecular interactions than the monohydrate.

3.1.4. Partition Coefficient

Lipophilicity is an important factor affecting the transport process across the biological membrane. The lipophilicity of a compound is usually measured in terms of its partition coefficient between octanol and water at a defined pH. Molecular weight of the compound and its capability to form hydrogen bonds are two major determinations of partition coefficient (Waterbeemd *et al*, 2001).

The partition coefficient of quercetin and four related glycosides were determined in the octanol/water system. The results are summarized in Table 3.3. Lipophilicity was seen to decrease in the order: quercetin > quercetin-3-rhamnoside > quercetin-3-glucoside > quercetin-3-galactoside > quercetin-3-rutinoside. This result suggests that sugar substitution at position 3 reduces the lipophilicity of quercetin. The order of lipophilicity is consistent with the number of hydrophilic OH group present in the sugar substituents, as referred to in the preceding discussion on ΔH^{S} .

Table 3.3. Partition coefficient of quercetin and its glycosides (n = 4).

Compound	MW (g/mole)	Log P
Quercetin	302	1.81 ± 0.49 ^a
Quercetin-3-glucoside	464.38	0.816 ± 0.0049
Quercetin-3-galactoside	464.38	0.785 ± 0.0046
Quercetin-3-rhamnoside	448.4	1.36 ± 0.047
Quercetin-3-rutinoside	610.5	-0.236 ± 0.0090

^a Partition coefficient of quercetin was obtained from Murota *et al.* (2000).

3.2. Validation of *in vitro* models

3.2.1. Selection of Marker Compounds

Validation of the *in vitro* models employed six marker compounds, namely mannitol, propranolol, lucifer yellow, atenolol, L-leucine and PEG-4000. These are widely used and well documented marker compounds (Dowty, 1997; Lennernäs, 1997; Reardon, 1993). Table 3.4. shows the diversity in physical properties of the marker compounds. The values shown for % absorbed in humans are literature data, ranging from less than 1% for PEG-4000 to 100% for L-leucine and propranolol.

Table 3.4. Physicochemical data, MW, pK_a values, LogP (Octanol/Water, pH 7.4) and absorption in human of 6 markers studied in the Ussing Chamber and Caco-2 cell monolayers

Compound	MW (g/mole)	pK _a	Log P (oct/water pH 7.4)	Percentage of oral absorption (human)	Transport mechanism/ route	References
Mannitol	182	N/A	-3.10	65	Paracellular	Dowty, 1997
Propranolol	259	9.5	1.3	100	Passive diffusion	Lennernäs, 1997
Lucifer yellow	457.2	N/A	N/A	N/A	Paracellular	Reardon, 1993
Atenolol	266	9.6	-1.8	50	Paracellular	Lennernäs, 1997 Grès, 1998
L-leucine	131	2.3	N/A	100	Carrier mediated	Lennernäs, 1997 Grès, 1998
PEG-4000	4000	9.6	-5.1	0	paracellular	Dowty, 1997 Grès, 1998

N/A: data is not available

Mannitol is widely used as low molecular weight markers. Being hydrophilic, it

has very limited partition into the lipophilic cell membranes. As with mannitol, atenolol is transported by the paracellular route through the tight junction.

Lucifer yellow and PEG-4000 represent the medium and high molecular weight compounds. They are used as non-absorbable markers. Propranolol, a β -receptor antagonists, is a marker of the transcellular (passive diffusion) route (Lennernäs, 1997), which is the major transport pathway for many compounds.

L-leucine, an amino acid, is a carrier-mediated transport marker (Grès, 1998). Its transport across the intestinal cells is an active process involving ATP and carrier. Active transport is normally characterized by bi-directional difference in permeability of the compound being transported across the cells, with a higher permeability from the apical to basolateral (AP \rightarrow BL) side than in the reverse direction (BL \rightarrow AP).

3.2.2. Validation of Ussing Chamber

The results of the transport studies on rat ileum using the Ussing Chamber are summarized in Table 3.5. The results were generally comparable to the published data. The apparent permeability coefficient P_{eff} of L-leucine was 6 times greater from AP to BL than from BL to AP, confirming the involvement of carriers in the transport of amino acid. For propranolol and atenolol, the permeability was 2 and 3 times greater from BL to AP than in the reverse direction. However, as have been well established, they are transported by passive diffusion and paracellular route respectively and thus should not have shown any bi-directional differences in permeability across the cells. Tomita *et al*, (2000) also found the permeation of lucifer yellow and mannitol across rat colonic mucosa were 3 and 2.3 times greater from BL to AP than in the opposite direction. At present, the reason for such discrepancy in the directional differences in permeability of transcellular and paracellular markers remains obscure. In view of this

problem and the difficulties in data interpretation, the Ussing Chamber technique was relinquished in the subsequent transport studies with the flavonoids.

Table 3.5. Apparent Permeability Coefficients of 6 marker compounds obtained in rat ileum using the Ussing Chamber (n = 3-6).

Compound	Concentration	$P_{\text{eff}} \times 10^5$ (cm/s) rat ileum		$P_{\text{eff}} \times 10^5$ (cm/s) (references)
		AP to BL	BL to AP	AP to BL
Mannitol	0.8 $\mu\text{ci/ml}$	1.24	N/A	0.7 (0.28) ^a
Propranolol	2 mM	2.66 (0.35)	4.62 (1.04)	4.13 (0.38) ^b
Lucifer yellow	0.33 mg/ml	0.503 (0.027)	N/A	N/A
Atenolol	1 mM	0.464 (0.132)	1.29 (0.226)	0.508 (0.076) ^b
L-leucine	0.5 $\mu\text{ci/ml}$	3.3 (0.878)	0.564 (0.033)	1.964 (0.579) ^b
PEG-4000	1 $\mu\text{ci/ml}$	0.332	N/A	0.167 (0.033) ^a

^aDowty *et al*, 1997.

^bUngell *et al*, 1997.

Permeabilities from BL to AP of marker compounds are not available (N/A).

3.2.3. Validation of Caco-2 Cell Monolayers

3.2.3.1. Integrity of Caco-2 Cell Monolayers

Transepithelial electrical resistance (TEER) is widely used to assess the integrity of the Caco-2 cell monolayers. TEER is determined primarily by the ion flux through paracellular space. A constant TEER value of $1015 \pm 137 \text{ ohm}\cdot\text{cm}^2$ was found in DMEM culture medium for a 3-week culture of Caco-2 cell monolayers in our laboratory.

Throughout the course of all the experiments, the integrity of cell monolayers was preserved as monitored by TEER. The TEER value was $574 \pm 103 \text{ ohm}\cdot\text{cm}^2$ before transport experiments and $431 \pm 64 \text{ ohm}\cdot\text{cm}^2$ at the end of transport experiments conducted in transport buffer PBS⁺. The percentage of the remaining TEER was $76 \pm 11\%$ (n = 64). TEER was affected by the integrity of the cell monolayers, temperature

and ingredient of transport buffer. Thus the experiments need to be conducted under defined culturing and experimental conditions.

3.2.3.2. Permeability of Marker Compounds

The permeability coefficient determined for the marker compounds using Caco-2 cell monolayers are presented in Table 3.6. Most of the values were comparable to the literature data. However, for the carrier-mediated marker L-leucine, the permeability obtained from our experiment was 20 times greater than the reference value. The difference may be due to the different level of expression of the transporters on Caco-2 cell monolayers under different culture conditions and cell passages.

For propranolol and mannitol that are transported by passive diffusion and paracellular transport route respectively, there were no significant differences in permeability between the two directions ($p > 0.05$). Since the Caco-2 cell monolayers are devoid of mucus layer, the technique is much simpler to handle than the Ussing Chamber involving the use of rat ileum.

Table 3.6. Apparent Permeability Coefficients of 5 marker compounds obtained in Caco-2 cell monolayers (n = 3).

Compound	Concentration	$P_{app} \times 10^6$ (cm/s)		$P_{app} \times 10^6$ (cm/s) (Reference, AP to BL)
		AP to BL	BL to AP	
Mannitol	1 μ ci/donor	1.48 (0.0432)	1.44 (0.225)	0.65 ^c
Propranolol	100 μ M	54.7 (10.17)	52.6 (0.205)	27.5 ^c
Lucifer yellow	0.33 mg/ml	0.259 (0.0933)	N/A	0.1- 0.7 ^d
Atenolol	3 mM	0.907 (0.0822)	N/A	1.16 ^e
L-leucine	0.5 μ ci/ml	9.19 (1.47)	1.71 (0.201)	0.47 ^f

^cYee, 1997

^dIrvine, 1998

^eGrès, 1998

^fLenneräs, 1997

Permeabilities from BL to AP of marker compounds are not available (N/A).

3.2.3.3. Selection of *in vitro* models

Compared with the Ussing Chamber technique, Caco-2 cell monolayers are more appropriate for investigating the possible involvement of the efflux systems in the transport process by comparison of permeability of marker compounds in the two directions (i.e. AP BL or BL AP). Area of the transport in the Caco-2 cell monolayers model is larger than that in Ussing Chamber, which will increase the flux across the cells and hence improve the ease of analysis. Thus, the Caco-2 cell monolayers model was preferred to the Ussing Chamber technique in the present study. Although the Ussing Chamber employs animal tissues and resembles more closely the *in vivo* situations, the observed discrepancy in the bi-directional permeability for some of the transport markers has rendered it a less desirable technique for mechanistic transport studies.

3.2.3.4. Validation of Sodium/glucose Co-transporter (SGLT1)

Phloridzin is a competitive inhibitor of D-glucose transporter SGLT1. It binds to the Na⁺-D-glucose cotransporter of the small intestine brush border membrane but cannot be transported by this way (Toggenburger *et al*, 1982).

Comparison of permeability and uptake of D-glucose into the Caco-2 cell monolayers with or without phloridzin is shown in Table 3.7. As can be seen, the permeability and uptake of D-glucose into the cell monolayers were decreased in the presence of phloridzin by 50% of the control. These results confirm the existence of the major transporter of sugars, SGLT1, in the current Caco-2 cell monolayers, under the stated culture conditions. Thus, this model was used to study the transport process potentially involving the sugar transporter, SGLT1.

Table 3.7. The effect of SGLT1 inhibitor Phloridzin (100 μ M) on P_{app} and uptake of D-glucose (100 μ M) from AP to BL on the Caco-2 cell monolayers (n = 3).

AP	BL	With Phloridzin	Without Phloridzin
$P_{app} \times 10^5$ (cm/s)		1.324 \pm 0.138*	2.318 \pm 0.250
Uptake P%		3.622 \pm 0.414*	6.773 \pm 0.438

* $p < 0.05$, significantly difference compared to control

3.3. Transport Studies on Quercetin and Related Flavonoids

3.3.1. Direction of Transport

To determine whether the transport of quercetin and its glycosides involved any active process like the efflux system, the bi-directional transport permeability of these compounds in Caco-2 cell monolayers was compared as shown in Table 3.8. Recovery was calculated as the percentage of total amount of the flavonoids in original form found on both donor and receiver sides at the end of the experiments. Apparent permeability was calculated in the original form of flavonoids by the equation described in chapter 2.

There was no significant difference in permeability between the two directions among the flavonoids except for quercetin-3-glucoside ($p = 0.0018$). Its permeability in the BL to AP direction was greater than in the AP to BL direction, which suggests the involvement of an efflux pump. Further studies using different concentrations of the glucosides and an efflux pump inhibitor were conducted to confirm this, and the results are discussed in the following section 3.3.2. The above findings suggest that quercetin, quercetin-3-galactoside, quercetin-3-rhamnoside and quercetin-3-rutinoside are transported by passive diffusion whereas the transport of quercetin-3-glucoside involves also the efflux P-gp.

The apparent permeability coefficient of quercetin (aglycone) was about 5 times and 10 times higher than those of the glycosides and mannitol respectively, consistent with its higher lipophilicity. Thus it appears that permeability is not a limiting step in

the absorption process of quercetin.

All of the above transport studies with quercetin were conducted at pH 6.8 instead of 7.4 based on the consideration of the cell viability and chemical stability of quercetin. Quercetin was more stable at pH 6.8 than at pH 7.4 but still yielded several degradation products as shown in Figure 3.2b. The measured quercetin would still be an underestimate as a result of the degradation-related losses. Thus future permeability measurement of quercetin need to take degradation into account.

Apart from potential loss due to degradation, quercetin may accumulate in the cell monolayers due to its higher lipophilicity. For these reasons, the recovery of quercetin in the original form in the donor and receiver sides after the experiments was poor (~ 46%).

Although the various quercetin glycosides differed in the sugar substituent at position 3 of the quercetin structure, their P_{app} were similar. Compared with the paracellular marker mannitol, quercetin glycosides displayed a higher P_{app} , by about 2 times. Thus poor permeability may limit their absorption.

To improve our understanding and prediction of the absorption of flavonoids, quantitative- structure-activity-relationship (QSAR) derived models may be employed to correlate structure-related physicochemical parameters with oral absorption. In the present study, we speculate that lipophilicity is a major contributor to the membrane permeability of flavonoids. However, other parameters such as polar surface area may also need to be considered in above models. The sugar moiety and its site of substitution in flavonoid glycosides may determine whether the transport could use specific transporters, and are worthy of further investigation.

Table 3.8. Bi-directional permeability of Quercetin (12.5 μM) and its glycosides (50 μM) in the Caco-2 cell monolayers (n = 3-5).

Compound	$P_{\text{app}} \times 10^6$ (cm/s)		Recovery %
	AP to BL	BL to AP	Two directions
Q-3-rutinoside	2.73 ± 0.32	2.15 ± 0.58	92.4 ± 8.2
Q-3-glucoside	1.50 ± 0.22	$2.43 \pm 0.19^*$	93.8 ± 5.5
Q-3-galactoside	2.46 ± 0.36	2.42 ± 0.13	84.2 ± 7.6
Q-3-rhamnoside	2.71 ± 0.61	2.67 ± 0.37	102.3 ± 9.4
Quercetin	15.5 ± 0.16	16.9 ± 0.61	45.7 ± 10

AP: Apical side, BL: Basolateral side

* $p < 0.05$, significant different between two directions

3.3.2. Concentration Dependence

The flux of quercetin-3-glucoside across Caco-2 cell monolayers is shown in Fig. 3.10a,b. The flux was essentially linear for up to 2 hours for all quercetin-3-glucoside concentrations studied (25-100 μM). The flux from the basolateral side to the apical side was 12.6-, 3.4-, 1.6- and 1.3- folds greater than that from the apical side to the basolateral side, indicating the involvement of the efflux system.

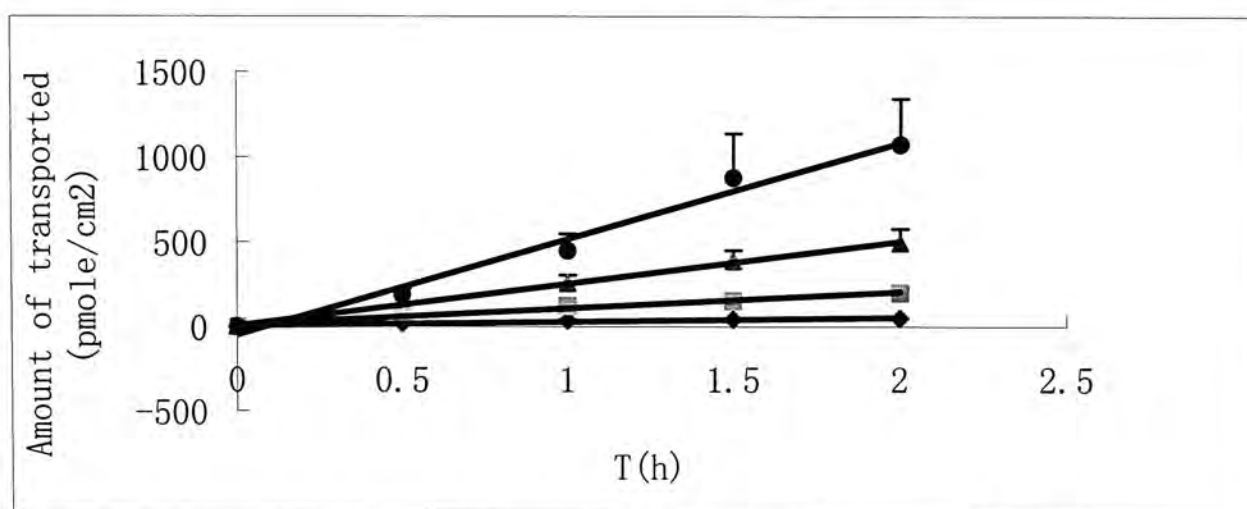


Fig.3.10a. Transepithelial flux of quercetin-3-glucoside across the Caco-2 cell Monolayers from AP to BL (n = 3).

The Quercetin-3-glucoside concentrations used were 25 μM (), 30 μM (), 50 μM () and 100 μM ()

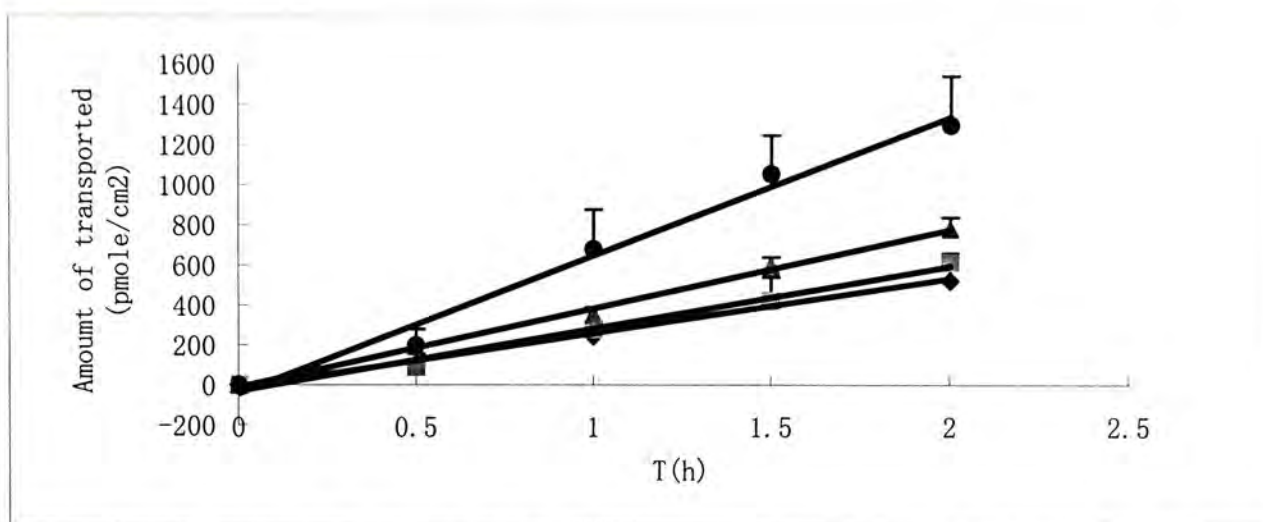


Fig. 3.10b. Transepithelial flux of Quercetin-3-glucoside across the Caco-2 cell monolayers from BL to AP (n = 3). The Quercetin-3-glucoside concentrations used were 25 μM (◆), 30 μM (◻), 50 μM (▲) and 100 μM (●).

As shown in Figure 3.10c, there was no significant correlation between the apparent permeability of quercetin-3-glucoside and TEER. $1/P_{\text{app}}$ in the AP to BL direction varied by several folds within a narrow range of $1/\text{TEER}$ values. The variation may be due to the efflux effects but not to the paracellular transport pathway. This suggests that quercetin-3-glucoside is predominantly transported across the intestinal cells by the transcellular route.

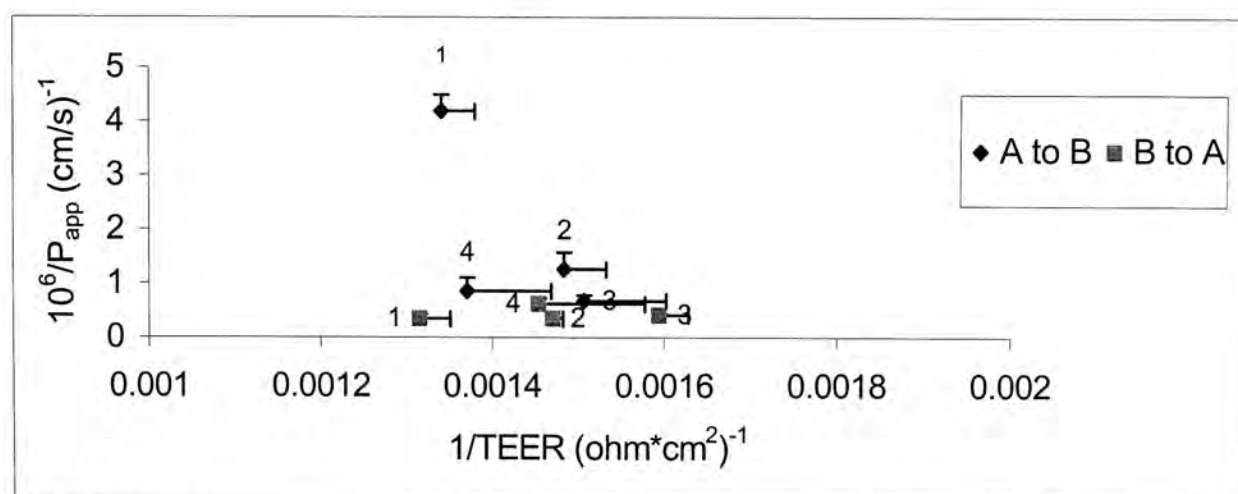


Fig. 3.10c. $(P_{\text{app}})^{-1}$ plotted against $(\text{transepithelial Electrical resistance, TEER})^{-1}$ of Caco-2 cell monolayers after transport studies with different concentration of quercetin-3-glucoside from two directions. Each point is expressed as mean \pm SD (n = 3). The Quercetin-3-glucoside concentrations used were 25 μM (1), 30 μM (2), 50 μM (3) and 100 μM (4).

3.3.3 Inhibition of P-gp by Verapamil

Transport studies were conducted in the presence of a P-gp inhibitor to confirm the involvement of the efflux system. Verapamil, a substrate of P-glycoprotein is generally used as an inhibitor at 100 μM in Caco-2 study to serve this purpose (Hosoya *et al*, 1996; Hunter *et al*, 1993). In addition, verapamil has the advantage that it does not alter the permeability of those markers for the paracellular and passive diffusion routes in Caco-2 cell monolayers (Hosoya *et al*, 1996).

As shown in Fig. 3.11, verapamil at a concentration of 100 μM reduced the permeability of quercetin-3-glucoside at 30 μM across the epithelial cell layers in the BL to AP direction from $(2.84 \pm 0.20) \times 10^{-6}$ cm/s to $(2.05 \pm 0.19) \times 10^{-6}$ cm/s. Furthermore, the inhibition was accompanied by an increase in permeability in the AP to BL direction from $(0.842 \pm 0.19) \times 10^{-6}$ cm/s to $(1.58 \pm 0.14) \times 10^{-6}$ cm/s. No decrease in TEER was observed upon verapamil treatment, indicating that the integrity of the cells was maintained during the experiment.

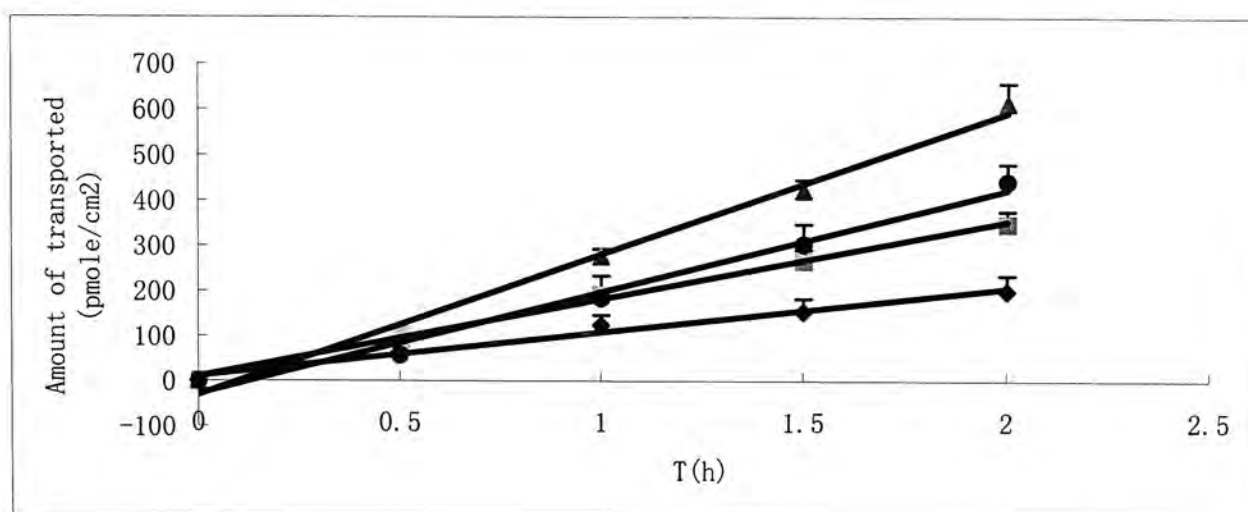


Fig. 3.11. Time course of 30 μM Quercetin-3-glucoside transport across the Caco-2 cell monolayers in the absence or presence of 100 μM verapamil ($n = 3$). Key: \blacktriangle , A \rightarrow B (control); \bullet , B \rightarrow A (control); \blacksquare , A \rightarrow B (with verapamil); \blacklozenge , B \rightarrow A (with verapamil).

These results suggest that quercetin-3-glucoside is a substrate of the P-glycoprotein efflux pump, and interaction of verapamil with P-glycoprotein reduces

the efflux of quercetin-3-glucoside.

Walgren *et al* (1998) found that both quercetin 3,4'-diglycoside and quercetin 4'- β -glucoside showed prominent efflux in the Caco-2 cells. These authors further demonstrated that the efflux of quercetin 4'- β -glucoside across the Caco-2 cell monolayers was associated with the apical multidrug resistance-associated protein 2 (Walgren *et al*, 2000).

Taking the findings from present study and those reported by other groups together into consideration, it appears that some of the quercetin glucosides are substrates of the efflux pumps, and several efflux pumps may be responsible for the efflux of quercetin glucosides.

3.3.4. Metabolism of Quercetin in Caco-2 Cells

Fig. 3.12. shows the concentration of quercetin (aglycone) on the basolateral side before and after enzymatic hydrolysis of quercetin glucuronide when quercetin was loaded on apical side.

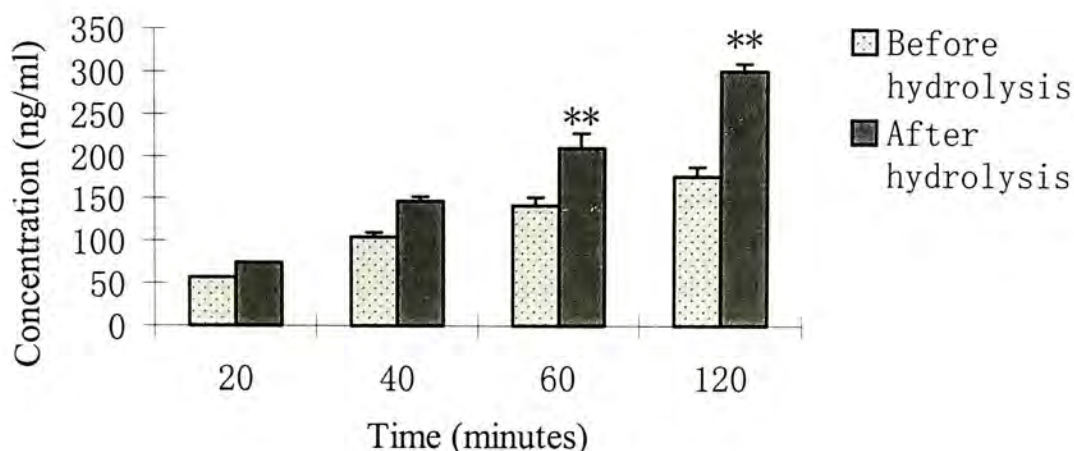


Fig. 3.12. Concentration of quercetin aglycone in basolateral side before and after hydrolysis. The transport studies were performed from apical to basolateral side with Caco-2 cell monolayers (n = 3). Initial concentration of quercetin aglycone in apical solution was 12.5 μ M. ** p<0.01, significantly different before and after hydrolysis.

As can be seen from Fig. 3.6, the concentration of quercetin after hydrolysis by β -glucuronidase was increased on the receiver side. These results suggest that quercetin aglycone is transported into the cell membrane and metabolized by the Phase II enzymes expressed on Caco-2 cell monolayers (Bjorge *et al*, 1991; Abid *et al*, 1995) to its conjugate forms, and then secreted into the basolateral side.

Although the present study confirmed that quercetin could be metabolized by Phase II enzymes in the intestinal cells, further studies are required to identify the chemical structures of the metabolites.

3.3.5. Studies of Quercetin-3-glucoside with Sugar Transporters

In recent years, Hollman *et al*, (1995;1997;1999) have conducted a series of absorption studies of quercetin and its glycosides in human subjects. They suggested that intestinal glucose transporter (SGLT1) may be involved in the absorption of quercetin glucosides.

To verify if this was indeed the case, the present study has employed the Caco-2 cell monolayers to investigate the transport of quercetin-glucosides across the cells. Our choice of the Caco-2 cell model was based on the early work of Blais *et al*, (1987) who had demonstrated the presence of a Na⁺-dependent sugar transport system in Caco-2 cell monolayers grown on petri dishes with properties similar to those normally found in brush-border membranes of human fetal colon. These authors used a nonmetabolizable sugar analog α -methylglucoside (AMG) and found that its accumulation in confluent monolayers was inhibited by sodium replacement, phloridzin and D-glucose. The existence of a Na⁺-dependent hexose transport system in Caco-2 cells was further confirmed by Riley *et al* (1991).

Using D-glucose as a marker, we have validated that our Caco-2 cell monolayers

also expresses the glucose transporter, SGLT1. As shown in Table 3.9, the permeability of quercetin-3-glucoside from AP to BL in the presence of sodium displayed no significant difference from that observed in the absence of sodium ($p > 0.05$).

Table 3.9. The effect of sodium ions on P_{app} of Quercetin-3-glucoside ($50 \mu\text{M}$) from AP to BL on Caco-2 cell monolayers ($n = 6$).

	$P_{app}(\text{AP} \rightarrow \text{BL}) \times 10^6 \text{ (cm/s)}$
With sodium ions	1.502 ± 0.22
Without sodium ions	1.288 ± 0.14

$p > 0.05$, no significant difference.

In addition, the SGLT1 inhibitor, phloridzin, at $100 \mu\text{M}$ did not decrease the permeability of quercetin-3-glucoside across the Caco-2 cell monolayers in the AP to BL direction, as expected (Fig. 3.13).

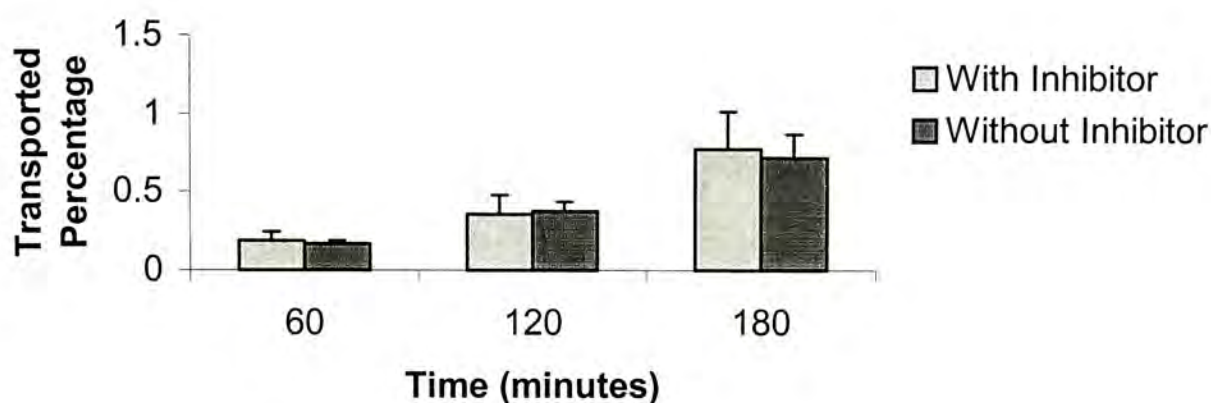


Fig. 3.13. The effect of SGLT1 inhibitor Phloridzin ($100 \mu\text{M}$) on the transport of Quercetin-3-glucoside ($100 \mu\text{M}$) from AP to BL on Caco-2 cell monolayers ($n = 3$).
 $p > 0.05$, no significant difference.

The above observations could be interpreted in several ways. As our previous

data have shown, the transport of quercetin-3-glucoside across the Caco-2 cells probably involves an efflux pump, i.e. P-gp. Regardless of whether quercetin-3-glucoside is actively transported by SGLT1 from AP to BL side or not, this efflux pump or P-gp would pump the compounds out of the cells if it had enough sites to bind quercetin-3-glucoside. Therefore, no directional difference in transport would be observed. The other possible explanation is that quercetin-3-glucoside is not a substrate of and cannot be transported by sodium/glucose cotransporter SGLT1. Hence, no difference in permeability from AP to BL was observed when replacing sodium or adding the SGLT1 inhibitor, phloridzin. Another possibility is that quercetin-3-glucoside could be actively transported into the cells and passively transported out of the cells concurrently. The relative slow passive diffusion process could result in an apparent lack of bi-directional differences in the measured permeability.

3.4. Uptake of D-glucose by BBMVs

Since the Caco-2 cells are derived from human colonic cell line, the observed lack of effect of the SGLT1 on the glucosides transport may not be fully reflective of the *in vivo* situation in the small intestine. To investigate this further, we have selected another well-established *in vitro* model utilizing isolated brush border membrane vesicles (BBMVs) with SGLT1 expression from the rabbit's small intestine.

BBMVs are a microvillar membrane preparation containing relatively small amount of metabolizing enzymes. It is a very well-characterized model for glucose uptake study (Hopfer *et al*, 1973; Kessler *et al*, 1978). The technique measures the interaction of glucoside with the SGLT1 indirectly in terms of its inhibition on the D-glucose uptake by SGLT1. This indirect verification of the SGLT1 involvement in the

glucoside transport will unlikely be obscured by any coexisting efflux action of P-gp which only competes for the glucoside, as could be the case with the Caco-2 cell technique.

Fig. 3.14. shows a typical time course plot of glucose uptake by BBMVs. Under a NaCl gradient, a very rapid initial uptake of D-glucose, marked by an 'overshoot' peak, was observed in 1 minute after the commencement of incubation, consistent with the result from Kessler *et al*, (1978). Thus for comparison of the rate of glucose uptake, all the uptake experiments were performed for exactly 1 minute.

The effect of quercetin-3-glucoside or quercetin-3-galactoside on the D-glucose uptake by rabbit's intestinal BBMVs is shown in Figs. 3.15a,b. Quercetin-3-glucoside and quercetin-3-galactoside at 0.05, 0.1 and 0.2 mM concentration appeared to have no significant inhibitory effects on the uptake of 0.1 mM D-glucose (t-test, $p > 0.05$).

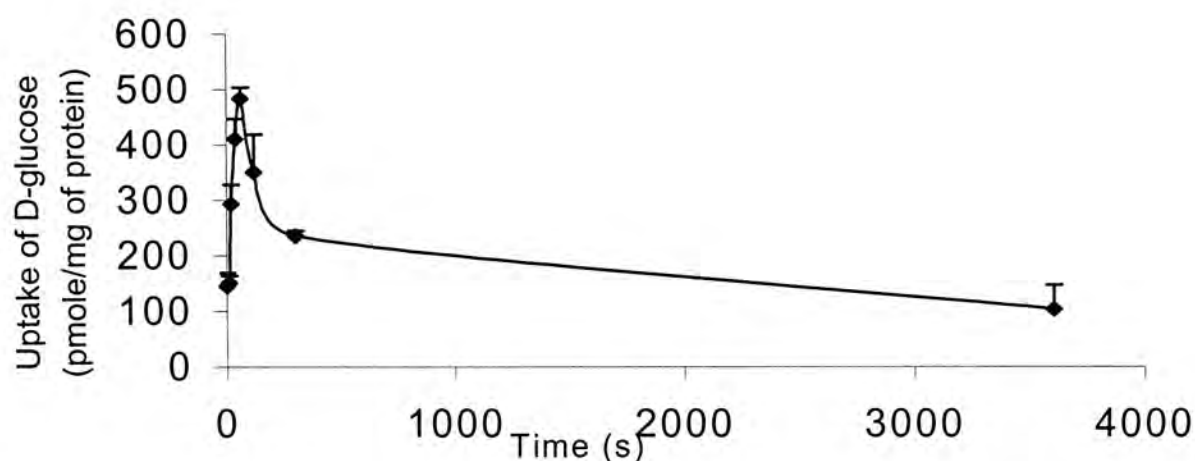


Fig. 3.14. Time course plot of D-glucose uptake by rabbit intestinal BBMVs ($n = 4$). 40 μ l of 0.1 mM D-glucose in incubation buffer (100 mM NaCl, 100 mM mannitol, 10 mM HEPES-Tris, pH 7.4).

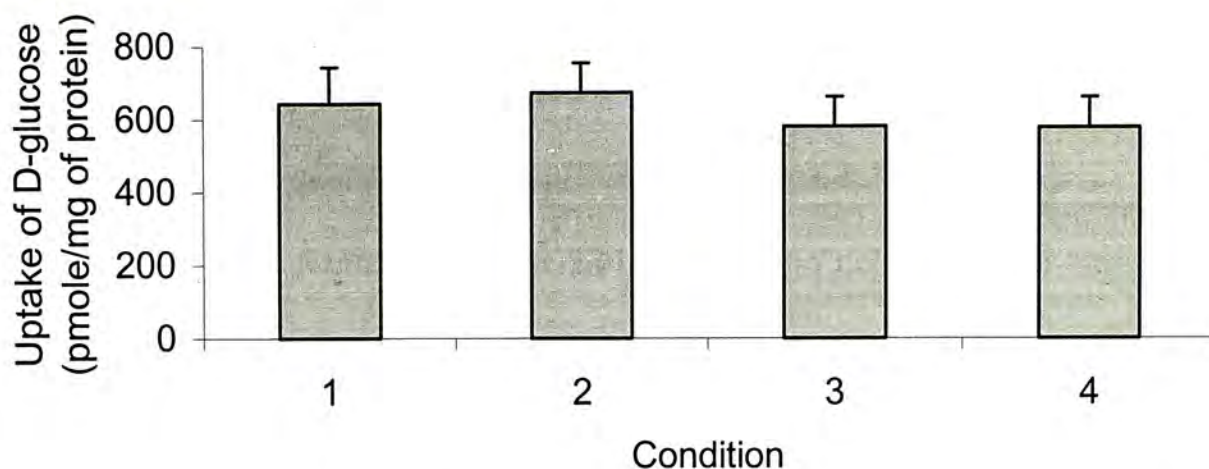


Fig. 3.15a. Uptake of D-glucose by rabbit intestinal BBMVs in the presence of Quercetin-3-glucoside (n = 6).
 Condition1: 0.1 mM D-glucose (control)
 Condition2: 0.1 mM D-glucose and 0.05 mM Quercetin-3-glucoside
 Condition3: 0.1 mM D-glucose and 0.1 mM Quercetin-3-glucoside
 Condition4: 0.1 mM D-glucose and 0.2 mM Quercetin-3-glucoside
 $p > 0.05$, no significant difference from the control.

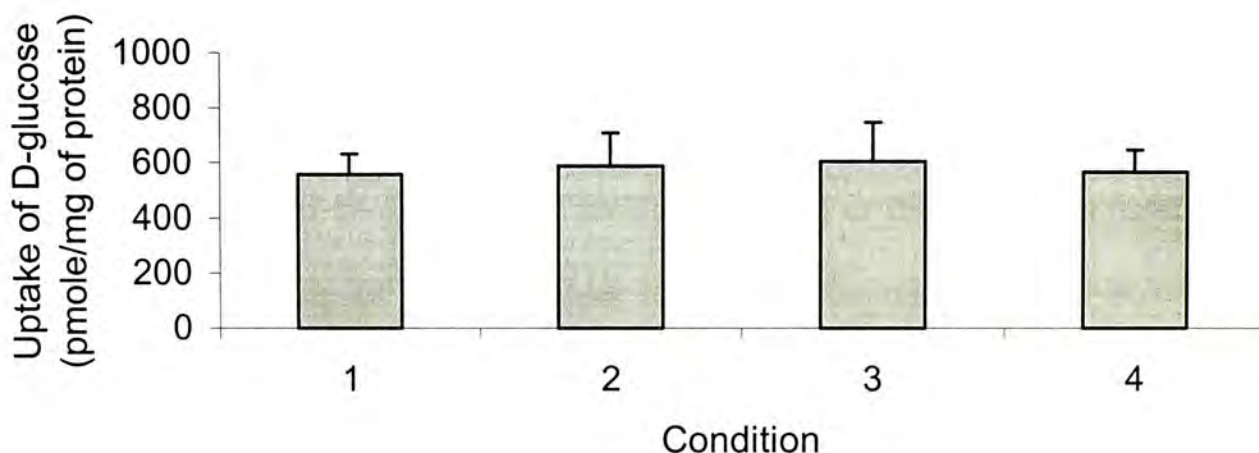


Fig. 3.15b. Uptake of D-glucose with Quercetin-3-galactoside by rabbit intestinal BBMVs (n = 5).
 Condition1: 0.1mM D-glucose (control)
 Condition2: 0.1 mM D-glucose and 0.05 mM Quercetin-3-galactoside
 Condition3: 0.1 mM D-glucose and 0.1 mM Quercetin-3-galactoside
 Condition4: 0.1 mM D-glucose and 0.2 mM Quercetin-3-galactoside
 $p > 0.05$, no significant difference from the control.

Ader *et al* (2001) suggested that quercetin-3-glucoside could compete with methyl- α -D-glucopyranoside (MDG), a non-metabolisable glucose analogue, for the intestinal glucose transporter SGLT1. They applied an *in vitro* method using rat small

intestine to investigate the mucosal uptake of MDG. They found that quercetin-3-glucoside and quercetin-4'-glucoside could inhibit SGLT1-mediated uptake of MDG, whereas the aglycone quercetin or the quercetin-3-rutinoside was ineffective.

Lee *et al* (1994) found that rat SGLT1 (665 amino acid residues) was 86-87% identical to SGLT1 in rabbit, pig and human. The inhibitory effect of phlorizin on MDG-evoked inward current in oocytes injected with rat or rabbit SGLT1 cRNA was more potent on rat SGLT1 than on rabbit SGLT1 (IC_{50} 0.17 μ M and 5 μ M), implying the existence of species difference in SGLT1. Using the same rats' SGLT1, the uptake of C^{14} -labelled MDG was observed to decrease in the presence of D-glucose, unlabelled MDG, D-galactose, 3-O-methyl-D-glucoside or uridine, suggesting that the binding to rat SGLT1 may not be very selective for D-glucose. This may compromise the utility of such an *in vitro* approach which relies on the use of an inhibitor to indirectly confirm the presence of the glucose cotransporters.

Further insight can be gained from studies designed to determine the structural requirement for binding of the glucosides to SGLT1. Nomoto *et al* (1997) have proposed the following structural requirements for the SGLT1 substrate: (1) the substrate must have a D-pyranose ring configuration, (2) it must possess a C1 chair form, and (3) the hydroxyl group in the glucose molecule at carbon 2 must be in the equatorial position. The authors found that β -form glucopyranoside had a higher affinity for SGLT1 than did the α - form.

Both quercetin-3-glucoside and quercetin-3-galactoside meet the above criteria and thus can potentially interact with SGLT1. Although the present findings seemed to suggest an absence of competition between quercetin-3-glucoside or quercetin-3-galactoside and D-glucose for the same binding sites on the sugar transporter, the possible involvement of this carrier in the transport of flavonoid glycosides cannot be

entirely ruled out and need to be investigated further.

The present project employed *in vitro* intestinal absorption models to explain some observations made *in vivo* on flavonoid absorption. The results suggest that relatively high permeability of quercetin across the intestinal epithelium may account for the short t_{\max} (time to peak concentration) observed *in vivo*. The lower concentration of quercetin in free form found *in vivo* may be due to its degradation under intestinal pH conditions, and metabolism by Phase II enzymes to its conjugate form across the intestinal cells. As for the selected quercetin glycosides, there was no significant difference in their permeabilities as determined by the Caco-2 cell monolayers model. Passive diffusion appears to be the major route of transport although some efflux systems like P-gp may also be involved in the absorption of quercetin-3-glucoside. The selected glycosides are stable under intestinal pH condition. Their poor permeabilities probably explain why they are generally not well absorbed *in vivo*, it is likely that the selected glycosides need be hydrolyzed first before being absorbed into the blood. This may account for the observed low concentrations of unchanged quercetin glycosides in the blood after oral consumption.

However, the possible involvement of glucose transporter in the transport process of flavonoids glycosides cannot be entirely ruled out and need to be further. The relationship between the structures of flavonoid glycosides and specific interactions with glucose transporter SGLT1 will provide valuable insight on the bioavailabilities of flavonoids. If specific carriers are indeed involved, the flavonoids that satisfy the structural requirements are expected to be absorbed better than the others which are predominantly transported by passive diffusion. Such structure-related difference in absorption may contribute to the inter-batch variations in the oral absorption of commercial flavonoid products.

**CHAPTER 4.
CONCLUSIONS**

In conclusion, the physicochemical properties (including chemical stability, aqueous solubility, formation of hydrates, heat of solution and partition coefficient of quercetin and its glycosides (quercetin-3-glucoside, quercetin-3-galactoside, quercetin-3-rutinoside and quercetin-3-rhamnoside) have been characterized. In addition, the intestinal transport mechanisms of these flavonoids have been investigated using validated *in vitro* models, namely, Caco-2 cell monolayers derived from human's colonic cancer cell and brush border membrane vesicles from rabbit's small intestine.

Quercetin (aglycone) has been shown to be poorly soluble in water and prone to hydrolytic degradation under intestinal pH condition. Incubation of quercetin in water at intestinal pH 6.8 resulted in the formation of three degradation products. Substitution of quercetin at position 3 with sugars lead to lower lipophilicity (partition coefficient) and higher stability and aqueous solubility.

Quercetin displayed a higher permeability than the various glycosides, and transport across the Caco-2 cell monolayers was accompanied by the formation of the glucuronide metabolite. Permeability does not appear to be a limiting factor for its absorption. However, metabolism by phase II enzymes in the intestine, poor aqueous solubility and the relative instability at intestinal pH may limit the amount of the free form of quercetin absorbed *in vivo*. In contrast, the various glycosides exhibited low partition coefficients and poor permeabilities, which may be a limiting factor for their absorption. All of these observations suggest that passive diffusion is the predominant transport mechanism for quercetin and its glycosides except for quercetin-3-glucoside, whose transport may also involve interaction with the efflux P-gp.

Quercetin-3-glucoside and quercetin-3-galactoside possessed no inhibitory effect on the uptake of D-glucose by BBMV, suggesting that they may not compete with

D-glucose for the glucose transporters, SGLT1.

The present thesis has generated some significant findings on the physical-chemical properties, intestinal absorption mechanisms and absorption-limiting factors of quercetin and four related glycosides. Apart from being useful for explaining some of the reported variations in oral bioavailabilities of these flavonoids in humans, the findings have important implications in the formulation of efficacious flavonoid products. As a follow-up on the present work, the following studies are worthy of consideration:

1. Immunostaining of the *in vitro* cell models employed would be worthwhile to assure the expression of specific transporters at the molecular level.
2. Since BBMVs experiments for verifying the involvement of SGLT1 was based indirectly on the inhibition of D-glucose binding with SGLT1 by the quercetin glycoside, it would be advisable to measure the direct uptake of the glycosides into BBMVs (i.e. direct binding with SGLT1) for further confirmation.
3. It would be necessary to use at least a few more structurally different flavonoids to further probe/confirm the relationship between chemical structure and intestinal absorption. If specific sugar substitution could indeed result in active absorption via sugar transporters, then appropriate structural modification could be used to enhance the oral absorption of flavonoids. This, couple with proper formulation strategies, will enable the formulation of efficacious flavonoid products.

References

- Abid A., Bouchon I., Siest G. and Sabolovic N. (1995) Glucuronidation in the Caco-2 human intestinal cell line: induction of UDP-glucuronosyltransferase 1*6. *Biochem. Pharmacol.* **50**, 557-561.
- Ader P., Blöck M., Pietzsch S., and Wolffram S. (2001) Interaction of quercetin glucosides with the intestinal sodium/glucose co-transporter (SGLT-1). *Cancer Lett.* **162**, 175-180.
- Artursson P. (1990) Epithelial transport of drugs in cell culture. I: a model for studying the passive diffusion of drugs over intestinal absorptive (Caco-2) cells. *J. Pharm. Sci.* **79**, 476-482.
- Artursson P. (1991) Cell culture as models for drug absorption across the intestinal mucosa. *Crit. Rev. in Ther. Drug Carrier Syst.* **8**, 305-330.
- Artursson P. Palm K. and Luthman K. (1996) Caco-2 monolayers in experimental and theoretical predictions of drug transport. *Adv. Drug Deliv. Rev.* **22**, 67-84.
- Aziz A.A., Edwards C.A., Lean M.E.J. and Crozier A. (1998) Absorption and excretion of conjugated flavonols, including quercetin-4'-O- β -glucoside and isorhamnetin-4'-O- β -glucoside by human volunteers after the consumption of onions. *Free Rad. Res.* **29**, 257-269.
- Bailey C.A., Bryla P. and Malick A.W. (1996) The use of the intestinal epithelial cell culture model, Caco-2, in pharmaceutical development. *Adv. Drug Deliv. Rev.* **22**, 85-103.
- Barthe L., Woodley J., and Houin G. (1999) Gastrointestinal absorption of drugs: methods and studies. *Fundam. Clin. Pharmacol.* **13**, 154-168.
- Bjorge S., Hamelehle K.L., Homan R., Rose S.E., Turluck D.A. and Wright D.S. (1991) Evidence for glucuronide conjugation of p-nitrophenol in the Caco-2 cell model. *Pharm. Res.* **8**, 1441-1443.
- Blais A., Bissonnette P., and Berteloot A. (1987), Common characteristics for Na⁺-dependent sugar transport in Caco-2 cells and human fetal colon. *J. Membrane Biol.* **99**, 113-125.
- Cavet M.E., West M. and Simmons N.L. (1996) Transport and epithelial secretion of the cardiac glycoside, digoxin, by human intestinal epithelial (Caco-2) cells. *Br. J. Pharmacol.* **118**, 1389-1396.
- Cook N.C. and Samman S. (1996) Flavonoids-Chemistry, metabolism, cardio-protective effects, and dietary sources. *Nutr. Biochem.* **7**, 66-76.
- Dantzig A. and Bergin L. (1990) Uptake of the cephalosporin, cephalixin by a dipeptide transport carrier in the human intestinal cell line, Caco-2. *Biochim. Biophys. Acta* **1027**, 211-217.
- Day A.J., DuPont M.S., Ridley S., Rhodes M., Rhodes M.J.C., Morgan M.R.A., and

- Williamson G. (1998) Deglycosylation of flavonoids and isoflavonoid glycosides by human small intestine and liver β -glucosidase activity. *FEBS Lett.* **436**, 71-75.
- Day A.J., Canada F.J., Diaz J.C., Kroon P.A., Mclauchlan R., Faulds C.B., Plumb G.W., Morgan M.R.A. and Williamson G. (2000a) Dietary flavonoid and isoflavone glycosides are hydrolysed by the lactase site of lactase phlorizin hydrolase. *FEBS Lett.* **468**, 166-170.
- Day A.J., Bao Y., Morgan M.R.A., and Williamson G. (2000b) Conjugation position of quercetin glucuronides and effect of biological activity. *Free Rad. Biol. & Med.* **29**, 1234-1243.
- Dowty M.E. and Dietsch C.R. (1997) Improved prediction of *in vivo* peroral absorption from *in vitro* intestinal permeability using an internal standard to control for intra- and inter-rat variability. *Pharm. Res.* **14**, 1792-1797.
- Erlund I., Kosonen T., Alfthan G. Mäenpää J., Perttunen K., Kenraali J., Parantainen J., and Aro A. (2000) Pharmacokinetics of quercetin from quercetin aglycone and rutin in healthy volunteers. *Eur. J. Clin. Pharmacol.* **56**, 545-553.
- Formica J.V. and Regelson W. (1995) Review of the biology of quercetin and related bioflavonoids. *Food. Chem. Toxic.* **33**, 1061-1080.
- Galijatovic A., Walle U.K., and Walle T. (2000) Induction of UDP-glucuronosyl-transferase by flavonoids chrysin and quercetin in Caco-2 cells. *Pharm. Res.* **17**, 21-26.
- Goldbohm R.A., van den Brandt P.A., Hertog M.G.L., Brants H.A.M. and van Poppel G. (1995) Flavonoids intake and risk of cancer: a prospective cohort study. *Am. J. Epidemiol.* **141**, s61.
- Graefe E.U., Derendorf H. and Veit M. (1999) Pharmacokinetics and bioavailability of the flavonol quercetin in humans. *International J. Clin. Pharmacol. and Therap.* **37**, 19-233.
- Graefe E.U., Witting J., Mueller S., Riethling A.K., Uehleke B., Drewelow B., Pforte H., Jacobasch G., Derendorf H., and Veit M. (2001) Pharmacokinetics and bioavailability of quercetin glycosides in humans. *J. Clin. Pharmacol.* **41**, 492-499.
- Grès M.C. and Julian B. (1998) Correlation between oral drug absorption in humans, and apparent drug permeability in TC-7 cells, a human epithelial intestinal cell line: comparison with the parental Caco-2 cell line. *Pharm. Res.* **15**, 726-733.
- Gutmann H., Fricker G., Török M., Michael S., Beglinger C. and Drewe J. (1999) Evidence for different ABC-transporters in Caco-2 cells modulating drug uptake. *Pharm. Res.* **16**, 402-407.
- Hertog M.G.L., Hollman P.C.H., and Venema D.P. (1992) Optimization of quantitative HPLC determination of potentially anticarcinogenic flavonoids in vegetables and fruits. *J. Agric. Food Chem.* **40**, 1591-1598.

- Hertog M.G.L., Kromhout D., Aravanis C., Blackburn H., Buzina R., Fidanza F., Giampaoli S., Jansen A., Menotti A., Nedeljkovic S., Pekkarinen M., Simic B.S., Toshima H., Feskens E.J.M., Hollman P.C.H., and Katan M.B. (1995) Flavonoids intake and long-term risk of coronary heart disease and cancer in the seven countries study. *Arch. Intern. Med.* **155**, 381-386.
- Hertog M.G.L., Sweetnam P.M., Fehily A.M., Elwood P.C. and Kromhout D. (1997) Antioxidant flavonols and ischemic heart disease in a welsh population of men: the Caerphilly study. *Am. J. Clin. Nutr.* **65**, 1489-1494.
- Hidalgo I.J., Raub T.J., and Borchardt R.T. (1989) Characterization of the human colon carcinoma cell line (Caco-2) as a model system for intestinal epithelial permeability. *Gastroenterology.* **96**, 736-749.
- Hollman P.C.H., Vries J.H.M., Leeuwen S.D., Mengelers M.J.B., and Katan M.B. (1995) Absorption of dietary quercetin glycosides and quercetin in healthy ileostomy volunteers. *Am. J. Clin. Nutr.* **62**, 1276-1282.
- Hollman P.C.H. and Hertog M.G.L. (1996) Potential health effects of the dietary flavonol quercetin. *Eur. J. Clin. Nutr.* **50**, 63-71.
- Hollman P.C.H., Trijp J.M.P., Buysman M.N.C.P., Gaag M.S., Mengelers M.J.B., Vries J.H.M. and Katan M.B. (1997) Relative bioavailability of the antioxidant flavonoid quercetin from various foods in man. *FEBS Lett.* **418**, 152-156.
- Hollman P.C.H. and Katan M.B. (1999) Dietary Flavonoids: Intake, Health Effects and Bioavailability. *Food and Chem. Toxicol.* **37**, 937-942.
- Hopfer U., Nelson K., Perrotto J., and Isselbacher K.J. (1973) Glucose transport in isolated brush border membrane from rat small. *J. Biol. Chem.* **248**, 25-32.
- Hosoya K.I., Kim K.J. and Lee. V.H.L. (1996) Age-dependent expression of P-glycoprotein gp170 in Caco-2 cell monolayers. *Pharm. Res.* **13**, 885-890.
- Hu M. and Borchardt R. (1990) Mechanism of L- α -methyldopa transport through a monolayer of polarized human intestinal epithelial cells (Caco-2). *Pharm. Res.* **7**, 1313-1319.
- Hunter J., Jepson M.A. Tsuruo T., Simmon N.L., and Hirst B.H. (1993) Functional expression of P-glycoprotein in apical membrane of human intestinal Caco-2 cells. *J. Biol. Chem.* **268**, 14991-14997.
- Hunter J. and Hirst B.H. (1997) Intestinal secretion of drugs. The role of P-glycoprotein and related efflux systems in limiting oral drug absorption. *Advan. Drug Deliv. Rev.* **25**, 129-157.
- Irvine J.D., Takahashi L. Lockhart K., Cheong J., Tolan J.W., Selick H.E., and Grove J.R. (1998) MDCK (Madin-Darby Canine Kidney) cells: A tool for membrane permeability screening. *J. Pharm. Sci.* **88**, 29-33.

- Justesen U. and Arrigoni E. (2001) Electrospray ionization mass spectrometric study of degradation products of quercetin, quercetin-3-glucoside and quercetin-3-rhamnoglucoside, produced by *in vitro* fermentation with human faecal flora. *Rapid Commun. Mass Spectrom.* **15**, 477-483.
- Karlsson J., Kuo S.M., Ziemniak J., and Artursson P. (1993) Transport of celiprolol across human intestinal epithelial (Caco-2) cells: mediation of secretion by multiple transporters including P-glycoprotein. *Br. J. Pharmacol.* **110**, 1009-1016.
- Keli S.O., Hertog M.G.L., Feskens E.J.M. and Kromhout D. (1996) Dietary flavonoids, antioxidant vitamins, and incidence of stroke. *Arch. Intern. Med.* **156**, 637-642.
- Kessler M., Acuto O., Storelli C., Murer H., Muller M., and Giorgio S. (1978) A modified procedure for the rapid preparation of efficiently transporting vesicles from small intestinal brush border membranes. *Biochim. Biophys. Acta.* **506**, 136-154.
- Knekt P., Järvinen R., Seppänen R., Heliövaara M., Teppo L., Pukkala E., and Aromaa A. (1997) Dietary flavonoids and the risk of lung cancer and other malignant neoplasms. *Am. J. Epidemiol.* **146**, 223-230.
- Kühnau J. (1976) The flavonoids. A class of semi-essential food components: their role in human nutrition. *World Rev. Nutr. Diet.* **24**, 117-191.
- Kuo S.M., Whitby B.R., Artursson P., and Ziemniak J.A. (1994) The contribution of intestinal secretion to the dose-dependent absorption of celiprolol. *Pharm. Res.* **11**, 648-653.
- Lee W.S., Kanai Y., Wells R.G., and Hediger M.A. (1994) The high affinity Na⁺/Glucose cotransporter. *J. Bio. Chem.* **269**, 12032-12039.
- Lennernäs H. (1995) Does fluid flow across the intestinal mucosa affect quantitative oral drug absorption? Is it time for a reevaluation? *Pharm. Res.* **12**, 1573-1582.
- Lennernäs H., Nylander S., and Ungell A.L. (1997) Jejunal permeability: A comparison between the Ussing Chamber technique and the Single-pass perfusion in humans. *Pharm. Res.* **14**, 667-671.
- Lowry O.H., Rosebrough N.J., Farr A.L. and Randall R.J. (1951) Protein measurement with the folin phenol reagent. *J. Biol. Chem.* **193**, 265-275.
- Manach C., Morand C., Crespy V., Demigné C., Texier O., Régéat F. and Rémésy C. (1998) Quercetin is recovered in human plasma as conjugated derivatives which retain antioxidant properties. *FEBS Lett.* **426**, 331-336.
- Martin A., Swarbrick J., and Cammarata A. (1992) *Physical Pharmacy*, Lea & Febiger press.
- Mayersohn M. (1996) Principles of drug absorption, in *Modern Pharmaceutics* pp 21-7, Marcel Dekker Inc., New York.

- Murota K., Shimizu S., Chujo Hitomi., Moon J.H., and Tergo J. (2000) Efficiency of absorption in metabolic conversion of quercetin and its glucosides in human intestinal cell line Caco-2. *Arch. Biochem. Biophys.* **384**, 391-397.
- Nielsen S.E. and Dragsted L.O. (1998) Column-switching high-performance liquid chromatographic assay for the determination of quercetin in human urine with ultraviolet absorbance detection. *J. Chromatogr. B.* **707**, 81-89.
- Nomoto M., Yamada K., Haga M. and Hayashi M. (1997) Improvement of intestinal absorption of peptide drugs by glycosylation: transport of tetrapeptide by the sodium ion-dependent D-glucose transport. *J. Pharm. Sci.* **57**, 326-332.
- Olthof M.R., Hollman P.C.H., Vree T.B., and Katan M.B. (2000) Bioavailabilities of quercetin-3-glucoside and Quercetin-4'-glucoside do not differ in humans. *J. Nutr.* **130**, 1200-1203.
- Peters W.H.N and Roelofs H.M.L. (1989) Time-dependent activity and expression of glutathione S-transferases in the human colon adenocarcinoma cell line Caco-2. *J. Biochem.* **264**, 613-616.
- Pinto M. Robine-Leon S., Appay M.D., Kedinger M., Triadou N., Dussaulx E., Lacroix B., Simon-assmann P., Haffen K., Fogh J., and Zweibaum A. (1983) Enterocyte-like differentiation and polarization of the Human colon carcinoma cell line Caco-2 in culture. *Biol. Cell.* **47**, 323-330.
- Polentarutti B.I., Peterson A.L., Sjöberg A.K., Anderberg E.K.I., Utter L.M., and Ungell A.L.B. (1999) Evaluation of viability of excised rat intestinal segments in the Ussing Chamber: Investigation of morphology, electrical parameters, and permeability characteristics. *Pharm. Res.* **16**, 446-454.
- Reardon P.M., Gochoco C.H., Audus K.L., Wilson G., and Smith P.L. (1993) *In vitro* nasal transport across ovine mucosa: effect of ammonium glycyrrhizinate on electrical properties and permeability of growth hormone releasing peptide, mannitol, and lucifer yellow. *Pharm. Res.* **10**, 553-561.
- Rice-Evans C.A., Miller N.J., and Paganga G. (1996) Structure-antioxidant activity relationship of flavonoids and phenolic acids. *Free Rad. Biol. & Med.* **7**, 933-956.
- Riley S.A., Warhurst G., Crowe P.T., and Turnberg L.A. (1991) Active hexose transport across cultured human Caco-2 cells: characterization and influence of culture conditions. *Biochim. Biophys. Acta.* **1066**, 175-182.
- Rimm E.B., Katan M.B., Ascherio A., Stampfer M.J., and Willett W.C. (1996) Relationship between intake of flavonoids and risk of coronary heart disease in male health professionals. *Ann. Intern. Med.* **125**, 384-389.
- Ritschel W.A. and Kearns G.L. (1999) *Handbook of Basic Pharmacokinetics* pp 45-70, American pharmaceutical association, Washington, DC.

- Rosenberg D.W. and Leff T. (1993) Regulation of cytochrome P450 in cultured human colonic cells. *Arch. Biochem. Biophys.* **300**, 186-192.
- Shoji A., Takashi M., Kunihiro O., and Masahiro H. (1992) Intestinal active absorption of sugar-conjugated compounds by glucose transport system: implication of improvement of poorly absorbable drugs. *Biochem. Pharmacol.* **43**, 2037-2039.
- Smith T., Gibson C., Howlin B. and Pratt J. (1991) Active transport of amino acids by gamma-glutamyl transpeptidase through Caco-2 cell monolayers. *Biochem. Biophys. Res. Commun.* **178**, 1028-1035.
- Smith P.L. (1996) Methods for evaluation intestinal permeability and metabolism in vitro, in *Models for Assessing Drug Absorption and Metabolism* pp 13-34, Plenum Press, New York and London.
- Spencer J.P.E., Chowrimootoo G., Choudhury R., Debnam E.S., Srai S.K. and Rice-Evans C. (1999) The small intestine can both absorb and glucuronidate luminal flavonoids. *FEBS Lett.* **458**, 224-230.
- Tanigawara Yusuke. (2000) Role of P-glycoprotein in Drug Disposition. *Ther. Drug Monit.* **22**, 137-140.
- Thiebaut F., Tsuruo T., Hamada H., Gottesman M.M., Pastan I., and Willingham M.C. (1987) Cellular localization of the multidrug-resistance gene product P-glycoprotein in normal human tissues. *Proc. Natl. Acad. Sci.* **84**, 7735-7738.
- Toggenburger G., Kessler M., and Semenza G. (1982) Phlorizin as a probe of the small intestine Na⁺, D-glucose cotransporter a model. *Biochim. Biophys. Acta.* **688**, 557-571.
- Tomita M., Menconi M.J., Delude R.L., and Fink M.P. (2000) Polarized transport of hydrophilic compounds across rat colonic mucosa from serosa to mucosal is temperature dependent. *Gastroenterology* **118**, 535-543.
- Tukker J.J. (2001) *In vitro* methods for the assessment of permeability, in *Oral Drug Absorption* pp 51-72,
- Thiebaut F., Tsuruo T., Hamada H., Gottesman M.M., Pastan I., and Willingham M.C. (1987) Cellular localization of the multidrug-resistance gene product P-glycoprotein in normal human tissues. *Proc. Natl. Acad. Sci.* **84**, 7735-7738.
- Ungell A.L., Nylander S., Sjöberg Å., Bergstrand S., and Lennernäs H. (1998) Membrane transport of drugs in different regions of the intestinal tract of the rat. *J. Pharm. Sci.* **87**, 360-366.
- Ussing H.H. and Zerahn K. (1951) Active transport of sodium as the source of electric current in the short-circuited isolated frog skin. *Acta Physiol. Scand.* **23**, 110-127.
- Walgren R.A., Walle U.K. and Walle T. (1998) Transport of Quercetin and its glucosides across human intestinal epithelial Caco-2 cells. *Biochem. Pharmacol.* **15**,

1721-1727.

Walgren R.A., Karl W., Lindermayer G.E., and Walle T. (2000a) Efflux of dietary flavonoid quercetin-4'- β -glucoside across human intestinal Caco-2 cell monolayers by apical multidrug resistance-associated protein-2. *J. Pharmacol. Exp. Ther.* **294**, 830-836.

Walgren R.A., Lin J.T., Kinne R.K.H., and Walle T. (2000b) Cellular uptake of dietary flavonoids quercetin-4'- β -glucoside by sodium-dependent glucose transporter SGLT1. *J. Pharmacol Exp. Ther.* **294**, 837-843.

Walle U.K., French K.L., Walgren R.A. and Walle T. (1999) Transport of genistein-7-glucoside by human intestinal Caco-2 cells: potential role for MRP2. *Res. Commun. Mol. Path.* **103**, 45-56.

Walle T., Otake Y., Walle U.K., and Wilson F.A. (2000) Quercetin glucosides are completely hydrolyzed in ileostomy patients before absorption. *J. Nutr.* **130**, 2658-2661.

Wang E.J., Casciano C.N., Clement R.P., and Johnson W.W. (2001) Inhibition of P-glycoprotein transport function by grapefruit juice psoralen. *Pharm. Res.* **18**, 432-438.

Waterbeemd H.V.D. (2001) Intestinal permeability: prediction from theory, in *Oral Drug Absorption* pp 31-49,

Wilson T.H., Wiseman G. (1954) The use of sacs of everted small intestine for the study of the transference of substances from the mucosal to the serosal surface. *J. Physiol.* **123**, 116-125.

Wright E.M. (1994) Intestinal sugar transport, in *Physiology of the Gastrointestinal Tract* pp1751-1772, Raven Press, New York.

Yee S.Y. (1997) *In vitro* permeability across Caco-2 cells (colonic) can predict *in vivo* (small intestinal) absorption in man — fact or myth. *Pharm. Res.* **14**, 763-766.

Yoshioka M., Erickson R.H., Matsumoto H., Gum E. and Kim Y.S. (1991) Expression of dipeptidyl aminopeptidase IV during enterocytic differentiation of human colon cancer (Caco-2) cells. *Int. J. Cancer.* **47**, 916-921.

CUHK Libraries



003952877